

AD719240

AD _____

COPY NO. 93



TECHNICAL REPORT 4168
FULL AND MODEL SCALE TESTS
OF
BAY STRUCTURE

STUART LEVY
RICHARD RINDNER
LEON W. SAFFIAN
STANLEY WACHTELL

PICATINNY ARSENAL

EDWARD COHEN
MICHAEL DEDE
NORVAL DOBBS

AMMANN & WHITNEY

FEBRUARY 1971

DDC
RECEIVED
FEB 28 1971
B

Reproduced by
NATIONAL TECHNICAL
INFORMATION SERVICE
Springfield, Va. 22151

PICATINNY ARSENAL
DOVER, NEW JERSEY

DISTRIBUTION STATEMENT A

Approved for public release;
Distribution Unlimited

165

DISPOSITION

Destroy this report when no longer needed. Do not return to the originator.

The findings in this report are not to be construed as an official Department of the Army position, unless so designated by other authorized documents.

ACQUISITION FOR	
OPDI	WHITE SECTION <input type="checkbox"/>
OPC	SOFT SECTION <input type="checkbox"/>
UNCLASSIFIED	<input type="checkbox"/>
CLASSIFICATION	<i>per Tabern</i>
BY	
DISTRIBUTION/AVAILABILITY CODES	
CODE	AVAIL. CODE/SPECIAL
<i>A</i>	

Details of illustrations in
this document may be better
studied on microfiche

TECHNICAL REPORT 4168

FULL AND MODEL SCALE TESTS OF BAY STRUCTURE

STUART LEVY
RICHARD RINDNER
LEON SAFFIAN
STANLEY WACHTELL

PICATINNY ARSENAL

EDWARD COHEN
MICHAEL DEDE
NORVAL DOBBS

AMMANN & WHITNEY

FEBRUARY 1971

AMMUNITION ENGINEERING DIRECTORATE
PICATINNY ARSENAL
DOVER, NEW JERSEY

TABLE OF CONTENTS

Section	Page
LIST OF ILLUSTRATIONS	iii
LIST OF TABLES	v
ACKNOWLEDGMENTS	vii
ABSTRACT	ix
DAMAGE CLASSIFICATION	xi
SUMMARY	xiii
CONCLUSIONS	xv
SECTION I - INTRODUCTION	1
1-1 Background	1
1-2 Scope of Report	1
1-3 Primary Objectives	1
1-4 Secondary Objectives	1
SECTION II - SCALED BAY TEST SERIES	5
2-1 Test Layout	5
2-1.1 Prototype Structure	5
2-1.2 Model Design.	10
2-1.3 Model Construction	15
2-1.4 Test Site	18
2-1.5 Explosive Charges	22
2-1.6 Instrumentation and Test Measurements	25
2-2 Discussion of Test Results	33
2-2.1 Structural Damage	33
2-2.2 Pressure, Deflection and Strain Test Measurements	53
SECTION III - ULTIMATE CAPACITY BAY TESTS	69
3-1 General	69
3-2 One-Tenth Scale Composite Bay Test	70
3-3 One-Eighth Scale Composite Bay Test	70
3-4 One-Eighth Scale Plain Reinforced Concrete Bay Test	77

TABLE OF CONTENTS (Cont'd)

Section	Page
REFERENCES	79
APPENDICES	
A. Geometrical Scaling	81
B. Analysis of Dynamic Response of Back Wall of Full Scale Bay Structure (Round 1)	89
TABLE OF DISTRIBUTION	165
ABSTRACT DATA	173

LIST OF ILLUSTRATIONS

<u>Number</u>	<u>Title</u>	<u>Page</u>
1	Prototype of Bay Structure	2
2	Layout of Full Scale Bay Structure	7
3	Cross Section Through Bay Structure Wall & Floor Slab	9
4	Placement of Concrete in Model Cubicle	16
5	Straightening of Coiled Annealed Wire	17-
6	Bending Methods for Lacing Reinforcement	19
7	Preassembly of Wall Reinforcement	20
8	Soil Conditions at Test Site for Bay Structure Test Series	21
9	Pre-shot Test Setup for Model Structures	23
10	Pre-shot Test Setup for Full Scale Bay	24
11	Electronic Deflection Gage Setup for Wall	29
12	Details of Electronic Deflection Gage	30
13	Deflection Gage Layout (Full Scale Structure)	32
14	Camera Layout (One-Tenth Scale Structure)	34
15	Model Scale Tests - Round 1 - Donor Side	36
16	Full Scale Test - Round 1 - 2000 lbs - Donor Side	37
17	Model Scale Tests - Round 1 - Receiver Side	39
18	Area of Main Damage to Floor Slab - Round 1 -One Tenth Scale	40
19	Damage to Structure - Plan View - Round 1 -One Tenth Scale	41
20	Full Scale Test - Round 1 - 2000 lbs. - End Panel	44

LIST OF ILLUSTRATIONS (Cont'd)

<u>Number</u>	<u>Title</u>	<u>Page</u>
21	Model Scale Tests - Round 2 - Donor Side	45
22	Model Scale Tests - Round 2 - Receiver Side	46
23	Full Scale Test - Round 2 - 3000 lbs. - Donor Side	47
24	Full Scale Bay Test - Round 3 - 5000 lbs. - Donor Side	49
25	Model Scale Tests - Round 3 - Donor Side	50
26	Full Scale Test - Round 3 - 5000 lbs. - Donor Side	51
27	Model Scale Tests - Round 3 - Receiver Side	52
28	One-Eighth Scale Test - Round 4 - Receiver Side	54
29	One-Eighth Scale Test - Round 4 - Donor Side	55
30	Full Scale Bay Test - Round 4 - 7500 lbs. - Donor Side	56
31	Full Scale Bay Test - Round 4 - 7500 lbs. - Receiver Side	57
32	Exterior Leakage Pressure vs. Scaled Distance (Front Direction)	58
33	Exterior Leakage Pressure vs. Scaled Distance (Side Direction)	59
34	Exterior Leakage Pressure vs. Scaled Distance (Rear Direction)	60
35	Suggested Pressure-Distance Curves	61
36	One-Tenth Scale Test Setup - 10 lb. Charge	71
37	One-Tenth Scale Bay Test - Receiver and Donor Sides - 10 lb. Charge	72
38	Simulation of Multi-Cubicle Structure Using Steel Plate Tie System	73
39	One-Eighth Scale Bay Test - Receiver Side - 15 lb. Charge	75
40	One-Eighth Scale Bay Test - Donor Side - 15 lb. Charge	76
41	One-Eighth Scale Plain Reinforced Concrete Bay Test	78

LIST OF TABLES

<u>Number</u>	<u>Title</u>	<u>Page</u>
1	Comparison of Scaled Properties of Bay Structure Test Series	13
2	Charge Weight Properties	26
3	Electronic Instrumentation	27
4	Pressure Gage Data	28
5	Summary of Scaled Explosive Bay Structure Tests	35
6	Maximum Permanent Deflections Obtained by Measurements	63
7	Maximum Deflections Obtained from Electronic Deflection Gage Measurements	64
8	Maximum Deflection - Second Round - Full Scale Bay Test	65
9	Summary of Strain Gage Measurements	67
10	Back Wall Fragment Velocities (Round 3)	68
11	Test Structure Dimensions	69

ACKNOWLEDGMENTS

The authors wish to express sincere appreciation to the many individuals for their cooperation in behalf of this project. Special acknowledgment is given to Mr. Russel G. Perkins of the Armed Services Explosives Safety Board and to Mr. Joseph Porcaro of Ammann and Whitney, Consulting Engineers, New York, New York.

ABSTRACT

This report contains the results of two explosive test series: (1) The Scaled Explosive Bay Test Series whose purpose was to validate the "Scaling Laws" as applied to model bays and (2) The Ultimate Capacity Bay Test Series whose purpose was to determine the ultimate explosive resistance of a given explosive bay configuration.

The results of these tests indicated that scale models may be used to evaluate the blast-resistant capabilities of a laced reinforced concrete cubicle-type structure and that the total explosive capacity of the tested structure (at incipient failure) is at least equal to 7,500 lbs. of high explosives.

The Explosive Bay Test Series was carried out under the supervision of the Ammunition Engineering Directorate's Process Engineering Laboratory with technical assistance relating to structural design and testing provided by Ammann & Whitney of New York, New York.

The smaller models (1/10 and 1/8 scale) were fabricated at the Civil Engineering Laboratories, Columbia University, and Ohio River Division Laboratories, Cincinnati, Ohio and tested at Picatinny Arsenal. The 1/3 and 1/5 scale models were built and tested by the Arthur D. Little Corporation at its Keene, New Hampshire test facility and the full scale structure was constructed and tested at the U.S. Naval Weapons Center, China Lake, California.

DAMAGE CLASSIFICATION

In this report relating to results of structural damage, certain terms will be used to describe the degree of damage to a reinforced concrete wall. Definitions of these terms are:

Incipient Failure - on the verge of collapse

Partial Failure - breaking of concrete into two or more sections that do not disengage from each other as a result of either failure of the tension reinforcement and/or shear failure in the concrete

Total Failure - failed sections of the element are disengaged and/or complete disengagement of the concrete from the reinforcement occurred

Heavy Damage - element is at or near incipient failure

Medium Damage - large cracking (no reinforcement failure), local crushing, surface pitting

Light Damage - minimum damage, hairline or slightly larger cracks

In composite wall construction, the classification of the overall damage to the element is based on the damage sustained by the receiver panel.

SUMMARY

The Explosive Bay Test Series was conducted to establish "scaling factors" that would relate the test results of model cubicle structures to the full scale structure, and to evaluate the blast resistance of specific cubicle arrangements that might be used in the processing of explosive materials.

Twenty tests were conducted on eight structures, distributed in the following manner: three on the 1/10 scale, four on the 1/8 scale, three on the 1/5 scale, three on the 1/3 scale and four on the full scale structure. The remainder: three tests consisted of single tests on three different model bay structures (one 1/10 and two 1/8 scale). The three latter tests were performed separately from the scaling series tests and were primarily conducted to evaluate the ultimate capacity of the structure and/or compare the use of composite construction with that of plain reinforced concrete.

The charges were either single spheres or a cluster of spheres of Composition B. However, because of the large quantities of explosives involved, boxes of TNT were used in the last two rounds of the full scale test. The charge weights used were 2,000, 3,000, 5,000, 7,500 and 10,000 lbs. or their scaled equivalents. These charges were placed in the geometric center of each cubicle. Each structure of the scaling series was successively tested three or four times with increasing HE charges until the point of incipient failure or total destruction occurred. Three exceptions to this were the ultimate capacity structure tests where a single shot equivalent to 10,000 lbs. was fired in the 1/10 scale structure while the explosive weight in each 1/8 scale model was equivalent to 7,500 lbs.

All the bays tested had walls of composite-type construction (concrete-sand-concrete) except for one 1/8 scale model which utilized plain reinforced concrete. The concrete walls of both types of construction used laced reinforcement. The interior cell dimensions of the prototype structure were 40 feet long by 20 feet wide by 10 feet high. It had no roof and was open at one side.

The first round (2,000 lbs.) in the scaling test series produced light cracking in the 1/10, 1/8 and 1/5 scale models and hairline cracks in the 1/3 and full scale models. The damage sustained in the second round (3,000 lbs.) consisted of heavy cracking of the 1/10 scale model, medium cracking of the 1/5 scale model and minor cracking of the remainder of the models. The third round (5,000 lbs) caused partial destruction of the 1/10 scale model, medium damage to the 1/8 scale model, incipient failure of the 1/5 scale model and minor cracking of the 1/3 and full scale structures. Partial destruction was sustained by both the 1/8 and full scale structures in the fourth series of tests.

In the Ultimate Capacity Tests, the 10,000 pound equivalent charge in the 1/10 scale model produced complete destruction of the back wall while the side walls cracked and sheared at their supports. A 7,500 lb. equivalent charge caused incipient failure of the 1/8 scale composite-type model. However, when the 1/8 scale plain reinforced concrete model was tested with an equivalent charge of 7,500 lbs., the damage sustained was less than incipient failure. No reinforcement failure occurred in either test of the 1/8 scale model. In general, the bay successfully withstood the blast effects of detonations up to 7,500 lbs. of HE as evidenced by a single shot test with the 1/8 scale composite and plain wall construction.

The instrumentation used in the bay structure tests consisted of photographic coverage, deflection gages and pressure gages. All the instruments were not used in any one test.

CONCLUSIONS

The Scaled Bay Test Series proved that the so-called "Geometrical Scaling" laws are applicable and that scaled models can be used to simulate full scale response tests of laced reinforced concrete cubicle structures. Although test results show that models as small as 1/10 scale may be used to obtain a reasonable estimate of the blast-resistant capabilities of a full scale cubicle, it was found that the use of 1/8 scale and larger models will usually be more practical for testing and construction purposes and will not significantly increase the test costs.

The results of this test series indicated that the test structure, originally designed to withstand the blast effects of 2,000 lbs. of TNT, had an explosive storage capacity in the order of 7,500 lbs. of TNT.

The most satisfactory measurements of the structural motions were recorded by the deflection gauges. These measurements included a deflection-time history of the wall movements and indicated the maximum deflection which a wall could attain under given applied blast loads. Also, measurements were made of the overall movement of the test structure due to sliding. Although damage to the individual structures differed somewhat after each round of tests, the differences after the first two rounds of tests are not attributed entirely to scaling factors themselves. These differences could be directly related to variations which existed in construction methods, materials and/or test site conditions.

SECTION I

INTRODUCTION

1-1 Background

During the last several years, Picatinny Arsenal, as part of its Supporting Studies Program, has been carrying out an overall experimental and analytical program to establish safety criteria for the design of protective structures used in high explosive processing and storage facilities. This program was funded by the Armed Services Explosives Safety Board. The firm of Ammann & Whitney provided technical assistance on structural and other aspects of the program.

Because full scale testing in connection with the above program would have been prohibitively expensive, a test series was designed to evaluate the validity of utilizing models in place of full scale structures.

At the suggestion of the Armed Services Explosives Safety Board it was decided to design, construct and test a structure having the interior dimensions of a typical explosive manufacturing bay (Figure 1) that would withstand the effects of a detonation of 2,000 lbs. of HE (Ref. 1).

1-2 Scope of Report

This report is divided into two main parts:

- 1) Discussion of the bay structure test series (Section II)
- 2) Discussion of the ultimate capacity test series (Section III)

1-3 Primary Objectives

The two main objectives of the test series were to:

- 1) Establish "model factors" that will relate the test results of model structures to those of their prototype (full scale) and to each other.
- 2) Evaluate the explosive-resistant capacity of a specific cubicle arrangement.

1-4 Secondary Objectives

The secondary objectives were to:

- 1) Evaluate blast load parameters for the design of protective structures.

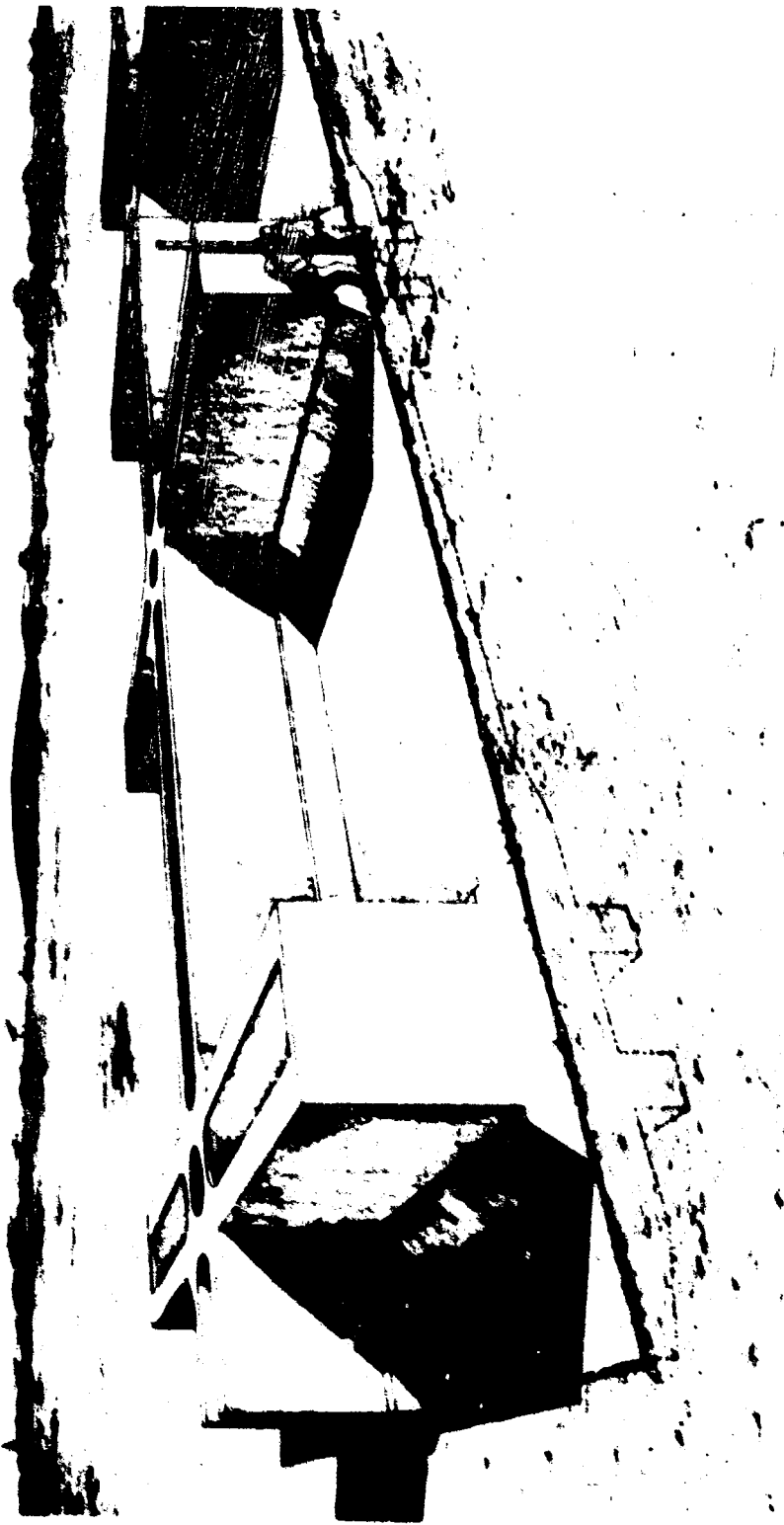


FIGURE 1 - PROTOTYPE OF BAY STRUCTURE

- 2) Determine experimentally the structural response of laced reinforced concrete to the applied blast loads.
- 3) Establish construction details to afford the required strength to resist the applied blast loads.
- 4) Accumulate data pertaining to leakage pressures.

SECTION II
SCALED BAY TEST SERIES

2-1 Test Layout

2-1.1 Prototype Structure

The bay structure was designed to include the effects of adjoining cells that would exist in an actual explosive manufacturing facility (Figure 2). All the structural elements were constructed of reinforced concrete and consisted of a floor slab, back wall and two side walls. The front and top of the structure remained open to the atmosphere. The interior dimensions of the prototype cubicle were 40 ft.-0 in. long by 20 ft.-0 in. deep by 10 ft.-0 in. high.

The walls of the structure were built using composite (sandwich) construction where two concrete panels were separated by sand fill. Each wall had an overall thickness of eight feet and was divided into a two foot thick donor panel, a four foot wide sand-filled cavity, and a two foot thick receiver panel. In the side walls, closure of the sand cavity at the open end of the structure was provided by an end panel. At the intersection of each side wall with the back wall, a sand-filled cylindrical cavity, which extended from the top of the walls down to the pedestal, was provided. Figure 3 illustrates a typical cross section through a composite wall.

To resist the buildup of blast pressures in the corners, two foot high by two foot wide concrete haunches were located at the intersections of all three walls with the floor slab. Also, concrete pedestals were used to separate the base of the individual panels of each wall. The haunches and pedestal of each wall were interconnected by reinforcing bars which were continuous across the base of the wall. This system formed a monolithic connection between the wall and the slab.

Adjacent to the walls was the peripheral floor slab which had a thickness of two feet and surrounded the one foot thick central floor slab. The transition between the two thicknesses was accomplished by an intermediate taper.

High strength billet steel bars conforming to ASTM Specification A432 (new ASTM designation is A615 Grade 60) were used throughout for reinforcement of the concrete. The main horizontal and vertical reinforcement in both the back and side walls consisted of 1-1/8 inch diameter bars located 10 inches on center and was identical at both surfaces of each panel. The horizontal reinforcement was bounded by the vertical reinforcing bars. As was the case with the horizontal reinforcement, the adjacent vertical bars in the walls were tied together by means of diagonal lacing reinforcement (Refs. 2 and 3) having a diameter

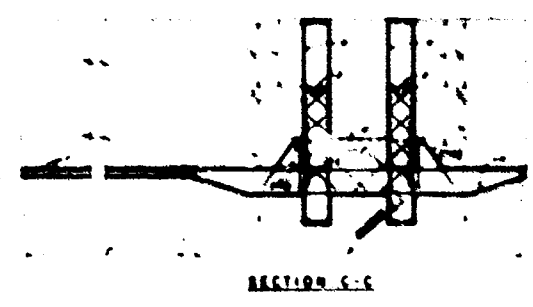
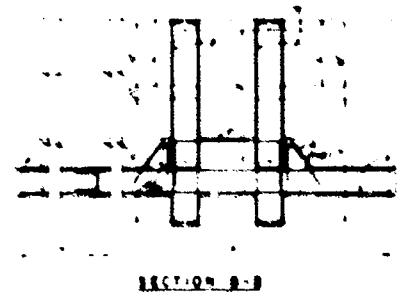
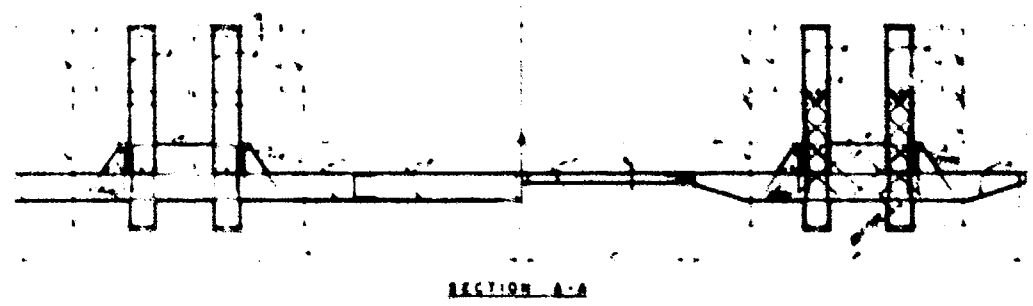
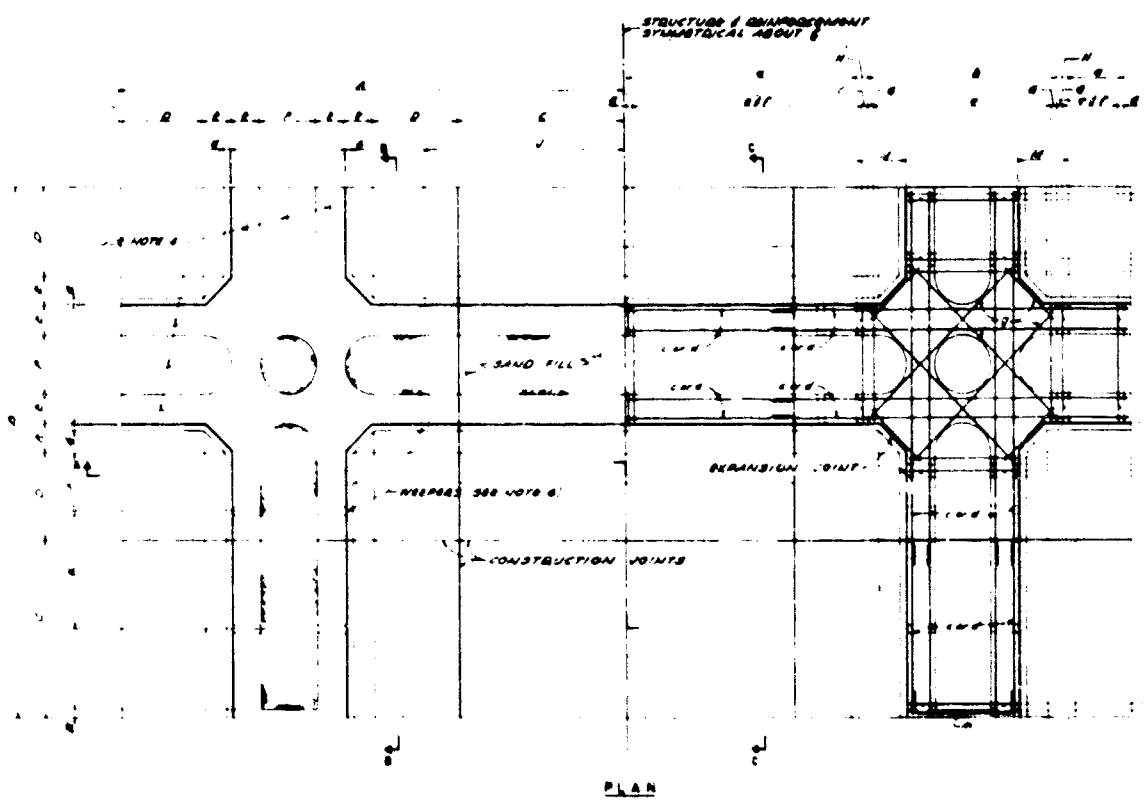
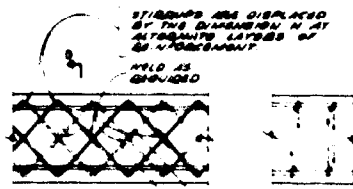
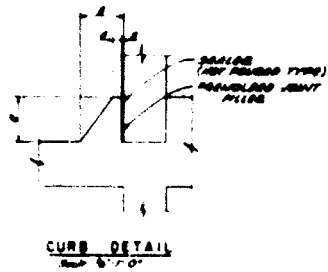
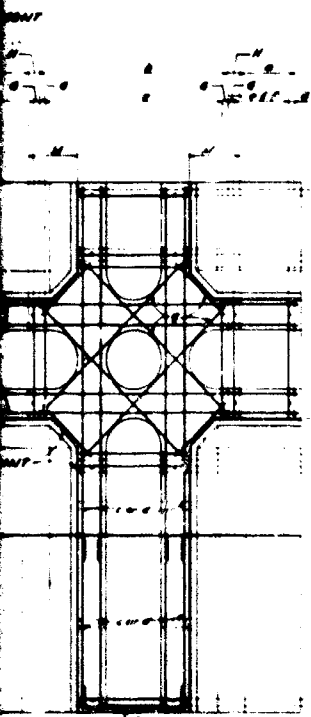


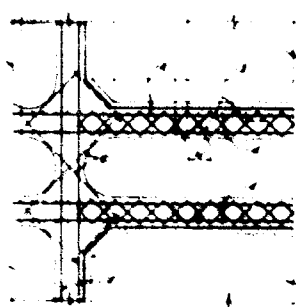
FIGURE 2 - LAYOUT OF FULL SCALE BAY STRUCTURE

A

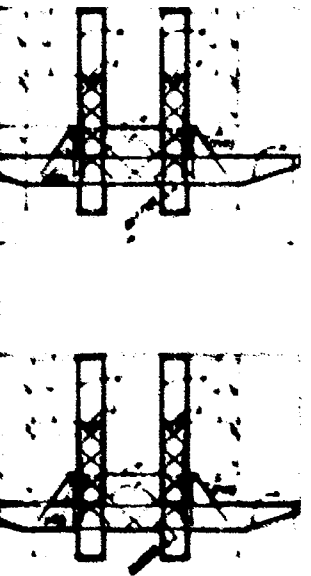


SECTION B-B
STIRRUP DETAILS

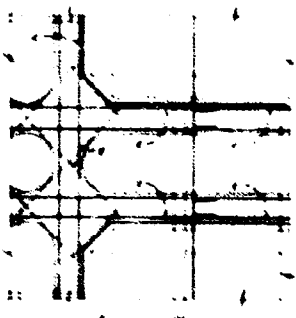
		SCHEDULE				
ITEM	NO. OF SIZE	F.S.	1/3	1/5	1/8	1/10
DIMENSIONS	A	20.0	1.0	1.75	0.8	1.75
	B	20.0	1.0	1.75	0.8	1.75
	C	20.0	1.0	1.75	0.8	1.75
	D	20.0	1.0	1.75	0.8	1.75
	E	20.0	1.0	1.75	0.8	1.75
	F	20.0	1.0	1.75	0.8	1.75
	G	20.0	1.0	1.75	0.8	1.75
	H	20.0	1.0	1.75	0.8	1.75
	I	20.0	1.0	1.75	0.8	1.75
	J	20.0	1.0	1.75	0.8	1.75
	K	20.0	1.0	1.75	0.8	1.75
	L	20.0	1.0	1.75	0.8	1.75
	M	20.0	1.0	1.75	0.8	1.75
	N	20.0	1.0	1.75	0.8	1.75
	REINFORCEMENT	O	20.0	1.0	1.75	0.8
P		20.0	1.0	1.75	0.8	1.75
Q		20.0	1.0	1.75	0.8	1.75
R		20.0	1.0	1.75	0.8	1.75
S		20.0	1.0	1.75	0.8	1.75
T		20.0	1.0	1.75	0.8	1.75
U		20.0	1.0	1.75	0.8	1.75
V		20.0	1.0	1.75	0.8	1.75
W		20.0	1.0	1.75	0.8	1.75
X		20.0	1.0	1.75	0.8	1.75
Y		20.0	1.0	1.75	0.8	1.75
Z		20.0	1.0	1.75	0.8	1.75
AA		20.0	1.0	1.75	0.8	1.75
AB		20.0	1.0	1.75	0.8	1.75



PARTIAL PLAN OF UPPER SECTION OF WALL



SECTION C-C

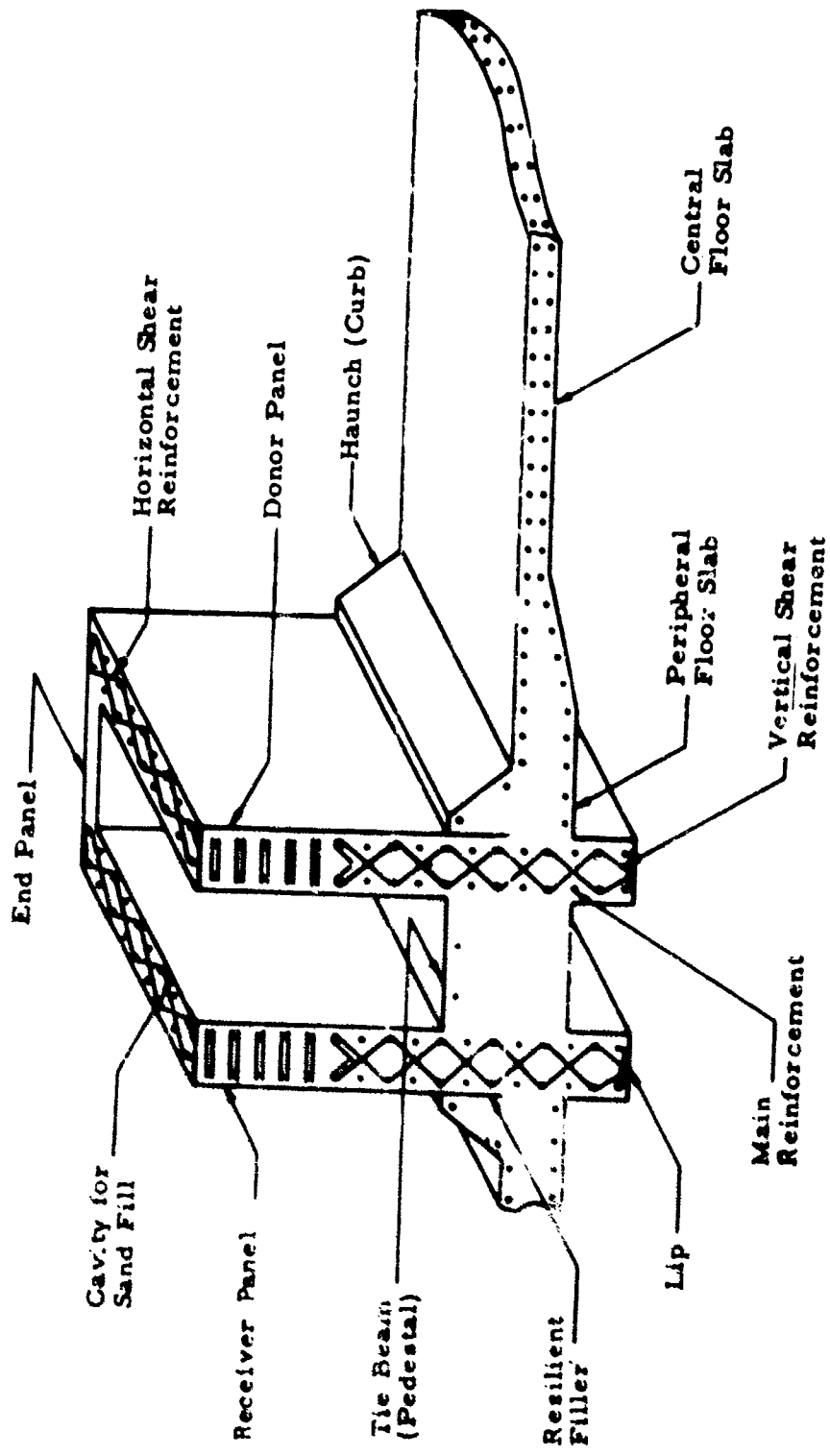


PARTIAL PLAN OF LOWER SECTION OF WALL

- GENERAL NOTES**
1. ALL DIMENSIONS SHALL HAVE UNLESS OTHERWISE SPECIFIED IN THIS DRAWING AND SHALL BE IN FEET AND INCHES.
 2. ALL DIMENSIONS SHALL BE TAKEN FROM THE EXTERIOR FACE OF THE WALL UNLESS OTHERWISE SPECIFIED.
 3. ALL DIMENSIONS SHALL BE TAKEN FROM THE CENTERLINE OF THE WALL UNLESS OTHERWISE SPECIFIED.
 4. ALL DIMENSIONS SHALL BE TAKEN FROM THE FACE OF THE WALL UNLESS OTHERWISE SPECIFIED.
 5. ALL DIMENSIONS SHALL BE TAKEN FROM THE FACE OF THE WALL UNLESS OTHERWISE SPECIFIED.
 6. ALL DIMENSIONS SHALL BE TAKEN FROM THE FACE OF THE WALL UNLESS OTHERWISE SPECIFIED.
 7. ALL DIMENSIONS SHALL BE TAKEN FROM THE FACE OF THE WALL UNLESS OTHERWISE SPECIFIED.
 8. ALL DIMENSIONS SHALL BE TAKEN FROM THE FACE OF THE WALL UNLESS OTHERWISE SPECIFIED.
 9. ALL DIMENSIONS SHALL BE TAKEN FROM THE FACE OF THE WALL UNLESS OTHERWISE SPECIFIED.
 10. ALL DIMENSIONS SHALL BE TAKEN FROM THE FACE OF THE WALL UNLESS OTHERWISE SPECIFIED.

LAYOUT OF FULL SCALE BAY STRUCTURE

B



Note: In-plane flexural reinforcement not shown

FIGURE 3 - CROSS SECTION THROUGH BAY STRUCTURE WALL AND FLOOR SLAB

of 5/8 inch. The lacing in the vertical direction was continuous over approximately the lower half of the wall height whereas the lacing in the horizontal direction was continuous across the full length of the wall. In the peripheral floor slab the reinforcement was identical to that utilized in the walls (1-1/8 inch diameter bars) but in the central floor slab, only minimum reinforcement of 1/2 inch diameter bars was provided.

2-1.2 Model Design

All models used in the test series were designed according to the principles of "Geometrical Scaling" to insure that the model test data can be applied to the prototype. The "Geometrical Scaling Laws" state that there is a linear relationship between the dimensions of the model cubicle and full scale prototype. However, the charge weights of explosives used vary as the cube root of the scale factor. A more detailed discussion of the principles of "Geometric Scaling" is presented in Appendix A. Theoretically, all structural parameters of a model should scale in relation to those of its prototype structure. However, because different materials are used in the model than in the full scale structure, exact scaling seldom can be achieved. The effects of these differences depend on the structure's response (stresses and strains) to the applied loads; that is, in a structural arrangement where the tension stresses are significant, the material differences affecting this type of action will be important in the model design. However, for models where the loads produce primarily compression, the differences in material affecting the tensile strength require less consideration.

Because the concrete and reinforcement used in model construction can be placed with 1/32 inch and 1/16 inch of the required dimensions, respectively, the minimum size model considered for use in the Bay Structure Test Series was 1/10 scale (Figure 2). Although models of the bay structure whose sizes are smaller than 1/10 scale could have been fabricated without difficulty, the reduced dimensions associated with the smaller models in combination with a slight misplacement of the explosive may have produced blast loads which were significantly different from those scaled from the prototype. The larger models provided more flexibility for locating the explosives, and therefore, greater reliability in the test results. Also, because of the handling problems which occurred during construction, the cost of fabrication of the smaller cubicle models probably would have been in the order of, or greater than, that of the 1/10 scale model.

The properties of the reinforcement, other than the spacing, needed major adjustments in the design. In the prototype and larger scale model (1/3 scale), the reinforcement consisted of standard ductile reinforcing bars which were commercially available. However, models smaller than 1/3 scale, the use of ductile steel wire was required to simulate the other physical (diameter and area) and mechanical (strength and ductility) properties of the reinforcing steel in the prototype structure.

Most wire sizes were available to scale the physical characteristics of the reinforcing bars for 1/10 scale models and larger. However, because the available steel wire was cold drawn, and therefore, brittle, adjustments of the wire properties to simulate the mechanical properties of the hot rolled reinforcement of the larger models had to be accomplished by annealing the wire.

As can be seen from Table 1, all dimensions of the bay structure models were scaled in accordance with the General Scaling Laws (Appendix A) whereas, except for the spacing and diameter of the main reinforcement in the 1/10 scale model, all physical properties of the reinforcement in the models were scaled within 10% of those of the main steel in the full scale structure. In the case of the 1/10 scale model, scaling of the area of the reinforcement was achieved with 4% of that of the prototype structure reinforcing steel.

Because the annealed wire used in the model construction was available before the test series was conceived, exact scaling between the mechanical properties of the reinforcement in the three smaller models and the prototype structure could not be fully achieved. The strength of the wire used in the three smaller models exceeded the strength of the reinforcing bars used in the 1/3 scale and full scale structures. However, this increased strength was partially offset by the reduced ductility of the wire. It should be noted that the tensile tests of both the reinforcing bars and wire were performed using an 8-inch specimen length. If the length of wire used for the tensile tests had been scaled according to model size, then the percent elongations recorded for the wire would have been larger than those given in Table 1 resulting in a closer comparison between the potential energy of the models and the prototype. Even though the variations in the mechanical properties of the various test structures were slight, these differences were evident in the results of the individual tests which will be explained later in this report.

The ultimate strength of the concrete in all four models and the full scale structure was within 10%. For the type of structure considered, where the major portion of the shear strength was afforded by the lacing bars and the compression forces were resisted by the compression reinforcement, this degree of duplication of the concrete strength of the individual structures was considered adequate. On the other hand, the concrete aggregate in the smaller scale models (1/8 and 1/10 scale) generally consisted of sand whose gradation, strength and shape did not necessarily simulate the crushed stone (coarse aggregate) of the prototype structure. Also, the sand (fine aggregate) used in the concrete mix of the full scale structure could not be simulated for the smaller models. As will be shown, this variation in the concrete components did not produce a significant variance in those test results where the concrete response was the controlling factor.

TABLE 1 - COMPARISON OF SCALED PROPERTIES OF BAY ST
TEST SERIES

UNIT	FULL-SCALE UNIT	ONE-THIRD-SCALE		ONE-FIFTH-SCALE	
		UNIT	S.F.	UNIT	S.F.
1. Charge Weight (lbs.)					
a. Test Series 1	2260	75	0.320	16	0.192
b. Test Series 2	3390	112.5	0.333	24	0.192
c. Test Series 3	5000	112.5	(4)	40	0.200
d. Test Series 4	7500	-		-	-
2. Cell Dimension (1)	40'x20'x10'	13'4"x6'8"x3'4"	0.333	8'x4'x2'	0.200
3. Thickness (in)(2)	24 [48]	8 [16]	6.333	$4\frac{13}{16}$ [$9\frac{5}{8}$]	0.200
4. Flexure Reinforcement					
a. Type	ASTM A432	ASTM-A432	-	Annealed Wire	-
b. Size	#9	#3	-	4g	-
c. Spacing (in.)	10	3.125	0.300	2	0.200
d. Diameter (in.)	1.128	0.375	0.333	0.234	0.207
e. Area (in ² /ft)	1.2	0.425	0.354	0.026	0.214
5. Stress (psi)					
a. Yield, f_y	73,700	73,100		100,000	
b. Ultimate, f_u	108,700	107,600		126,000	
6. Ductility (3)	17.3	(5)		9.3	
7. Bond	Laps	Continuous Bars		Continuous Bars	
8. Concrete Strength, f'_c , (PSI)	4,940	3,240		5550	

- (1) Feet and inches
(2) Number in [] indicate thickness of sand fill.
(3) Percent Elongation of 8 in. Specimen.
(4) Location of charge adjusted to simulate blast load.
(5) Data not available.
(6) Straight bars
(7) Data not reliable.

1 - COMPARISON OF SCALED PROPERTIES OF BAY STRUCTURE
TEST SERIES

ONE-THIRD-SCALE		ONE-FIFTH-SCALE		ONE-EIGHTH-SCALE		ONE-TENTH-SCALE	
	S.F.	UNIT	S.F.	UNIT	S.F.	UNIT	S.F.
	0.320	16	0.192	4	0.121	2.00	0.096
	0.333	24	0.192	6	0.121	3.24	0.101
	(4)	40	0.200	10	0.125	4.24	0.095
		-	-	15	0.125	-	-
3'4"	0.333	8'x4'x2'	0.200	5'x2'-6"x1'3"	0.125	4'x2'x1'	0.100
	6.333	$4\frac{13}{16}$ [$\frac{5}{8}$]	0.200	3 [6]	0.125	$\frac{7}{16}$ [$\frac{3}{4}$]	0.100
32	-	Annealed Wire	-	Annealed Wire	-	Annealed Wire	-
	-	4g	-	9-1/2g	-	10-1/2g	-
	0.300	2	0.200	1.25	0.125	1.25	0.125
	0.333	0.234	0.207	0.143	0.127	0.127	0.113
	0.354	0.026	0.214	0.151	0.121	0.013	0.104
	73,100		100,000		91,300		80,900
	107,600		126,000		100,000		90,800
	(5)		9.3		(7)		7.3
Knucous Bars		Continuous Bars		Continuous Bars		Continuous Bars	
	5,240		5550		5670		5840

2-1.3 Model Construction

The 1/5 scale and larger cubicles of the Bay Structure Test Series were constructed at the test site. The smaller (1/8 and 1/10 scale) models were built in a laboratory workshop and then shipped to the test site. Because of the inherent strength of the cubicle, transportation of the smaller models did not create a problem. A sufficiently strong pallet was designed using steel beams which allowed for raising and lowering of the model as required. The strong back and rigging system for moving the model was fabricated prior to construction of the model.

Unique problems of placing concrete were encountered in the construction of the smaller reinforced concrete models. The relatively large quantities of flexural reinforcement, the presence of lacing, and the unique detailing of the steel (Figure 4) required to develop the full capacity of the structure, minimized the space available for placement of the concrete. Fortunately, however, because of the interlocking of the flexural and lacing reinforcement which produced a rigid assembly (Figure 3), the concrete could be vibrated to the bottom of the walls merely by vibrating the top of the reinforcement assembly. In addition, by placing the vibrators against the exterior surfaces of the wall forms (1/4-inch plywood) and beneath the floor forms, complete vibration of the concrete was achieved without honeycombs. In the case of the larger models, the larger spacing of the reinforcement in these structures permitted the passage of vibrators down through the steel, which eliminated the need for consolidating the concrete by vibrating the reinforcement assembly.

As mentioned, the properties of the reinforcement in the models must be similar to those used in the prototype structure. For the cubicle model sizes tested, the reinforcement used in the 1/3 scale model bay structure was commercially available and had similitude with that used in the full scale structure. However, in the cubicles smaller than 1/3 scale, special annealed wire was used to produce similitude between the reinforcement of the models and that of the prototype. This wire was shipped in coils and required straightening before being used in the model construction. Two straightening methods were developed and used without significantly changing the properties of the annealed wire. The first method (used in the construction of the two small models) consisted of cutting the coiled wire to desired lengths and then stretching it in a universal testing machine. Care was taken to only slightly exceed the elastic limit of the wire. The second method consisted of passing the wire through a die and around a wheel (Figure 5). The die and wheel were so placed as to produce a reverse curvature in the wire. However, for the models considered, where the reinforcing steel was designed to attain inelastic deformations including the strain hardening region, this change in the elastic properties had only negligible effects in altering the overall potential energy of the structure to resist the applied blast loads.

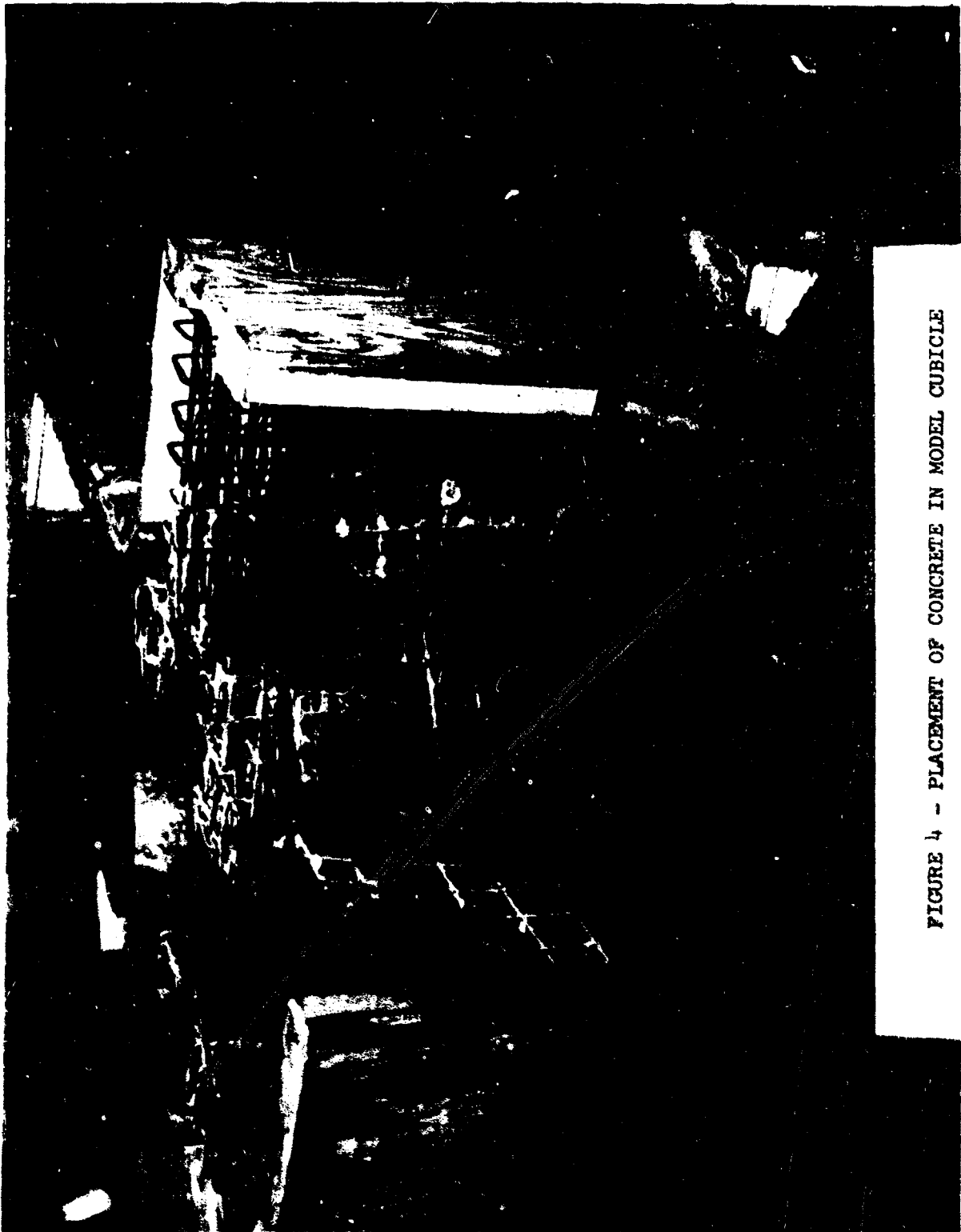


FIGURE 4 - PLACEMENT OF CONCRETE IN MODEL CUBICLE

NOT REPRODUCIBLE

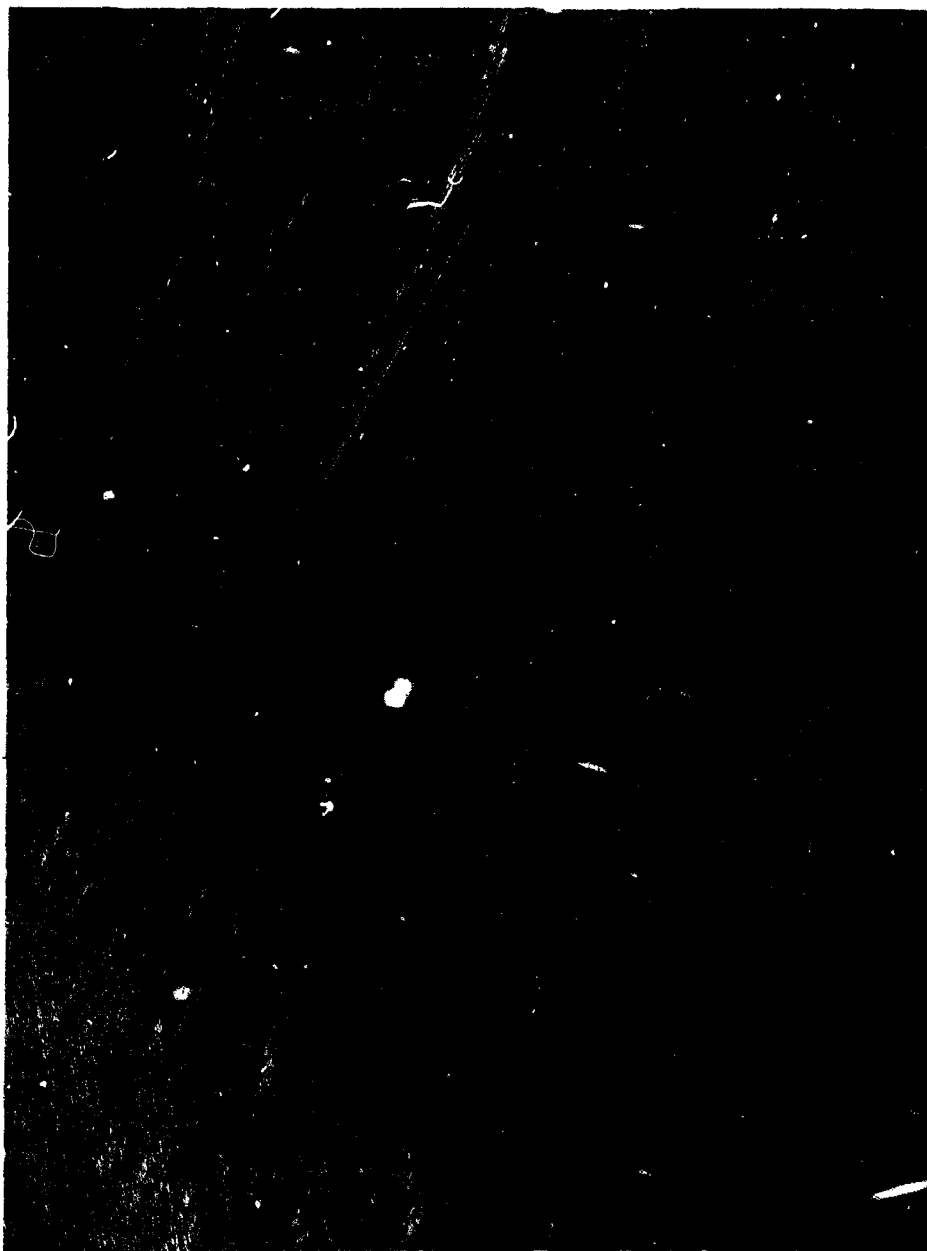


FIGURE 5 - STRAIGHTENING OF COILED ANNEALED WIRE

In addition, it was necessary to develop a different method for bending the reinforcing bars and wire than used for the lacing steel. For the heavier bars of the full scale structure, a series of dies were manufactured to give the correct bends. One die was fixed in place while the other die was attached to a hydraulic jack (Figure 6). The straight bars were then placed between the stationary die and the movable die and crimped by the action of the movable die. A similar method was used for the wire in the smaller models. In this case the crimping was achieved by hand rather than by hydraulic jack (Figure 6).

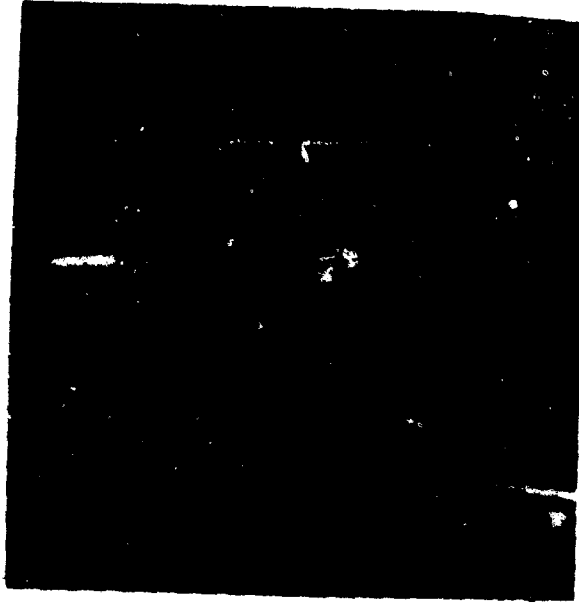
In the construction of the two small scale cubicles, the reinforcement for the individual walls of each cubicle was assembled in the shop (Figure 7). After the walls were erected, the floor reinforcement was threaded through the wall sections. In this case, all the reinforcement for the entire model was in place before any concrete was placed. The two larger models on the other hand were constructed using ordinary construction methods.

2-1.4 Test Site

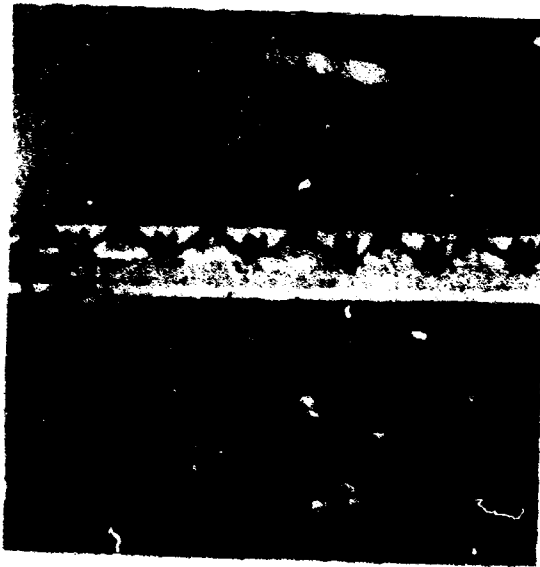
Both the small and large models of the reinforced concrete cubicles of the Bay Structure Test Series were tested in the field because of the relatively large quantities of explosives required in these tests. In addition, the possibility of the occurrence of high velocity concrete fragments predetermined open air testing. Provisions were made to prepare the site for the model tests so that they would simulate the site conditions of the prototype tests.

The 1/10 scale model, which was the initial structure tested, was placed on lightly compacted fill (Figure 8) used to level the site area before the test. The final results of this test indicated that the soft soil condition had a contributory effect on the final failure of the structure.

Based on the results of the 1/10 scale model test, the 1/3 and 1/5 scale structures were tested at another site where a more stable subgrade existed. Also, the use of the alternate site was required because of the larger explosive quantities involved in these tests. The substrata at the new site consisted of a rock ledge situated approximately two feet below the ground surface (Figure 8) and an overburden of natural soft top soil. The soil was excavated down to the rock ledge and this resulted in an overexcavation of approximately 8 inches more than that required for the wall footing. The overexcavation was then backfilled and compacted to 90% CE-55 to the depth required for construction. This stabilization of the subgrade appreciably increased the overall capacity of the larger models relative to that of the 1/10 scale structure.



a) HEAVY LACING



b) LIGHT LACING

FIGURE 6 - BENDING METHODS FOR LACING REINFORCEMENT

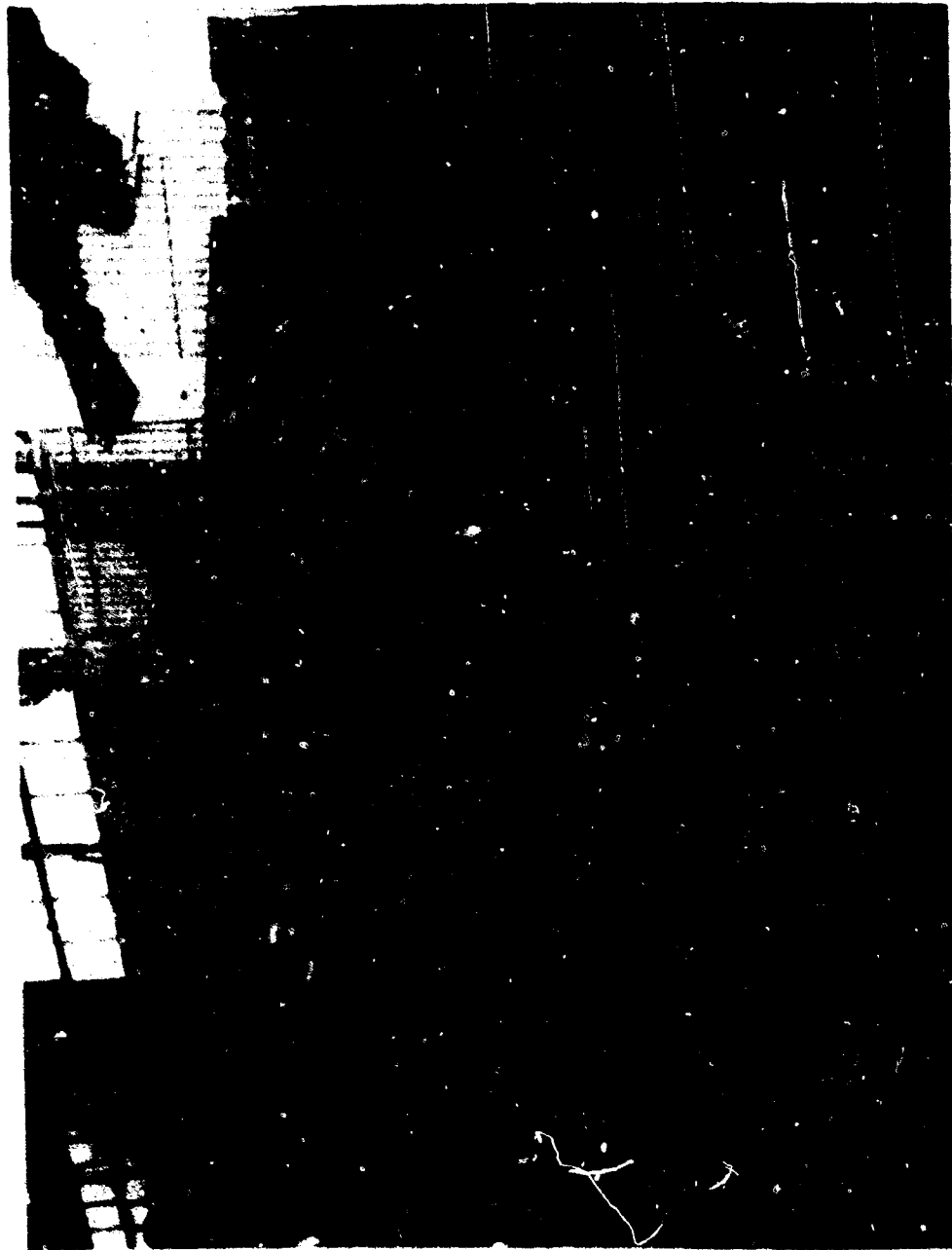
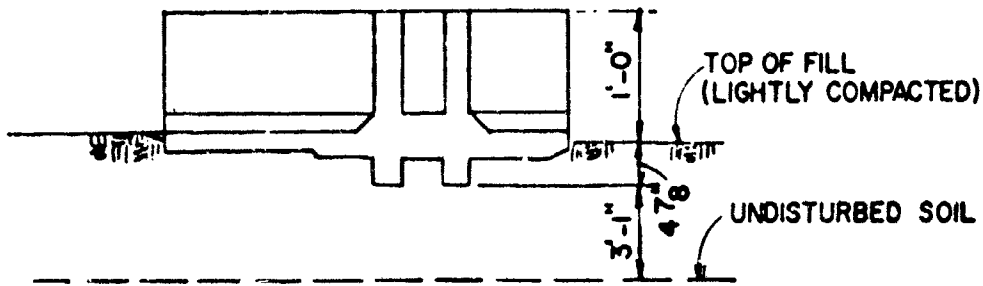
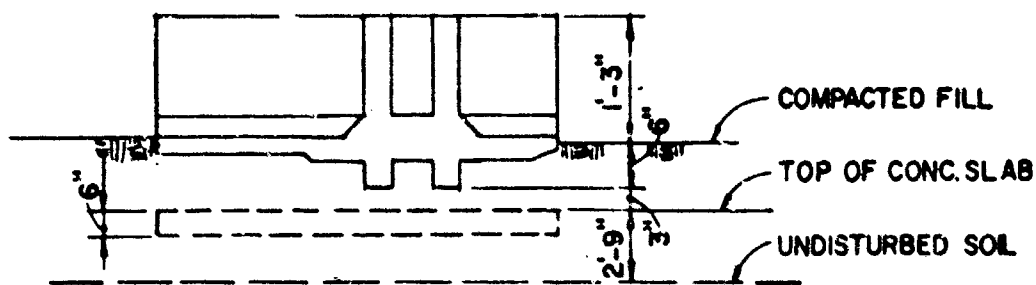


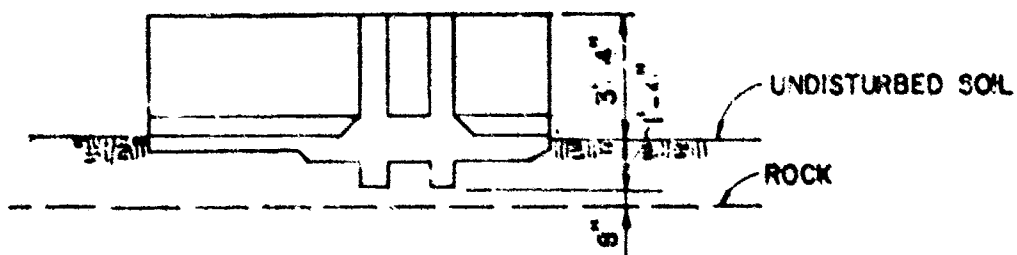
FIGURE 7 - PREASSEMBLY OF WALL REINFORCEMENT



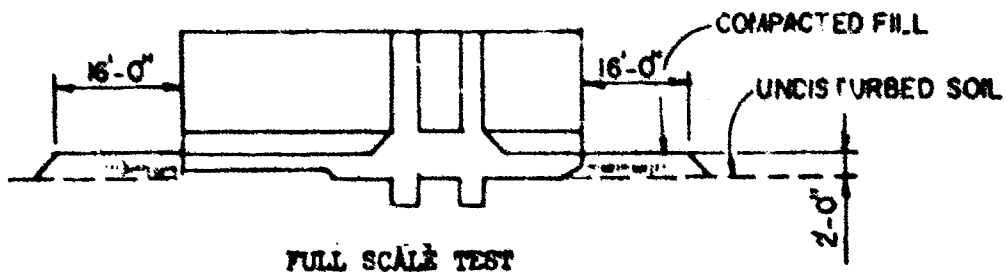
ONE-TENTH SCALE TEST



ONE-EIGHTH SCALE TEST



ONE-FIFTH AND ONE-THIRD SCALE TESTS



FULL SCALE TEST

FIGURE 8 - SOIL CONDITIONS AT TEST SITE FOR BAY STRUCTURE TEST SERIES

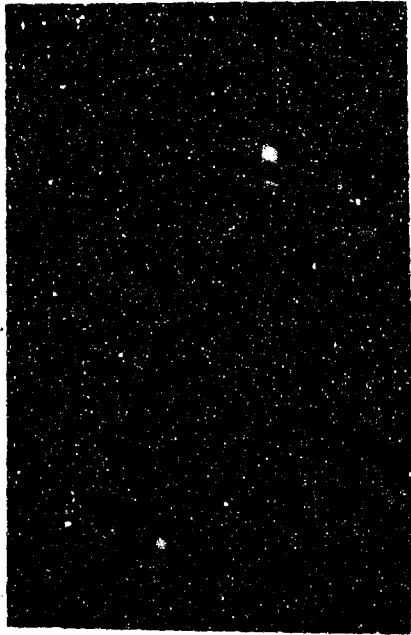
To establish a closer degree of similitude between the subgrades for the various models, the soil strength below the 1/8 scale model was considerably improved. The backfill was excavated to a depth of approximately one foot below the bottom of the floor slab (Figure 8). The sand fill was then compacted and a 6-inch thick lean concrete slab, used to simulate the rock ledge of the larger scale model test, was located at the bottom of the excavation. Sand was compacted on top of the slab to a depth required for positioning the model. As was evident from the test results, the stabilization of the subgrade resulted in a closer degree of similitude between the damage sustained by the larger structures and the 1/8 scale model than was produced in the 1/10 scale model test.

The full scale structure was constructed on the shore of a former lake at the Naval Weapons Center. The soil condition at this lake consisted of a calcium deposit which (until disturbed) was well compacted and dense. The strength of this cemented material was greatly reduced after being disturbed. To maintain a stable substrata similar to that of the 1/5 and 1/3 scale models, the full scale bay structure was built with a minimum of excavation. Here, the bottom of the floor slab was located on the existing ground surface (Figure 8). Excavation was required only for the wall footings. Lean concrete rather than soil was used as backfill around the footings to simulate the density of the undisturbed soil below the floor slab. Because the top of the floor slab of each model was placed flush with the ground surface, compacted fill had to be placed adjacent to the edges of the floor slab of the full scale structure. The purpose of the backfill was to prevent excessive absorption of the blast energy by sliding of the structure which in turn would affect the similitude between the models and the prototype.

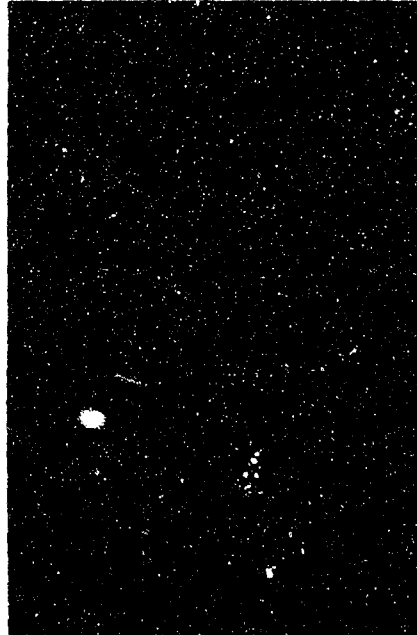
2-1.5 Explosive Charges

All five structures were tested twice under similar conditions, with quantities of explosives equivalent to 2,000 and 3,000 lbs. of Composition B in the first and second rounds, respectively. Except for the second round of the 1/10 scale model test, the explosives used in each test of each structure in the first two rounds were single spherical charges. The second round of the 1/10 scale model test utilized three spherical charges; the sum total of their weights was slightly greater than the equivalent weight of explosives used in the second test of other structures. Each charge was located at the geometric center of the structure. The typical pre-shot arrangement of each test is illustrated by the pre-shot test setup of the scaled structures (Figure 9) and full scale structure (Figure 10).

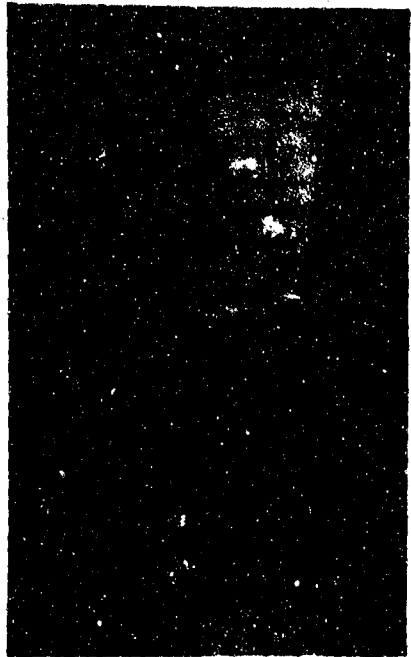
Except for the 1/3 and full scale structure tests, the explosives used in the individual tests of the third round were equivalent to 5,000 lbs. of Composition B. The quantity of explosives



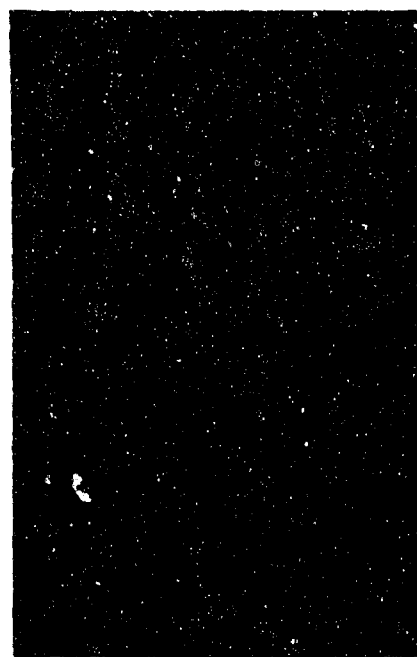
ONE - EIGHTH SCALE



ONE-TENTH SCALE



ONE - THIRD SCALE



ONE-FIFTH SCALE

FIGURE 9 - PRE-SHOT TEST SETUP FOR MODEL STRUCTURES

FIGURE 10 - PRE-SHOT TEST SET-UP FOR FULL SCALE BAY



utilized in the third test of the 1/3 scale structure was equal to 112.5 lbs. of Composition B (equivalent to 3,000 lbs. full scale) which was the maximum quantity of explosives permitted to be detonated at the test site. However, to simulate the blast loads acting on the back wall of the structure (in terms of impulse) which would be produced by the scaled equivalent of 5,000 lbs. of explosives, the 112.5 lb. charge was moved closer to the back wall. The explosives used in the third round of the full scale structure consisted of 100-50 lb. units of TNT. Each unit was contained in a light aluminum metal container. The containers were stacked in the shape of a square on the floor slab and at the center of the cell.

Only the 1/8 scale model and the prototype structure were tested in the fourth round because of the degree of damage after the third round. The equivalent weight of explosives used in each test was 7,500 lbs. A spherically-shaped charge of Composition B was suspended at the center of the bay used in the model test. In the full scale test 150-50 lb. containers stacked in a manner used in the third round were utilized.

Table 2 lists the charge properties, including the type, weight, location relative to the back wall (scaled distance) and full scale equivalent weight for each round of tests for each structure.

2-1.6 Instrumentation and Test Measurements

Pressure, deflection, and strain gages, and photographic coverage were the principal instruments used to record the physical state of the cubicle before, during and after the completion of each individual test. Table 3 lists the type and number of instruments used and the number which functioned during the test. A description of the physical and electronic measurements performed during each test follows.

Electronic Pressure Gages--Blast pressure measurements were made with Ballistic Research Laboratories' electronic pressure gages during the first three tests of the full scale test series at China Lake. Seven gages were placed at various distances from the outside walls of the cubicle to determine the blast pressures acting on the ground surface exterior of the test structure. The location of the gages varied from 90-1100 feet from the center of the donor cell which corresponded to estimated peak pressure levels of 30 and 0.4 psi, respectively. All gages were mounted flush with the ground surface in order that the side-on pressure produced by the leakage of the blast pressures over, around and through the structure to the exterior could be recorded. The location of these gages is shown in Table 4.

Electronic Deflection Gages--Electronic deflection gages (Figures 11 and 12) were used to determine the time-history movement of the walls of the 1/5, 1/3 and full scale structures. The deflection gages were linear displacement transducers which operate on the principle

Table 2 - CHARGE WEIGHT PROPERTIES

Structure	Round No.	Charge Properties			
		Type	Charge Wt. Lbs.	Z _A	E.F.S.Wt. Lbs.(1)
1/10 Scale	1	Single	2.0	0.8	2,000
	2	Cluster	3.24	0.675	3,240
	3	Cluster	4.25	0.62	4,250
1/10 Scale	1	Cluster	10.0	0.465	10,000
1/8 Scale	1	Single	4.0	0.79	2,000
	2	Single	6.0	0.69	3,000
	3	Single	10.0	0.58	5,000
	4	Cluster	15.0	0.50	7,500
1/8 Scale ⁽²⁾	1	Single	15.0	0.50	7,500
1/8 Scale ⁽³⁾	1	Single	15.0	0.50	7,500
1/5 Scale	1	Single	16.0	0.785	2,000
	2	Single	24.0	0.688	3,000
	3	Cluster	40.0	0.58	5,000
1/3 Scale	1	Single	75.0	0.775	2,025
	2	Single	112.5	0.680	3,040
	3	Single	112.5	0.530	3,040
Full Scale	1	Single	2,000	0.8	2,000
	2	Single	3,000	0.69	3,000
	3	Boxes	5,000	0.58	5,000
	4	Boxes	7,500	0.50	7,500

- (1) EFSWT. - Equivalent Full Scale Weight
- (2) Modified construction bay
- (3) Bay constructed of single reinforced concrete walls

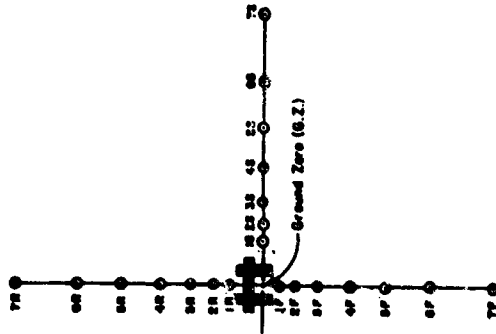
TABLE 3 - ELECTRONIC INSTRUMENTATION

STRUCTURE	ROUND	PRESSURE GAGE		DEFLECT. GAGE		STRAIN GAGE		PHOTOGRAPHY	
		Used	Oper.	Used	Oper.	Used	Oper.	Used	Oper.
One-Tenth Scale	1	-	-	-	-	-	-	4	4
	2	-	-	-	-	-	-	4	4
	3	-	-	-	-	-	-	3	3
One-Eighth Scale	1	-	-	-	-	-	-	3	3
	2	-	-	-	-	-	-	3	3
	3	-	-	-	-	-	-	3	3
	4	-	-	-	-	-	-	3	3
One-Fifth Scale	1	-	-	2	0	6	4	6	2
	2	-	-	2	2	-	-	4	4
	3	-	-	1	1	-	-	4	0
One-Third Scale	1	-	-	2	2	7	0	6	5
	2	-	-	2	2	-	-	4	4
	3	-	-	1	1	-	-	4	4
Full Scale	1	21	19	18	0	-	-	4	4
	2	21	17	17	17	-	-	4	4
	3	21	19	-	-	-	-	4	4
	4	-	-	-	-	-	-	4	4

TABLE 4 - PRESSURE GAGE LAYOUT

No.	GAGE		ROD NO. 1 (W-2260)				ROD NO. 2 (W-3390)				ROD NO. 3 (W-5000)			
	Location	R_c	Z_c	P_{so}	\bar{I}_g	Z_c	P_{so}	\bar{I}_g	Z_c	P_{so}	\bar{I}_g	Z_c	P_{so}	\bar{I}_g
1	P			-	-		-	-		-	-		-	-
	S	90	6.86	17.70	9.50	6.00	21.40	8.96	5.26	20.59	7.60			
	R			16.10	-		-	-		14.65	6.40			
2	P			11.60	9.37		14.15	9.90		15.50	-			
	S	150	11.45	7.90	7.46	10.00	8.97	5.90	8.00	10.37	7.04			
	R			7.20	6.91		7.95	5.56		8.66	4.90			
3	P			5.00	5.68		5.85	5.66		5.19	5.68			
	S	220	17.55	3.10	3.81	15.35	3.58	4.46	13.65	3.93	-			
	R			3.10	3.18		4.27	4.11		5.46	-			
4	P			2.60	3.29		3.65	4.36		-	-			
	S	340	25.95	1.90	2.05	22.70	2.57	3.64	19.90	3.16	4.42			
	R			1.80	2.04		2.29	2.42		2.89	2.81			
5	P			1.10	1.89		1.75	2.80		1.40	3.17			
	S	510	38.90	1.20	2.02	34.00	1.63	2.42	29.90	1.67	2.80			
	R			0.89	1.53		1.50	1.74		1.70	2.14			
6	P			0.75	1.46		1.01	2.05		0.88	2.35			
	S	740	56.50	0.61	1.33	49.40	-	-	43.40	1.02	1.55			
	R			0.73	-		-	-		1.12	1.47			
7	P			0.44	0.93		0.70	1.48		0.65	1.84			
	S	1100	84.10	0.43	-	73.60	0.54	-	64.50	0.62	1.63			
	R			-	-		0.40	0.87		0.48	0.95			

(1) GAGE LAYOUT



(2) NOMENCLATURE

1. Ground Distance from G.Z. (R_c), ft.
2. Sealed Ground Distance from G.Z. (Z_c), ft./lbe.^{1/3}
3. Side-on Pressure (P_{so}), psi
4. Scaled Side-on Impulse (\bar{I}_g), psi-ms/lbe.^{1/3}
5. Charge Weight (W), lbe.

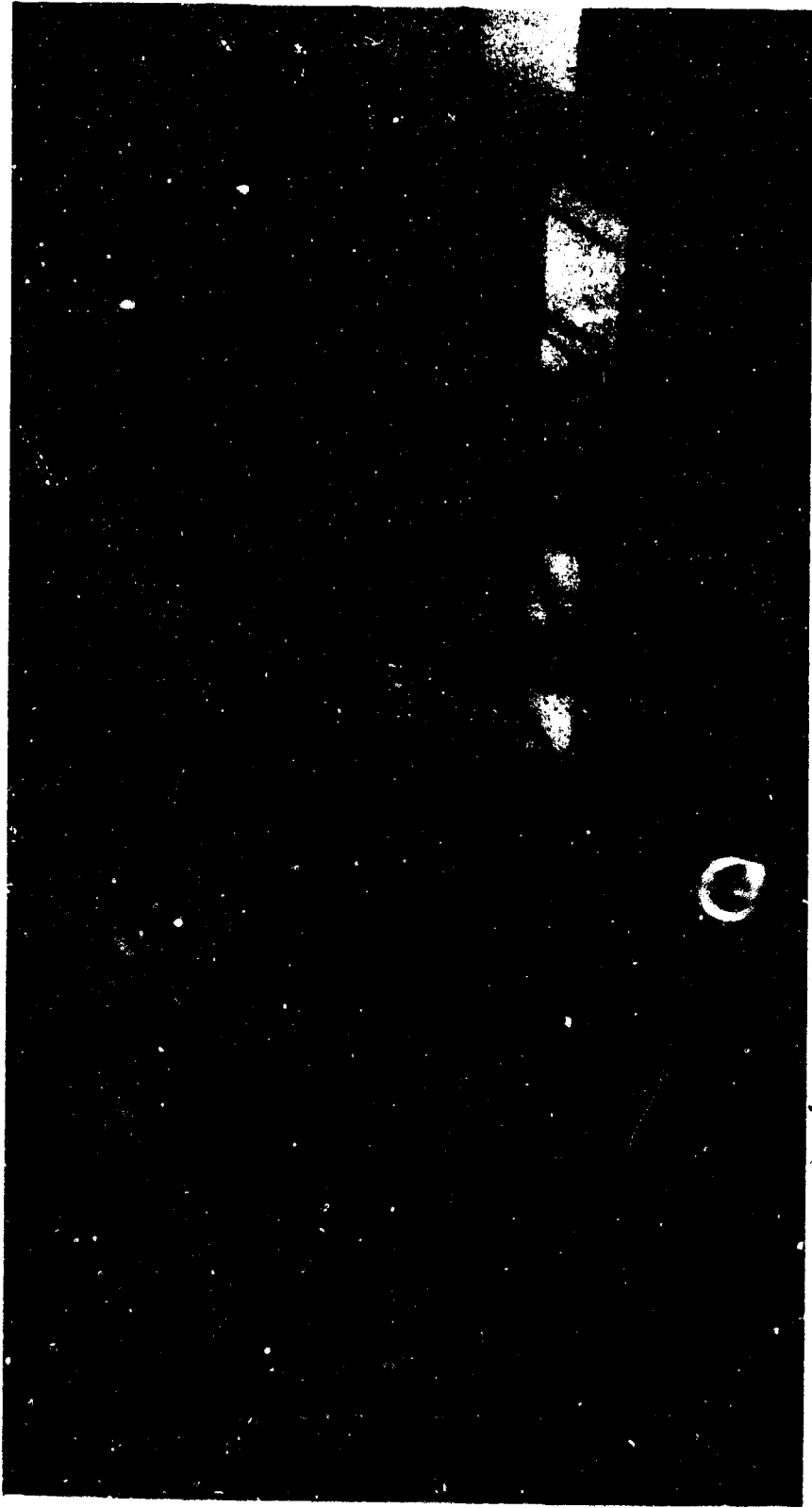


FIGURE 11 - ELECTRONIC DEFLECTION GAGE SETUP FOR WALL



FIGURE 12 - DETAILS OF ELECTRONIC DEFLECTION CAGE

of change in inductance in the coils of a linear differential transformer with changes in position of the core. These gages had either a 6 or 12 inch stroke and were used according to the magnitude of deflection anticipated. Each gage was mounted on the receiver side of each wall. In the full scale structure test, each gage was supported by its mount on the floor slab while in the 1/3 and 1/5 scale tests, the mounts were supported on concrete pedestals each of which was located adjacent to, but not connected to, the floor slab of its corresponding structure. The output of the transducer was recorded as a function of time giving a complete picture of the full scale structure wall deflections relative to the base slab. In the case of the models, the overall movement of the structure vs. time was recorded (Figure 12 shows some typical output of these instruments). The pre-shot and post-shot physical measurements indicated that the soil between the floor slab and pedestals remained elastic during the tests so that the overall movement of the structure contributed very little to the gross movement of the walls. No electronic deflection measurements were taken in the 1/10 or 1/8 scale test series.

Eighteen gages were used in each of the first three rounds of the full scale tests. Deflection measurements included those of both the receiver and donor panels of all three walls. The attachment points for the various gages are shown in Figure 13.

Two deflection gages were used in Rounds 1 and 3 of each 1/3 and 1/5 scale model tests. The gages in each test were located along the centerline and near the top of the back walls. One gage was attached to the donor panel while the other gage was attached to the receiver panel. In Round 3, one gage was attached to the receiver panel of the back wall of each of the two larger models.

Electronic Strain Gages--Strain gages were used to determine the mechanism of dynamic wall failure under explosive loading conditions. The strain gages were cemented directly to reinforcing bars at critical points within the structure before the concrete was poured in the 1/3 and 1/5 scale models. SR-4 post-yield gages were bonded to either the horizontal or vertical reinforcing bars where the development of maximum tension strains in either the side or back walls was anticipated. All gages were electrically shielded to minimize electrical interference from exterior sources. A total of six and seven gages were utilized in the 1/3 and 1/5 scale tests, respectively.

Physical Measurement--Except where structural failure occurred, post-shot permanent deflections of all the walls of each structure were measured before proceeding with the next round of tests. These deflections were obtained by hand measurements. Horizontal and vertical overall structural movements were determined by pre-shot and post-shot surveys of reference markers embedded within the concrete. To more closely define the damage sustained by each structure in each test

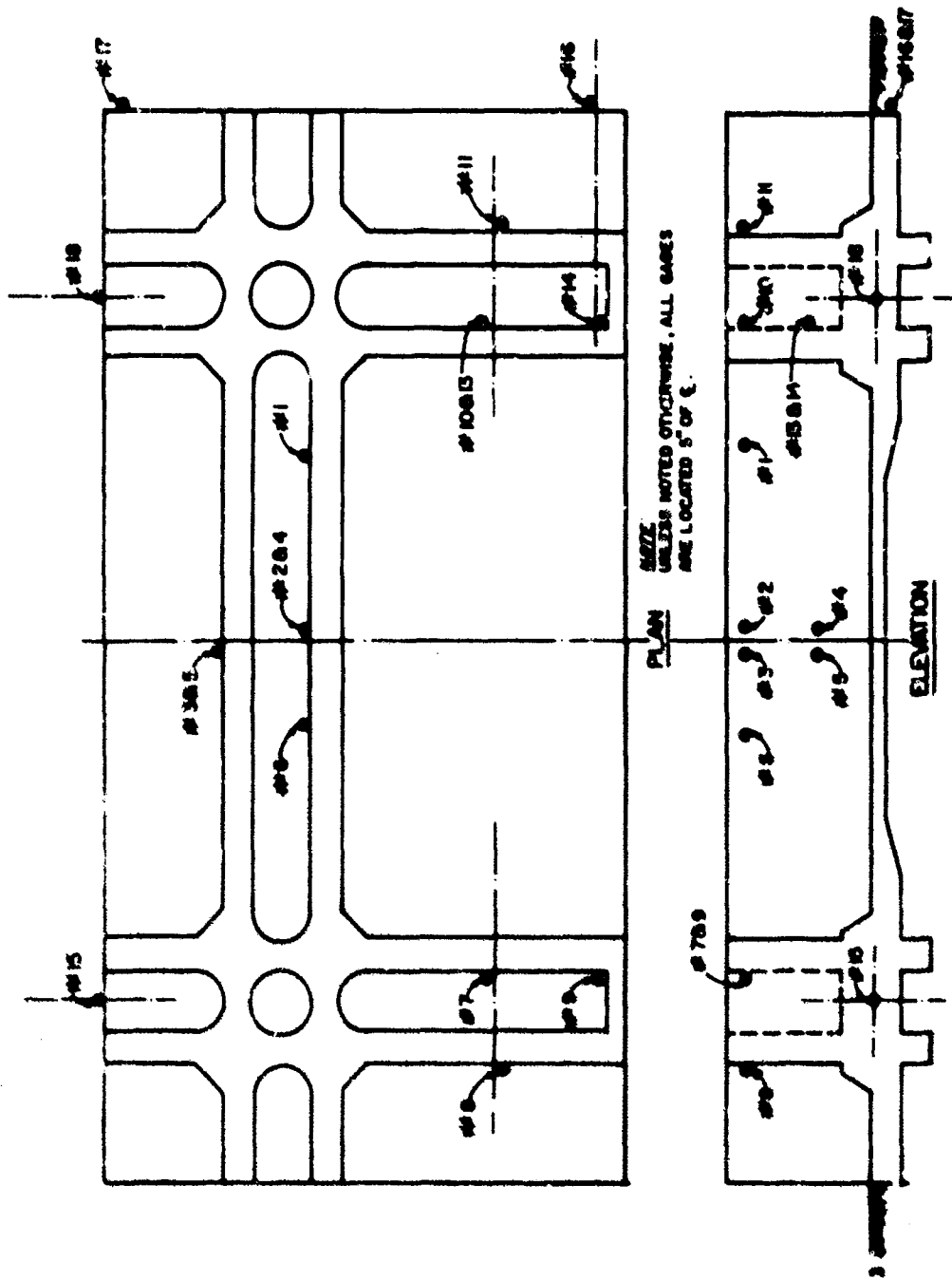


FIGURE 13 -- REFLECTION GAGE LAYOUT (Full Scale Structure)

series, post-shot crack patterns of the walls and floor slab of each structure were made. The patterns indicated the location and size of: concrete cracks, spalling, areas of exposed reinforcement, and areas of reinforcement failure.

Photographic Coverage—Both still and motion pictures were used to record test events. Still photography was used to record the construction phase of the test as well as pre-shot test arrangements and post-shot test results. Motion pictures were used principally to determine the damage characteristics of the test structure including sizes and velocities of fragments and their distribution resulting from the breakup of any portion of the test structure.

Four camera viewing methods were utilized: (1) the shadowgraph method, (2) backboard method (to determine fragment velocities), (3) rear viewing method, and (4) site viewing method. However, all the methods were not necessarily used in every test. The viewing method varied from found to round. Camera layouts and speeds for a typical test such as the 1/10 scale test series are illustrated in Figure 14.

2-2 Discussion of Test Results

2-2.1 Structural Damage

General—Since the scaled explosive equivalent of 2,000 lbs. and approximately 3,000 lbs. of HE were detonated in Rounds 1 and 2 of each model test, the discussion of the results and comparison of structural damage will concentrate on these rounds. Because of the variance of the individual test setups for Rounds 3 and 4, only a limited comparison of the results of these tests can be discussed. Emphasis has been placed on the discussion of the damage sustained by the back-wall since it was the critical element of the structure (Ref. 4). Table 5 is a summary listing the test setup and damage sustained by the back and side walls of each structure in each round of tests.

Round 1—In general, the overall damage sustained by all four models and the full scale structure was about the same. Surface spalling of the donor panel was slightly more severe in the 1/5, 1/3 and full scale structures (Figures 15 and 16) than the small scale structures. This apparently was caused by the failure of the thicker concrete cover over the reinforcement of the two larger models. The increased thickness was produced by accidental slippage of the wall forms during construction. The one-eighth scale model suffered the least damage because the bay was constructed under well controlled conditions in the laboratory. Additionally, the walls of the two larger models and the prototype structure needed patching after removal of the forms. Another contributing factor to the greater spalling of the walls of the larger structures was the greater

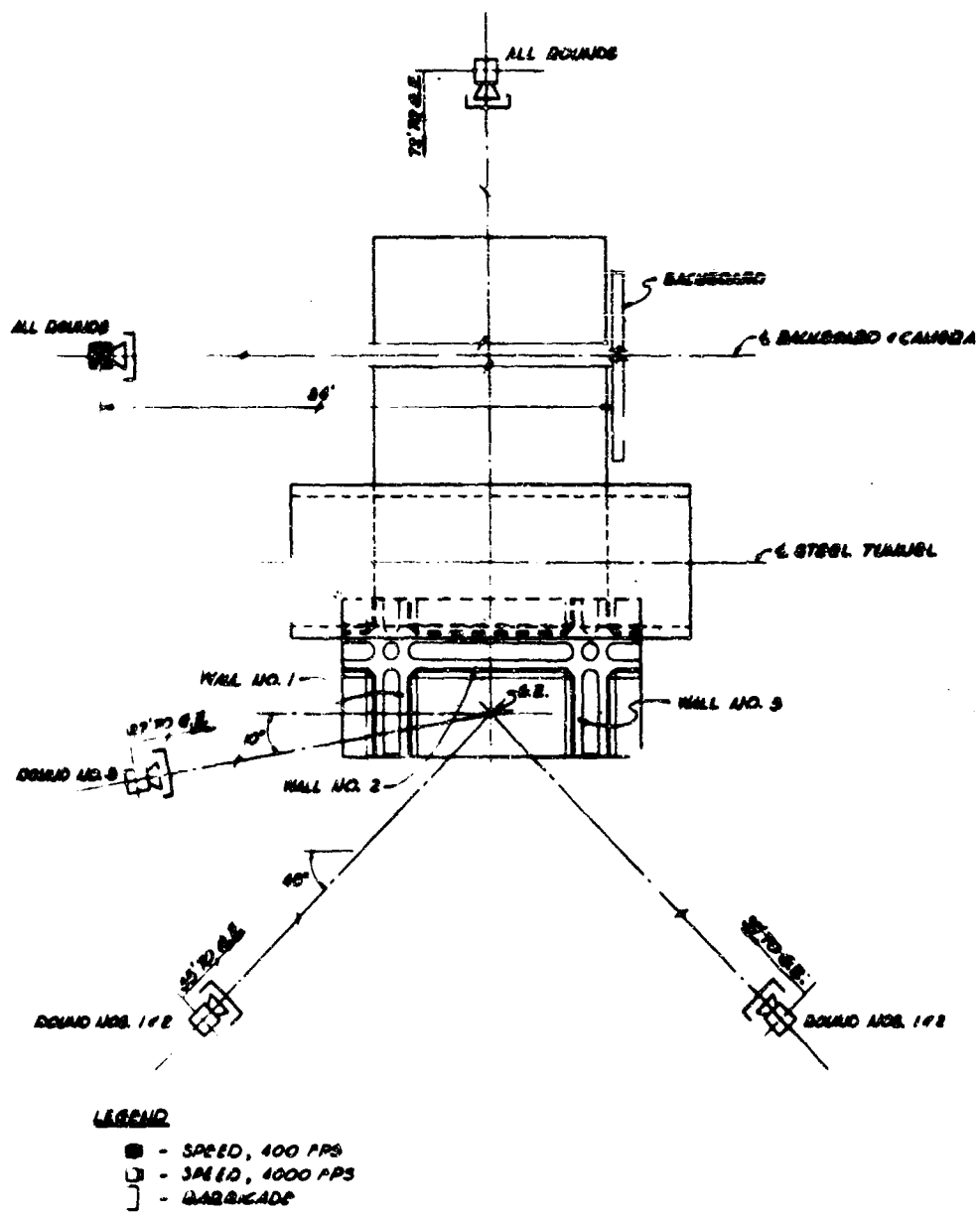


FIGURE 14 - CAMERA LAYOUT (One-Tenth Scale Structure)

TABLE 5 - SUMMARY OF SCALED EXPLOSIVE BAY STRUCTURE TEST

Structure	Rd. No.	Charge Properties			Summary of Results		
		Type	Charge Wt. Lbs.	Z ₄	E.F.S.Wt. Lbs.	Side Walls (RP)	Back Wall (RP)
1/10 Scale	1	Single	2.0	0.8	2,000	Scattered cracks	Light cracking
1/10 Scale	2	Cluster	3.24	0.675	3,240	Light cracking	Heavy cracking, some spalling
1/10 Scale	3	Cluster	4.25	0.62	4,250	Light cracking	Partial destruction (2)
1/10 Scale	4	Cluster	10.0	0.465	10,000	Cracked and sheared at supports	Complete destruction
1/8 Scale	1	Single	4.0	0.79	2,000	No damage	Few scattered cracks
1/8 Scale	2	Single	6.0	0.69	3,000	Few cracks	Light cracking (2)
1/8 Scale	3	Single	10.0	0.58	5,000	Light cracking	Medium damage (2)
1/8 Scale	4	Cluster	15.0	0.50	7,500	Medium damage (2)	Partial destruction (2) (Collapse of panels)
1/8 Scale (1)	1	Single	15.0	0.50	7,500	Heavy damage (2)	Incipient failure
1/8 Scale (3)	1	Single	15.0	0.50	7,500	Heavy damage (2)	Heavy damage (2)
1/5 Scale	1	Single	16.0	0.785	2,000	Few cracks	Light cracking
1/5 Scale	2	Single	24.0	0.688	3,000	Light cracking	Medium damage (2)
1/5 Scale	3	Cluster	40.0	0.58	5,000	Medium damage (2)	Incipient failure (2)
1/3 Scale	1	Single	75.0	0.775	2,025	No damage	Hairline cracks
1/3 Scale	2	Single	112.5	0.680	3,040	Few cracks (damage to end panels)	Few cracks
1/3 Scale	3	Single	112.5	0.520	3,040	Light cracking (heavy damage to end panels)	Light cracking
Full Scale	1	Single	2,000	0.8	2,000	No damage	Hairline cracks
Full Scale	2	Single	3,000	0.69	3,000	Light cracking (heavy damage to end panels)	Minor vertical cracks
Full Scale	3	Boxes	5,000	0.58	5,000	Minor cracks (heavy damage to end panels)	Cracking & spalling (in center)
Full Scale	4	Boxes	7,500	0.50	7,500	Major cracks (heavy damage to end panels)	Partial destruction (2)

ABBREVIATIONS: BW - Back Wall RP - Receiver Panel EFSWT - Equivalent Full Scale Weight
 GLOSSARY: Z₄ - Scaled distance from back wall (ft/lbs^{1/3})

(1) Modified construction bay

(2) Medium damage - Large cracks, surface pitting, some spalling
 Heavy damage - Somewhat less than incipient failure condition
 Partial destruction - Panel breaks up into few large sections
 Total destruction - Panel broken completely producing flying fragments
 Incipient failure - Element on verge of collapse

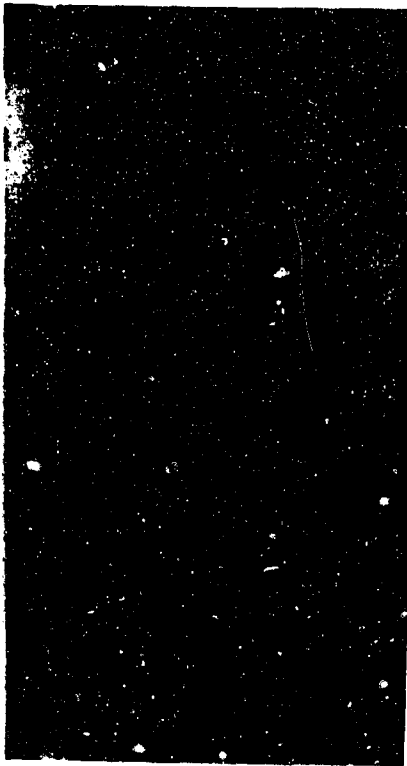
(3) Bay constructed of single reinforced concrete walls



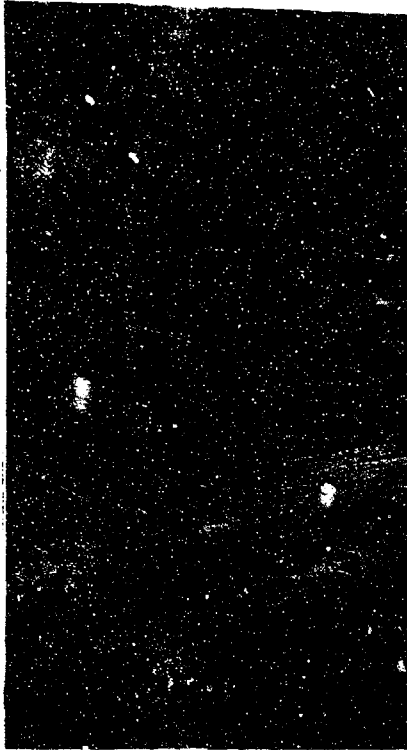
ONE - THIRD SCALE - 75 LBS.



ONE - EIGHTH SCALE - 4.0 LBS.



ONE - FIFTH SCALE - 16 LBS.



ONE - TENTH SCALE - 2.0 LBS.

FIGURE 15--MODEL SCALE TESTS - ROUND 1 - DONOR SIDE
(2000 lb. Explosive Equivalent)



FIGURE 16 - FULL SCALE TEST - ROUND 1 - 2000 LBS. - DONOR SIDE

elastic rebound of their back walls as compared to those of the smaller structures. This was evident by the protrusion of the vertical reinforcement past the back wall of each of the larger structures.

To prevent the vertical steel from buckling outward, the vertical bars should be placed inside the horizontal bars in the lower half of the wall. This follows an important conclusion that the controlling reinforcement should be placed internally of the secondary reinforcement. This principle will be applied in all cubicle designs that follow the Bay Tests.

The damage sustained by the back wall of each model and the full scale structure was similar. The major cracks were tension cracks formed at the supports on the donor side of the wall and at the middle of the wall at the receiver side where vertical cracks were produced. In areas of high compression stresses, the concrete was crushed on both the donor and receiver surfaces of the donor panel.

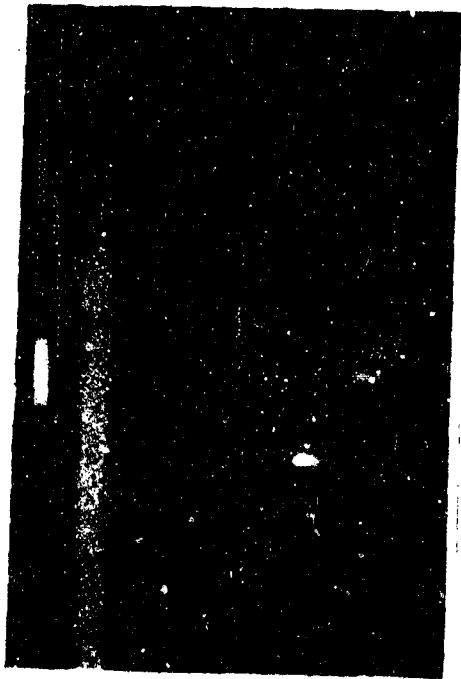
There was virtually no damage to the receiver panel of the back wall of each of the two larger structures (1/5 and 1/3 scale) while vertical cracks were formed near the center of the back wall of both smaller models (1/8 and 1/10 scale) (Figure 17). Both smaller structures were tested on partially compacted fill. These cracks were formed as a result of the vertical settlement of the center of the back wall relative to the sections of the structure where the side walls intersected the back wall. Since the soil stability of the 1/8 scale model was greater than that of the 1/10 scale model, the vertical cracks in the former were less severe. This reduced damage of the 1/8 scale model during the first test appreciably increased its blast-resistant capacity for subsequent tests.

After the first round of tests, the horizontal and vertical reinforcement in the receiver and donor panels of the back wall of all five structures remained intact. There was a minimum of cratering (Figures 15 and 16) of the floor slabs of the test structures. However, the depression in the floor slab of the full scale structure was slightly larger than the depression formed in the model floor slabs. The full scale structure crater was four inches deep and 45 feet in diameter. Figures 18 and 19 illustrate the extent of damage due to cratering in the one-tenth scale structure.

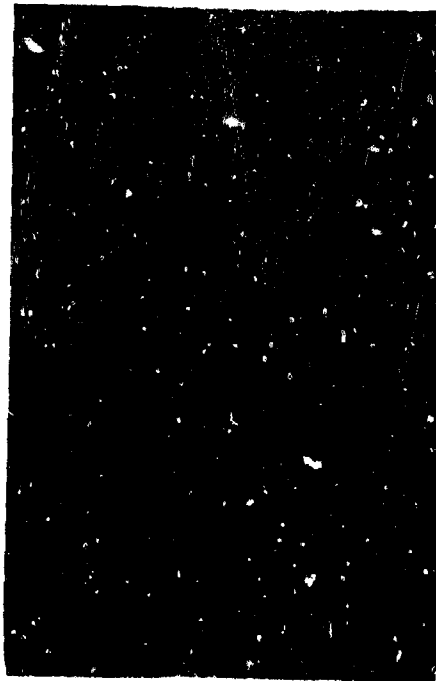
Except for the end panels, which retained the sand fill, the side walls of all test structures suffered little or no damage. Because the control of the placement of the reinforcement in the field-constructed structures was less than that which could be maintained in the laboratory, the damage to the end panels of the two larger models was slightly greater than that of the two smaller models. Post-shot investigations disclosed that the reinforcement in the end panels of the two larger models was not placed in the



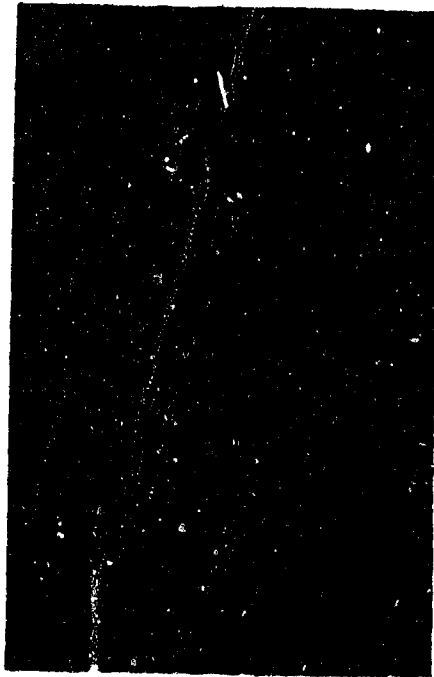
ONE - THIRD SCALE - 75 LBS.



ONE - EIGHTH SCALE - .0 LBS.



ONE - FIFTH SCALE - 16 LBS.



ONE - TENTH SCALE - 2.0 LBS.

FIGURE 17 - MODEL SCALE TESTS - ROUND 1 - RECEIVER SIDE

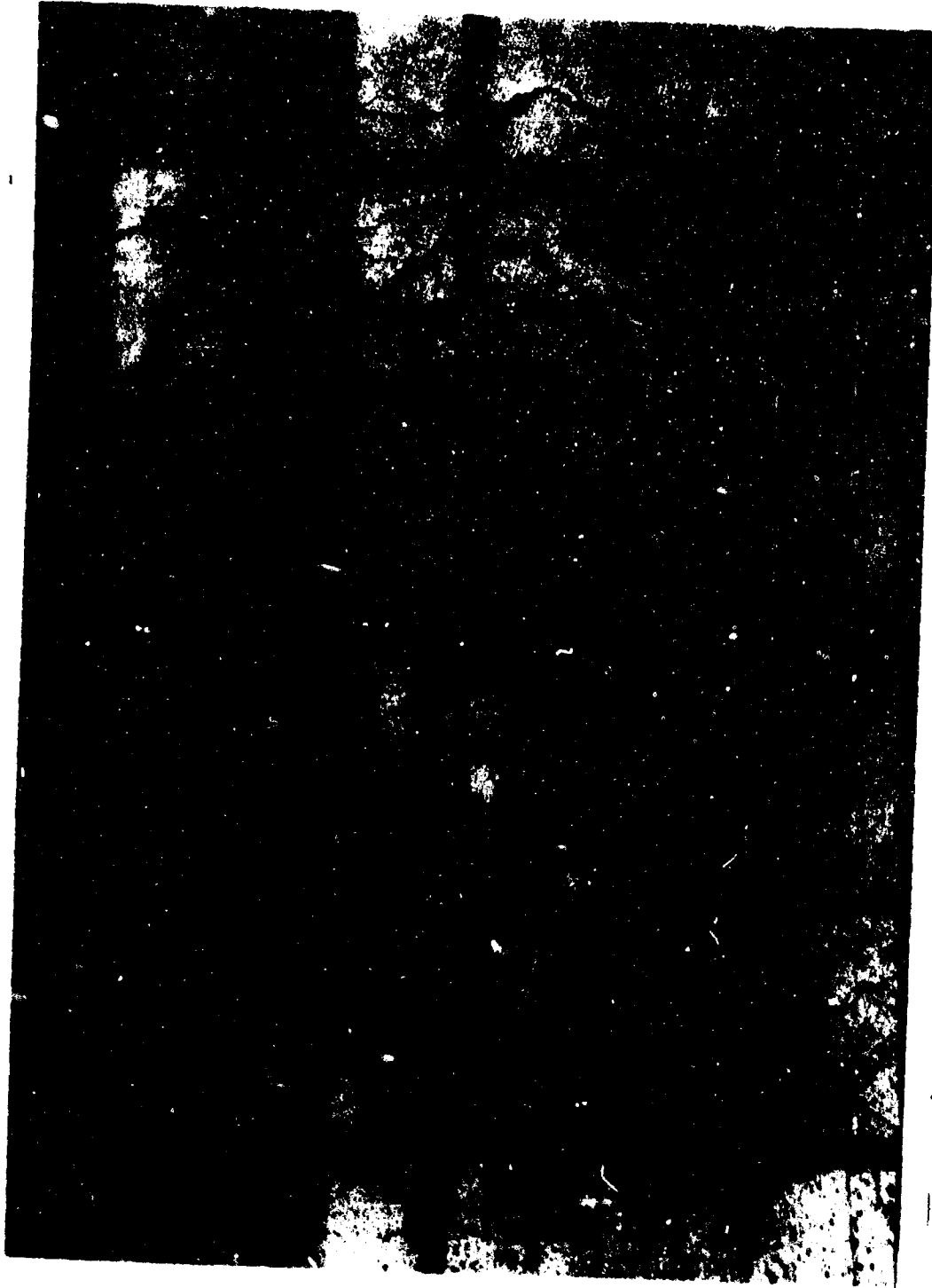


FIGURE 18 - AREA OF MAIN DAMAGE TO FLOOR SLAB - ROUND 1 - 1/10 SCALE

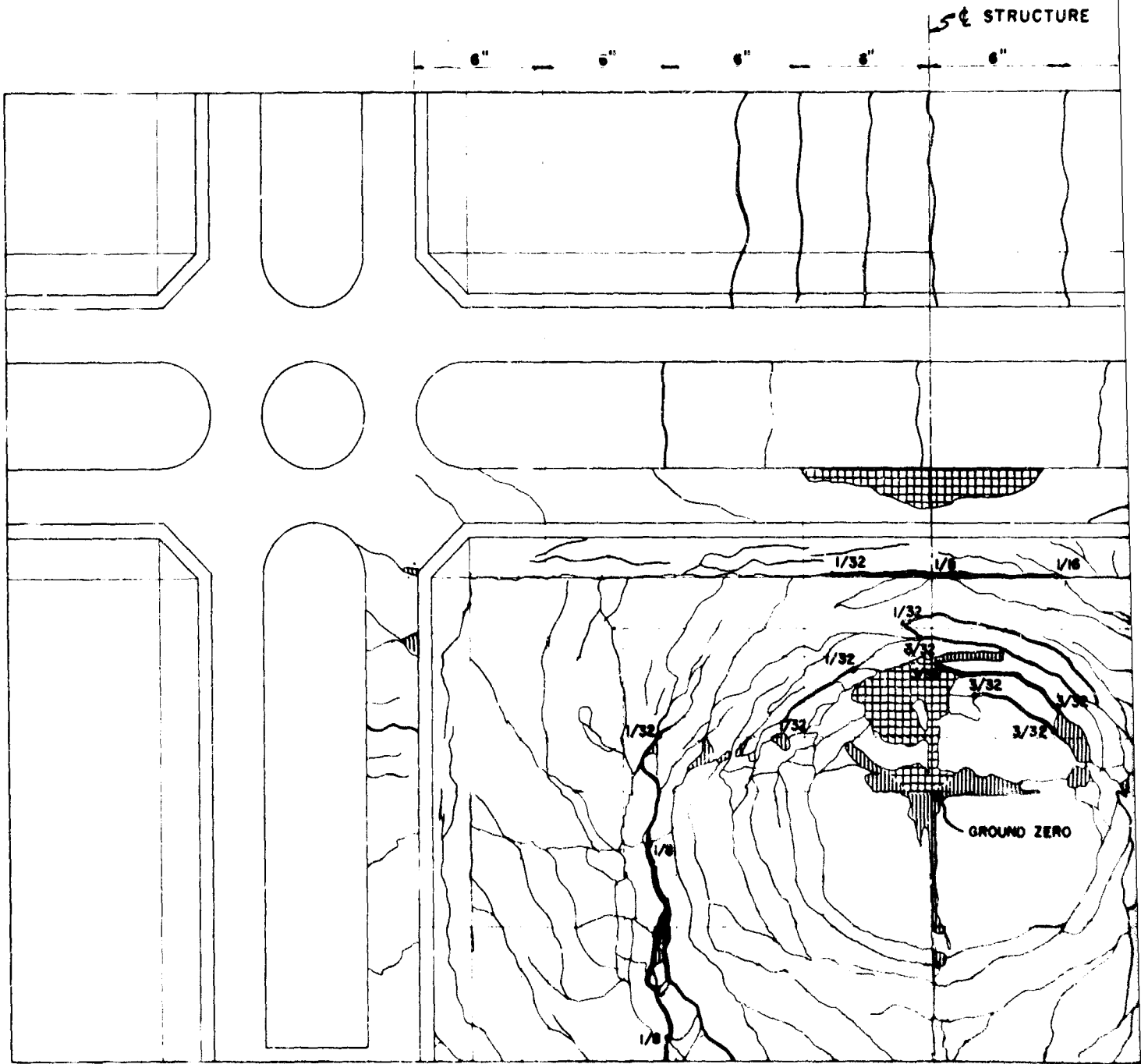
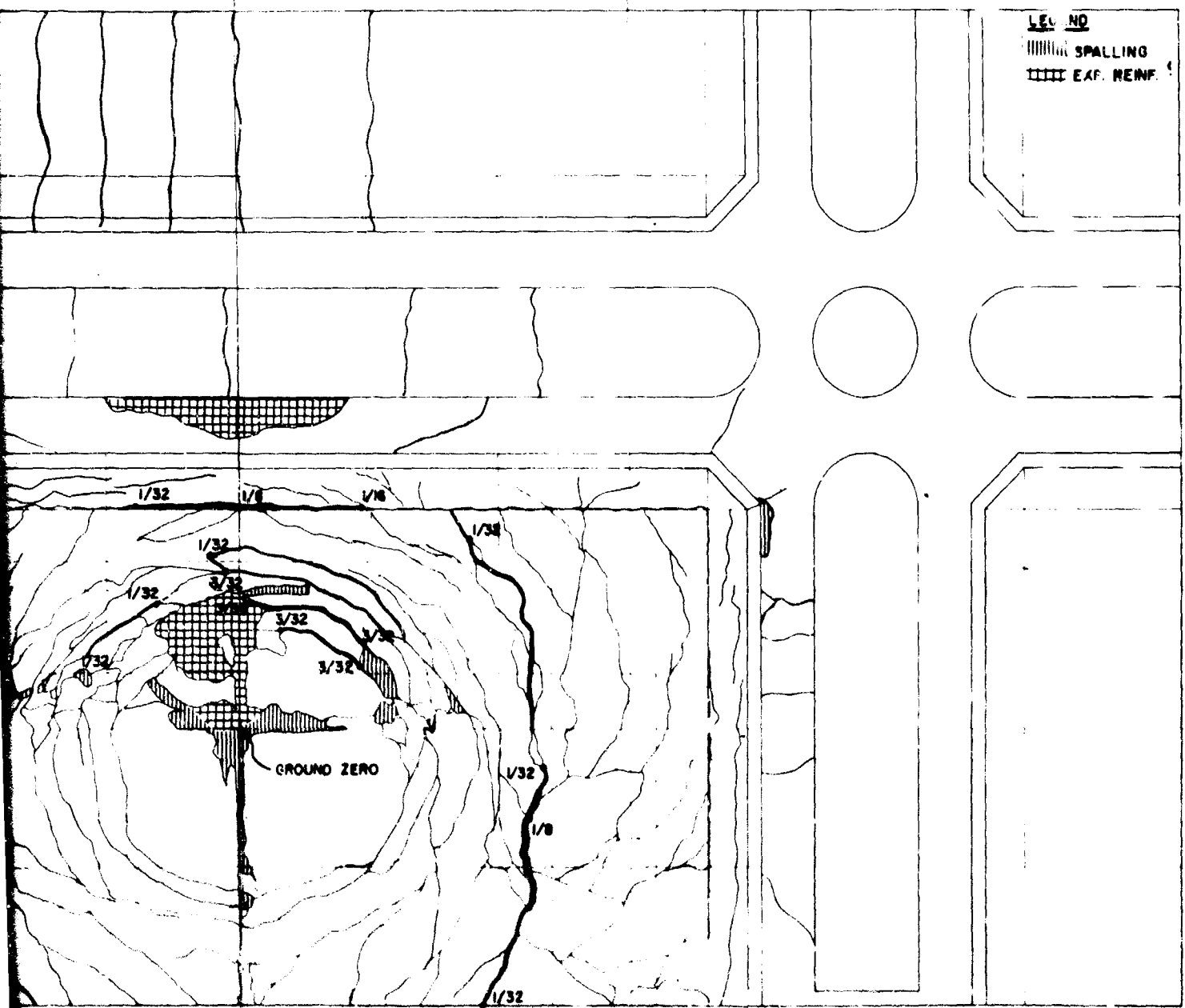


FIGURE 19 - DAMAGE TO STRUCTURE - PLAN VIEW - ROOM

A

STRUCTURE

LEGEND
SPALLING
EXP. REINF.



DAMAGE TO STRUCTURE - PLAN VIEW - ROUND 1 - 1/10 SCALE

B

center of the panels, but located near the interior surfaces, and therefore, providing little capacity against bending in these sections. In the full scale structure (Figure 20) and the two small scale models (Figure 15), more care was taken in the placement of the reinforcement in the end panels, and consequently, less damage occurred.

Round 2--The tension reinforcement in the back wall donor panel failed near the center of the 1/10 scale structure (above the floor slab haunch, Figure 2). The reinforcement in the remainder of the structure and in the other test structures remained intact although a shear plane was formed along each back wall donor panel support near the floor slab. The formation of the shear plane resulted in a reduction of the wall strength equivalent to a failure of the tension reinforcement. The length along the wall where the shear plane was formed in the 1/8 and full scale structures was shorter than those of the other three models. The shear failure of the concrete resulted in the formation of relatively large displacements of the donor panel which, in turn, caused excess scabbing (spalling produced by large straining of the reinforcement and/or displacement of the element). Spalling of the donor surface of each donor panel of the back walls of all structures was quite severe except in the 1/8 scale model where a smaller shear plane was formed (Figure 21).

The vertical cracks in the receiver panel of the back wall of each of the two smaller (1/8 and 1/10 scale) models (Figure 22) were quite large. However, these cracks were less pronounced in the 1/8 scale bay in comparison to those of the 1/10 scale model. Similar, but relatively smaller, cracks also were formed in the other three structures. The vertical cracks extended the full height of the wall while those of the other structures extended to approximately two-thirds of the wall height. Formation of these vertical fissures eventually produced failure of those structures.

The craters formed in the floor slabs in all test structures during the first round of tests were enlarged during the second round. With the exception of the 1/8 scale model, the crater penetrated the depth of each floor slab and displaced the subgrade.

The side walls of the models and the prototype structure suffered appreciably more damage than in Round 1. The walls of the full scale (Figures 21 and 23) and the two larger models (particularly the end panels) suffered more damage than those of the two smaller concrete models. Here again, the methods of pouring the concrete (which differed in the field from that of the laboratory) apparently contributed to the greater damage sustained by the larger structure.

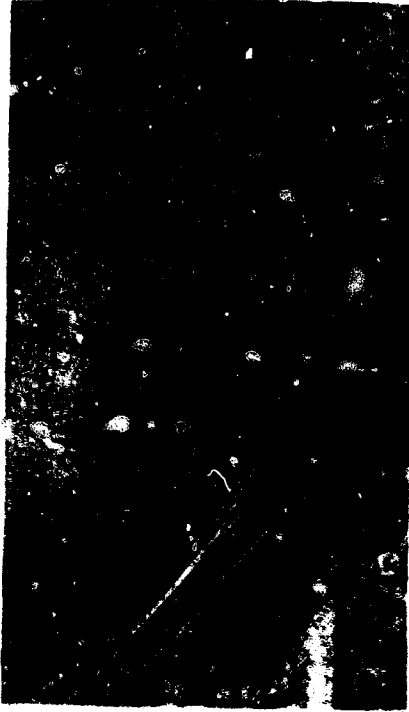
It is evident from the discussion so far that the comparatively insignificant differences in the damage to the various scale models can be attributed primarily to secondary causes such as method



FIGURE 20 - FULL SCALE TEST - ROUND 1 - 2000 LBS. - END PANEL



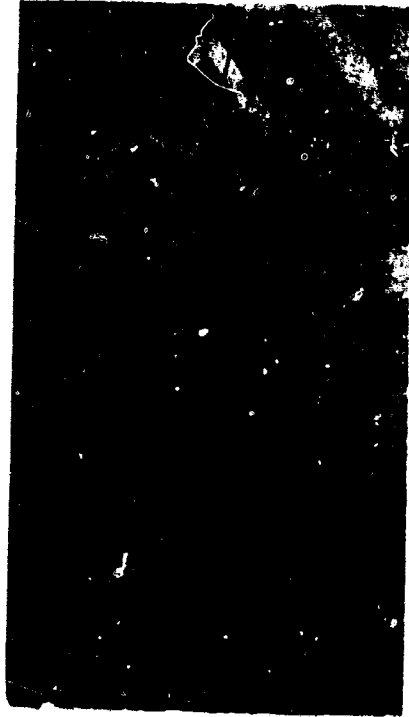
ONE - THIRD SCALE - 112.5 LBS.



ONE - EIGHTH SCALE - 6.0 LBS.



ONE - FIFTH SCALE - 24 LBS.

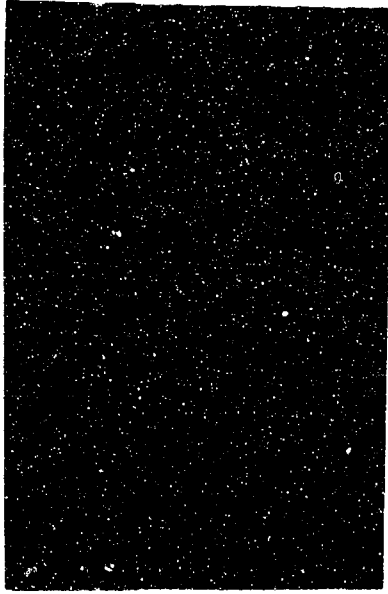


ONE - TENTH SCALE - 3.24 LBS.

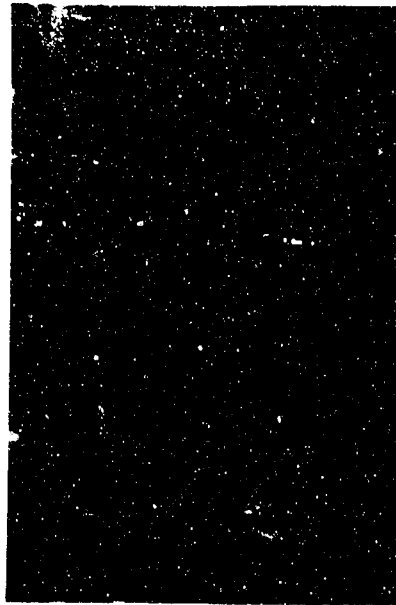
FIGURE 21-MODEL SCALE TESTS - ROUND 2 - DONOR SIDE
(3000 lb. Explosive Equivalent)



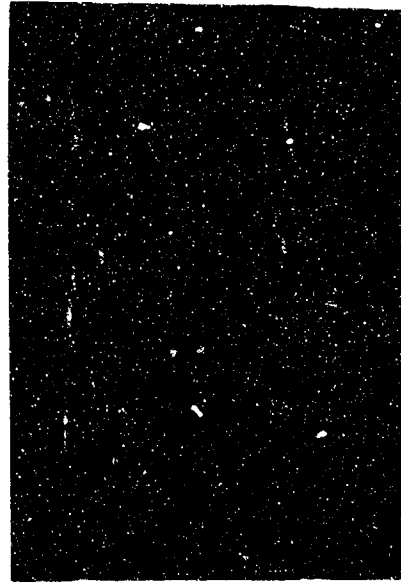
ONE - THIRD SCALE - 112.5 LBS.



ONE - EIGHTH SCALE - 6.0 LBS.



ONE - FIFTH SCALE - 24 LBS.



ONE - TENTH SCALE - 3.24 LBS.

FIGURE 22 - MODEL SCALE TESTS - ROUND 2 - RECEIVER SIDE
(3000 lb. Explosive Equivalent)



FIGURE 23 - FULL SCALE TEST - ROUND 2 -
3000 LBS. - DONOR SIDE

of pouring and differences in materials (reinforcement) and foundations (uncompacted vs. consolidated ground) rather than to scaling factors. In some instances more damage was sustained by the smaller models while in other cases the larger structures suffered a greater amount of damage. There was no definite pattern indicating that the degree of damage increased or decreased with the size of the model.

Round 3--A comparison of the damage sustained by the various test structures can be made only superficially since the test conditions (cluster of charges, charge limitations, etc.) were not exactly the same for all the scale models used in this round of tests. The difference between the individual tests of the first two test series also contributed to distorting the comparable results of the individual tests of the third round. However, the results of this round of tests did indicate test results which in general conformed to the scaling principles which, in turn, indicate that a wide deviation in test arrangements is necessary to significantly distort the results of one model test in comparison to those of similar model tests.

For the two larger structures (full and 1/3 scale) and the 1/8 scale model, the damage was comparable insofar as the donor panel of both the back and side walls sustained incipient failure (Figures 24 and 25). The post-shot condition of the receiver panels (Figures 26 and 27) was classified as heavy damage (less than incipient failure). The damage sustained by the donor and receiver panels of the back wall of the 1/5 scale model was partial destruction and incipient failure, respectively. This increased wall damage above that of the larger structures was attributed to the construction methods used in the field and the use of cluster charges to simulate the 5,000 lb. equivalent charge. The cluster of charges tended to produce a more severe loading condition on the wall insofar as: (1) the interaction of the blast waves of the individual charges enhances the blast pressures which increase the applied blast impulse, and (2) the use of multiple charges tends to direct more of the initial output of the explosion in one direction (in this case towards the back wall) compared to the spherical dispersion of the blast pressures associated with explosions of spherically-shaped charges. In the case of the full scale bay test, there was an enhancement of the blast output due to the use of multiple charges and because these charges were placed directly on the floor slab. However, the type of explosive used in the prototype test was TNT, which has a smaller blast output per unit weight than Composition B used in the model tests.

Both panels of the back wall of the 1/10 scale bay failed due to the enlargement of the previously mentioned vertical cracks which were originally formed during Round 1 as a result of the soil settlement beneath the center of the back wall. In addition, the blast loads acting on the side walls of the cubicle induced additional tension stresses in the horizontal reinforcement of the back wall. These stresses, which normally would be resisted by the mass of the adjoining sections in a multi-cubicle facility in combination



FIGURE 24 - FULL SCALE BAY TEST - ROUND 3
CHARGE WEIGHT = 5,000 LBS.
DONOR SIDE



ONE - THIRD SCALE - 112.5 LBS.



ONE - EIGHTH SCALE - 11.0 LBS.



ONE - FIFTH SCALE - 40 LBS.



ONE - TENTH SCALE - 4.25 LBS.

FIGURE 25 - MODEL SCALE TESTS - ROUND 3 - DONOR SIDE

(5000 lb. Explosive Equivalent)

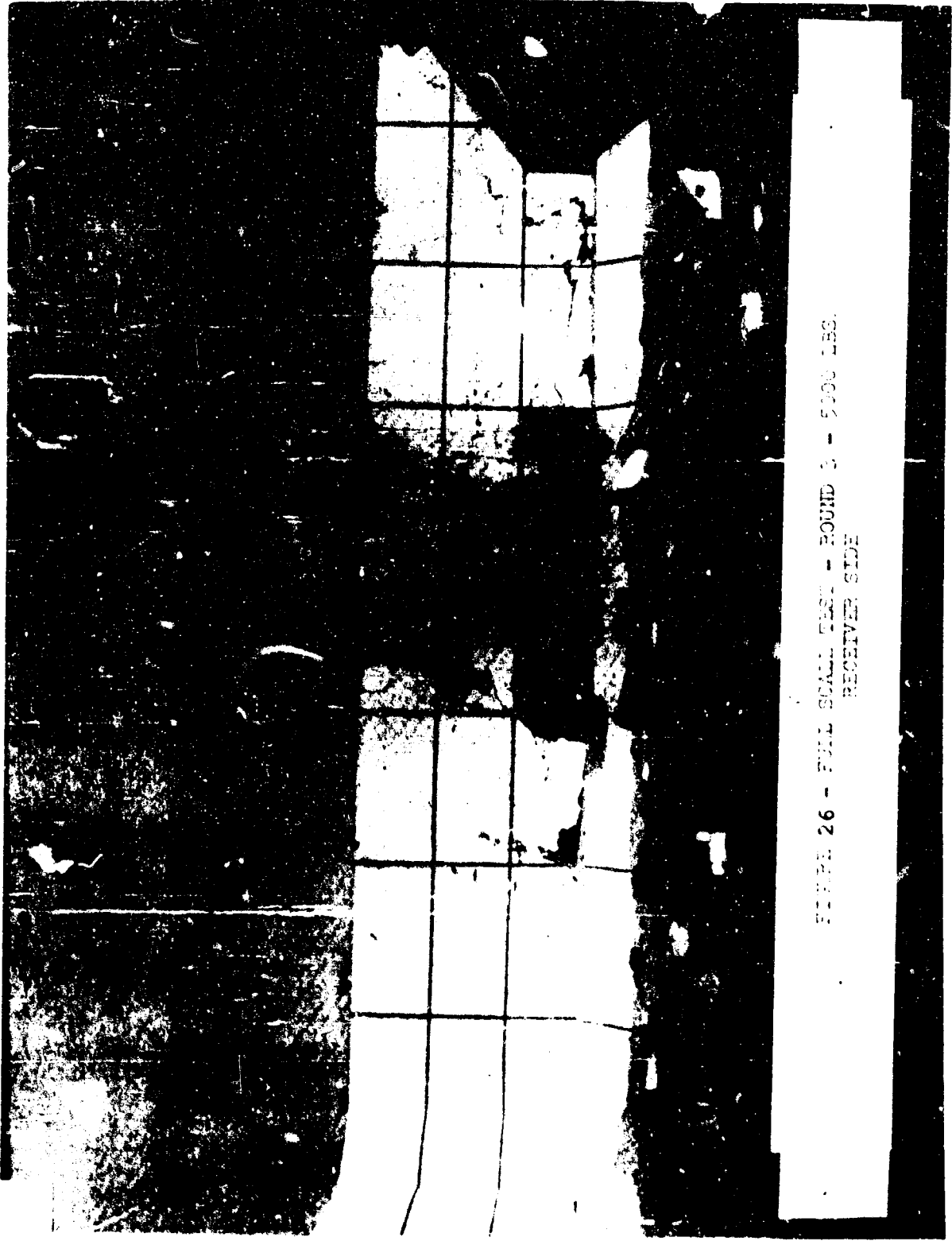
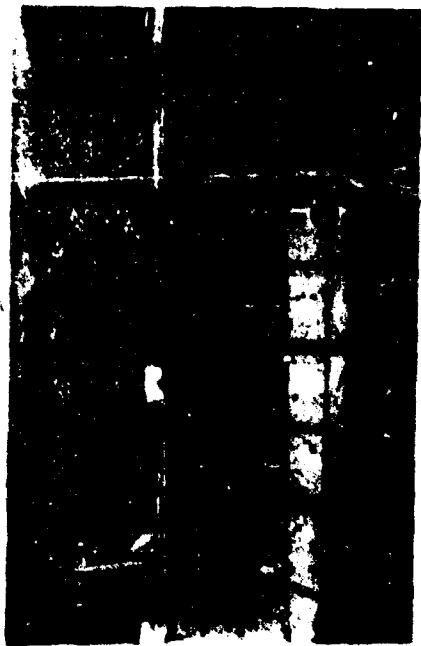
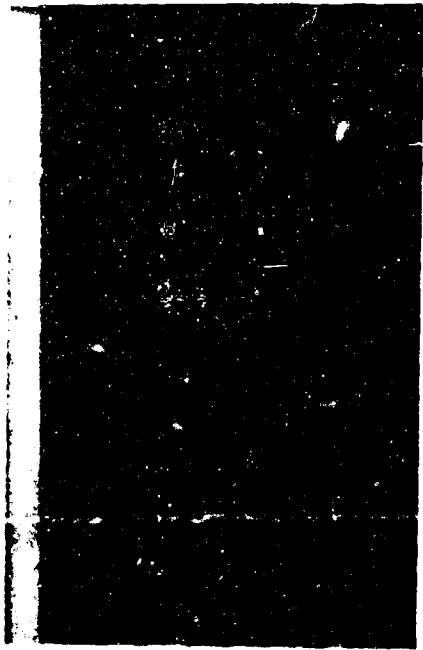


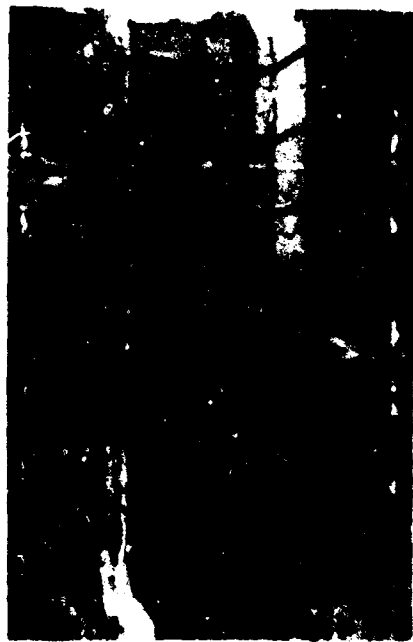
FIGURE 26 - FULL SCALE TEST - ROUND 3 - 5000 LBS.
RECEIVER SIDE



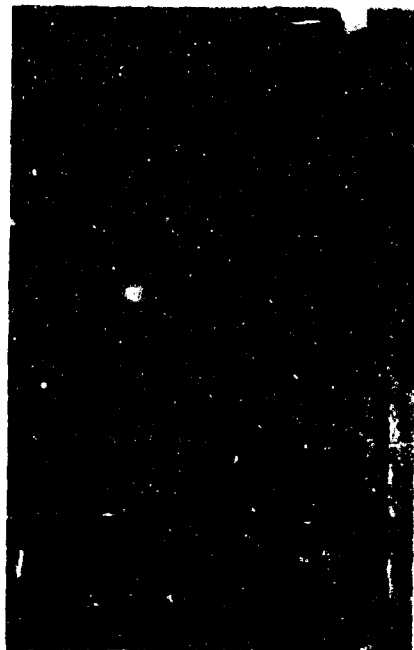
ONE - THIRD SCALE - 112.5 LBS.



ONE - EIGHTH SCALE - 10.0 LBS.



ONE - FIFTH SCALE - 40 LBS.



ONE - TENTH SCALE - 4.25 LBS.

FIGURE 27 - MODEL SCALE TESTS - ROUND 3 - RECEIVER SIDE
(5000 lb. Explosive Equivalent)

with the stresses produced by the subgrade and the normal bending stresses, failed the horizontal reinforcement in the back wall and enhanced the wall collapse.

Round 4--The 1/8 and full scale structures were tested in Round 4 to determine their ultimate capacity (Figures 28 to 31). The 1/8 scale model completely failed while the prototype structure was on the verge of collapse (incipient failure) as a result of an explosive equivalent equal to 7,500 lbs. The explosive used in the full scale structure was TNT while Composition B explosive was utilized in the 1/8 scale model test. Although the variation of the blast output of these two explosives did have an effect on the test results, the major reason for the variation in the structure's response was probably due to the greater potential energy of the full scale structure relative to that of the model. Although the yield and ultimate strength of the hot-rolled reinforcing bars of the full scale structure were less than those of the wire used in the model and the dynamic increase in the strength of the wire was higher than that of the reinforcement in the prototype, the ductility of the wire was significantly less than the ductility of the reinforcing bars. The extent of the damage to the full scale structure could have been reduced if the vertical reinforcement in the lower portion of the walls was placed inside the horizontal reinforcement. No instrumentation was used in this round.

2-2.2 Pressure, Deflection and Strain Test Measurements

Blast Pressures--The blast pressure gage data recorded in the first three rounds of the full scale structure tests is given in Table 5. This data includes gage location (distance and orientation), peak positive incident pressure r_{so} , and scaled impulse.

Figures 32 to 34 are plots of peak pressure, (acting on the ground surface) versus scaled distance for gages located adjacent to the open end (front), the side walls and the back wall of the structure, respectively. Also plotted are pressure-distance curves for unconfined surface explosions and leakage pressures resulting from explosions in partially confined cubicles (one back and two side walls).

In this test series, the reflection of the blast pressures off the back wall and the focusing of these pressures by the side walls resulted in a shotgun effect producing pressures adjacent to the open end of the structure larger than those which would have been produced by an unconfined surface explosion of equal magnitude. On the other hand, pressures acting on the ground in other areas around the structure were reduced below those of an unconfined burst by the shielding afforded by the walls. The walls focused the blast pressures at a higher altitude than would normally occur if the walls were not present.

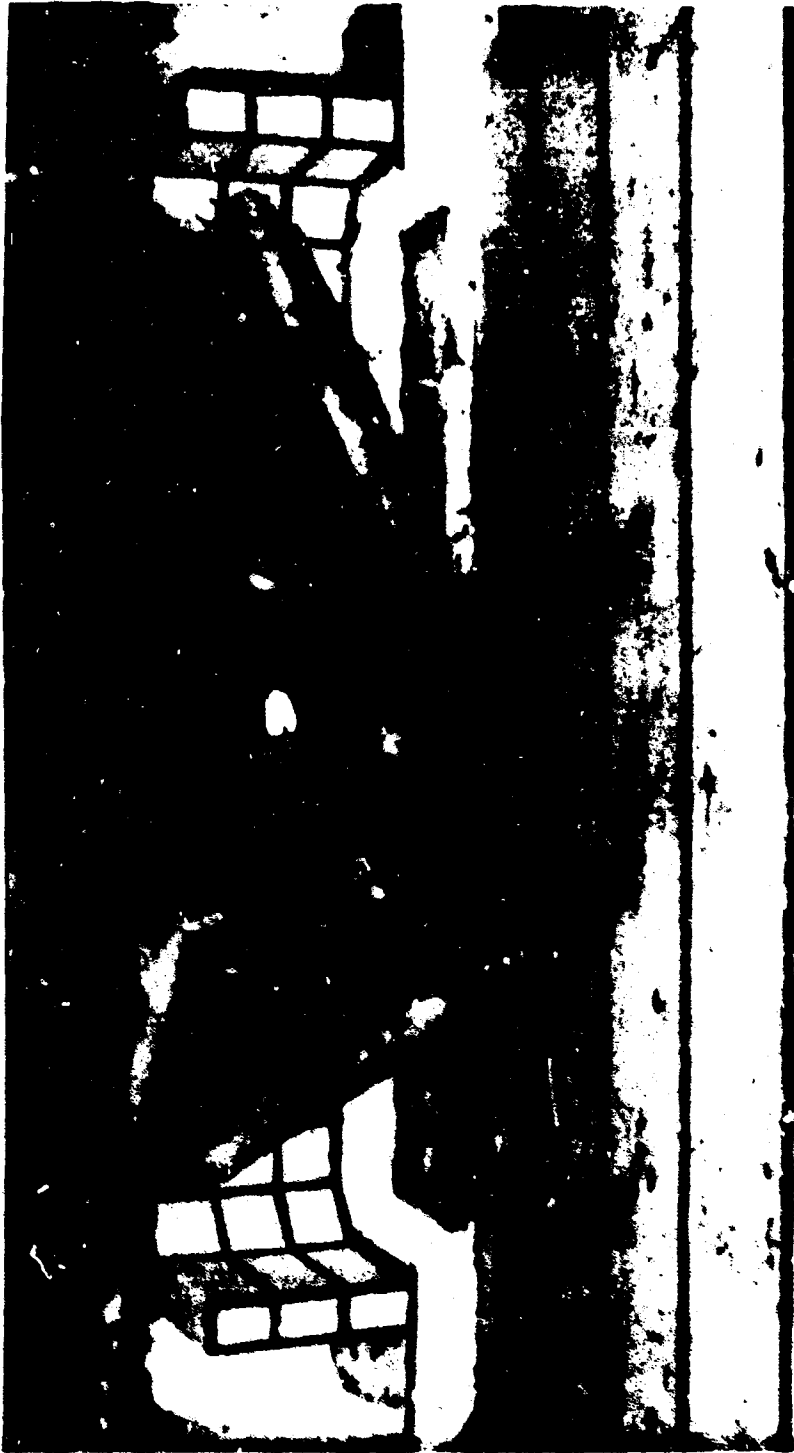


FIGURE 28 - ONE - ONE - EIGHTH SCALE TEST - ROUND 4 - RECEIVER SIDE

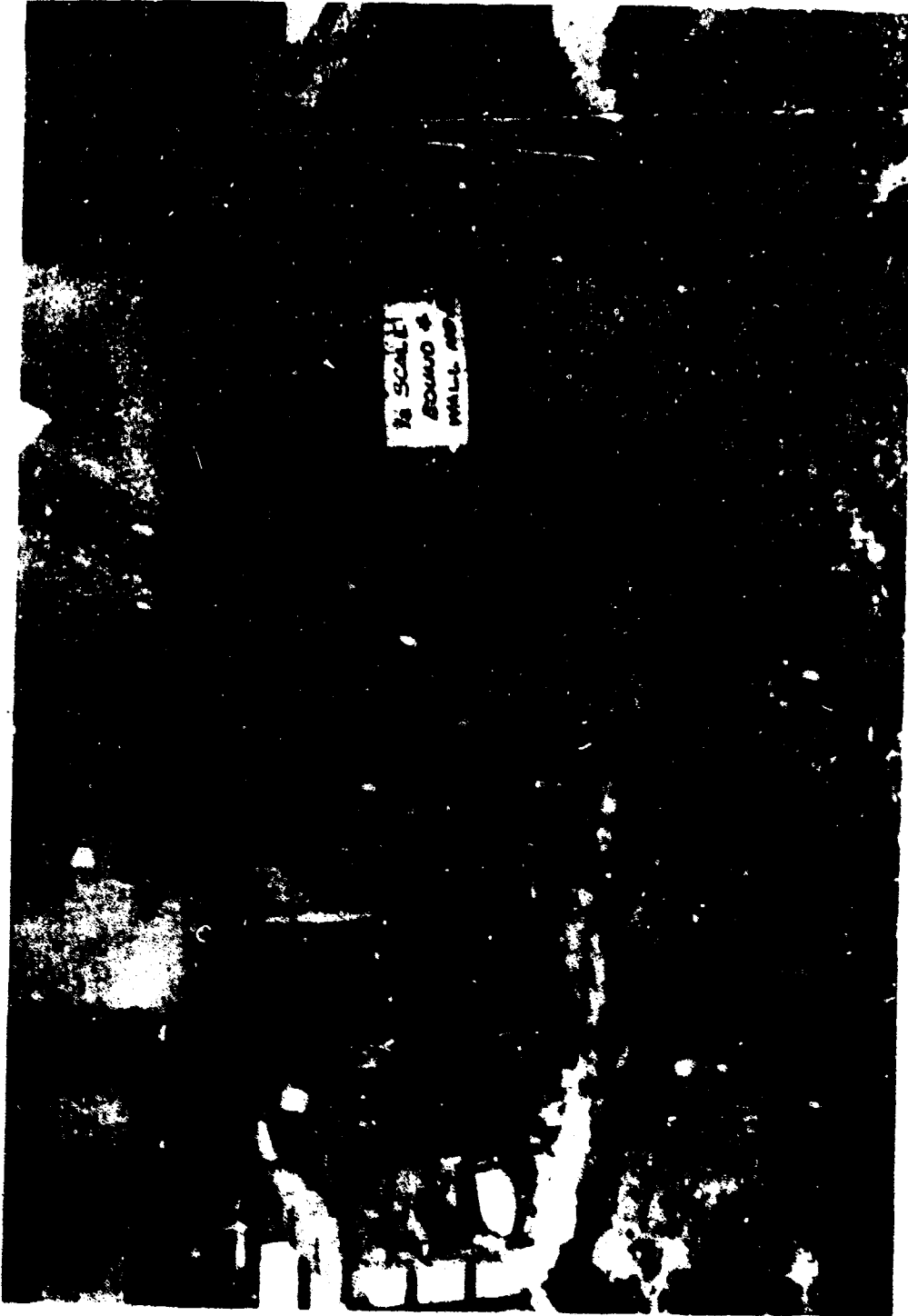


FIGURE 29 - ONE - EIGHTH SCALE TEST - ROUND 4 - DONOR SIDE



FIGURE 30 - FULL SCALE BAY TEST - ROUND 4
CHARGE WEIGHT = 7,500 LBS.
DONOR SIDE



FIGURE 1 - FULL SCALE, MAY TEST - POUND 4
GEAR WEIGHTS = 7,500 LBS.
RECEIVER SIDE

1000

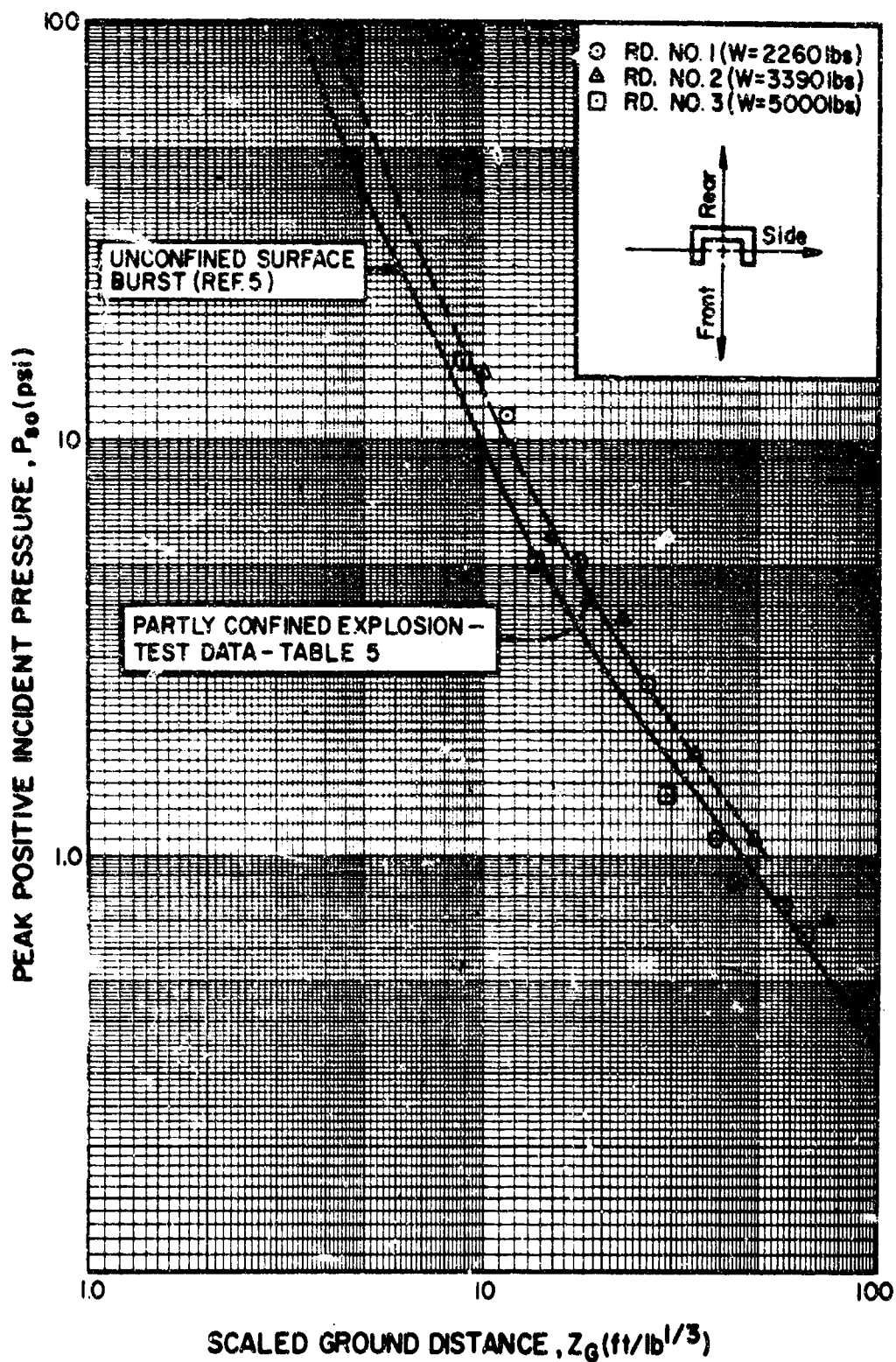


FIGURE 32 - EXTERIOR LEAKAGE PRESSURE VS. SCALED DISTANCE
 (FRONT DIRECTION)

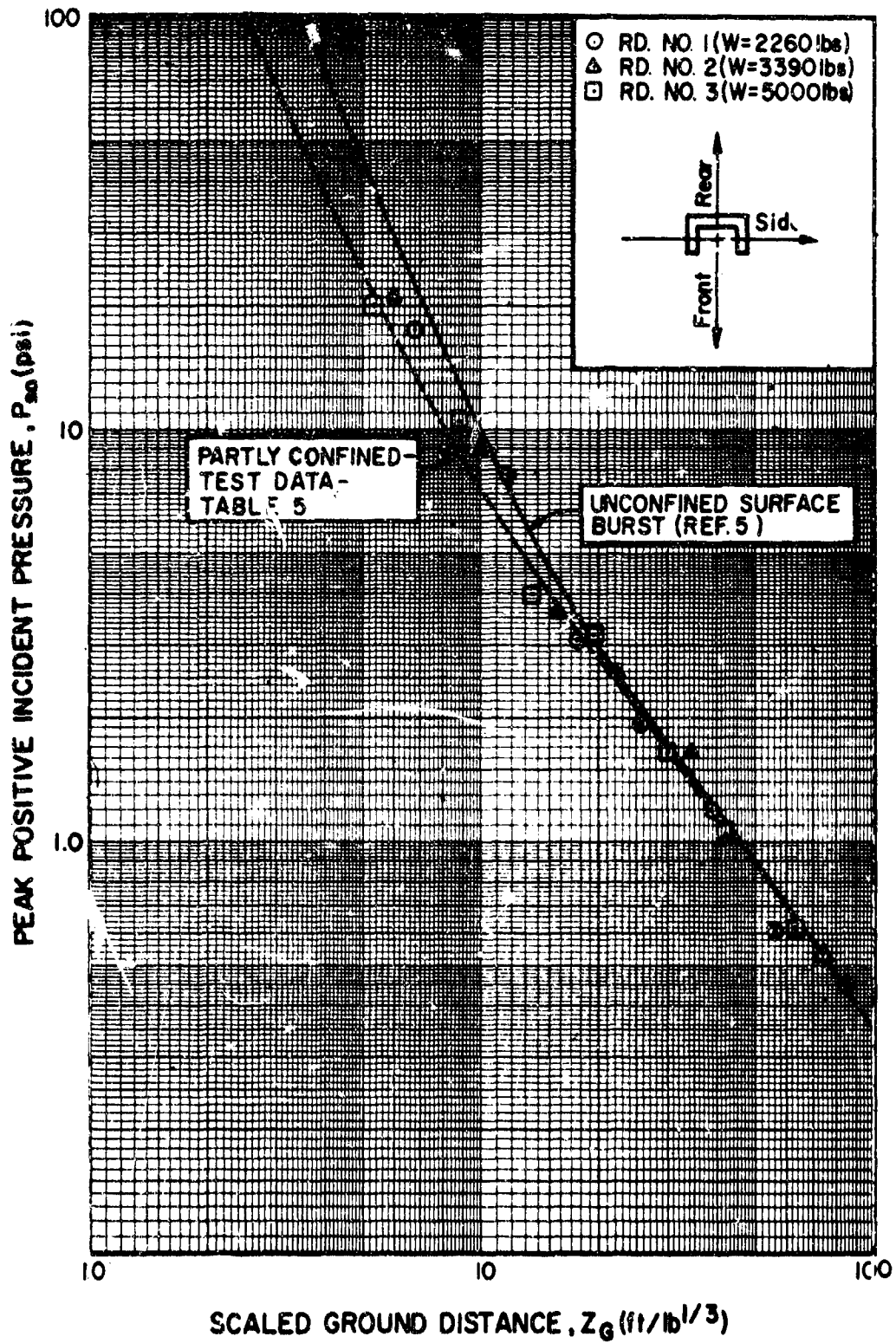


FIGURE 33 - EXTERIOR LEAKAGE PRESSURE VS. SCALED DISTANCE
 (SIDE DIRECTION)

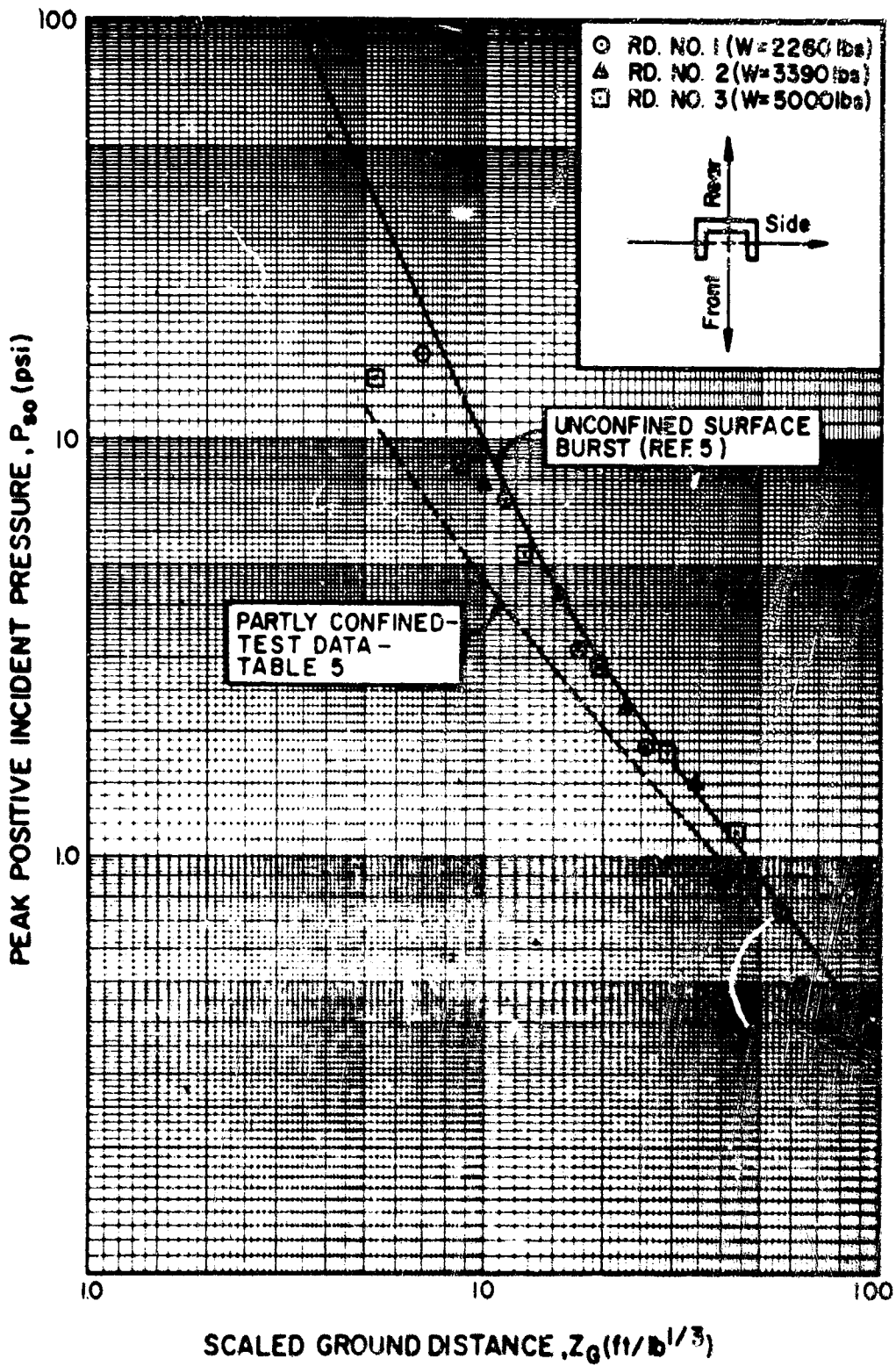


FIGURE 34 - EXTERIOR LEAKAGE PRESSURE VS. SCALED DISTANCE (REAR DIRECTION)

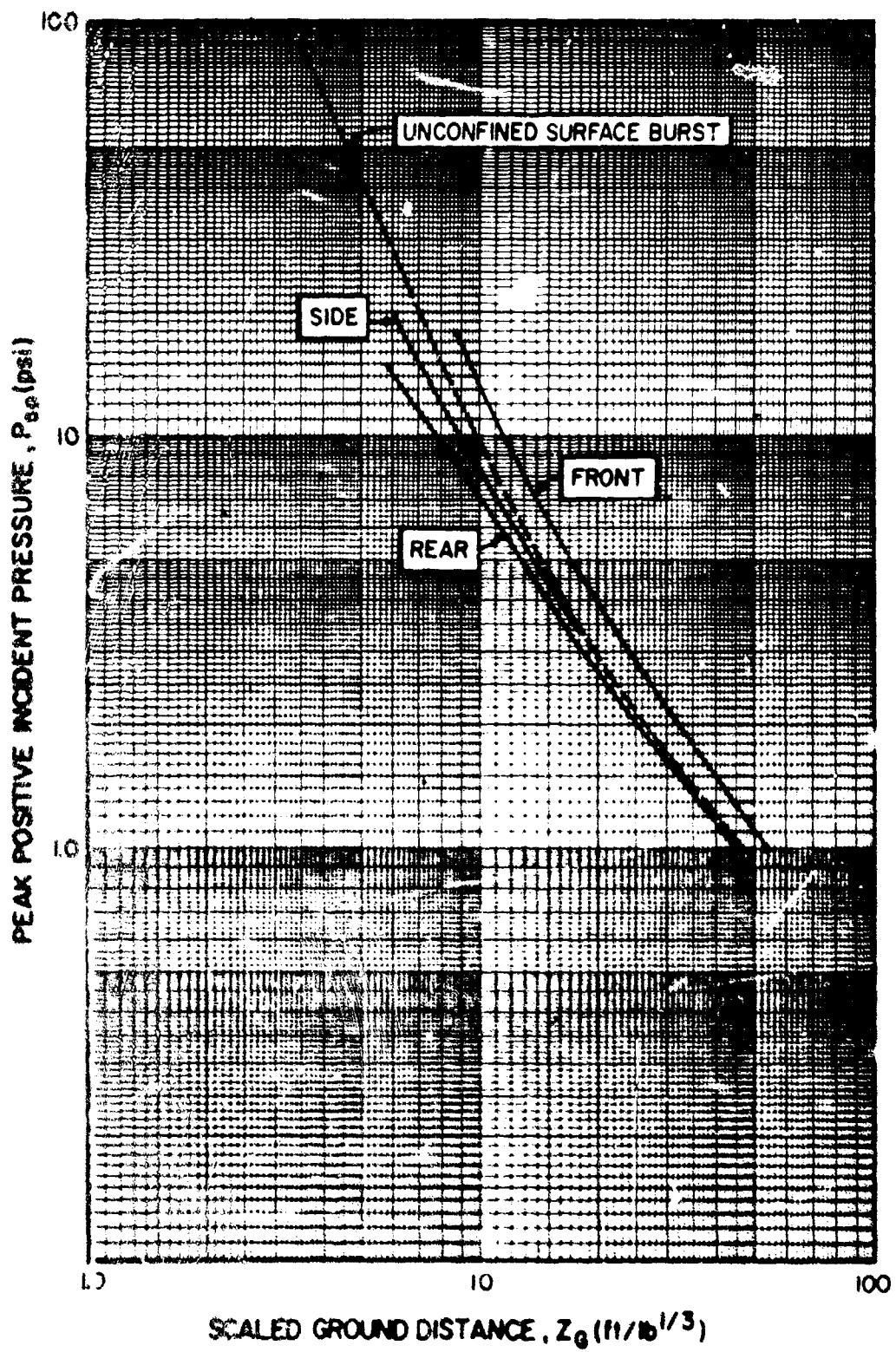


FIGURE 45 - INCIDENT PRESSURE - DISTANCE CURVES

It should be noted that the pressure-distance relationships are valid only for the structural arrangements and charge weights involved in this test series. A summary of these leakage pressures is given in Figure 35 while a summary of other leakage pressure data is presented References 6 to 8.

Deflections--As mentioned, electronic gage measurements indicating the deflection-time history of the walls and physical measurements of the permanent deflections were obtained in the Bay Structure Test Series. A typical deflection-time curve for a back wall is illustrated in Appendix B (Figure B-13) while Reference 9 contains a number of the other deflection measurements obtained during the test series. Electronic instrumentation was used in the two larger models and the full scale structure tests whereas permanent deflection measurements were obtained from all five structures tested. Tables 6 to 8 list the results of the various deflection measurements which were obtained from all five structures tested.

As may be expected, the permanent deflections of the back walls of the various test structures increased with increasing structure size (Table 8). However, except for Round 1, this increased magnitude of the deflections sustained by the 1/5 and 1/3 scale models deviated from the expected values. These deviations were primarily a function of field conditions where less control during construction could be maintained. Another factor affecting the scaling factors for the larger models was the effects produced by the lower density sand used in the cavities of these structures. The average sand density used in the 1/5 and 1/3 scale structures was approximately 80 pcf whereas the density used in the other structures varied between 85-90 pcf. This decrease in sand density resulted in the formation of larger and smaller deflections being sustained by the donor and receiver panels, respectively. However, the combined deflection of both panels was greater than that which would have occurred if the denser sand was used.

In the tests performed subsequent to Round 1, it could not be expected that scaling of deflections could be maintained. Here the settlement, rotation and sliding of the overall structure and the scaling factor variation of the individual elements which occurred during the first round seriously affected the pre-shot test conditions for subsequent tests.

Because of insufficient data from the electronic instrumentation (Tables 7 & 8), no estimate of the degree of scaling achieved between the maximum deflections of the various test structures could be made. However, the gage data did indicate that the maximum deflection of each wall was in the order of magnitude of approximately twice the permanent deflection. This is an indication that, for the magnitude of the deflections attained in these tests, the value of the maximum deflection and not only the permanent deflection must be considered in determining the potential energy developed by each wall in resisting the applied blast loads.

TABLE 6 - MAXIMUM PERMANENT DEFLECTIONS
OBTAINED BY MEASUREMENTS

STRUCTURE	ROUND	BACK WALL DEFLECTIONS (in.)		F.S. DEFLECTION
		DONOR PANEL	RECEIVER PANEL	MODEL DEFLECTION (5)
One-Tenth Scale	1	0.19	0.08	12.7
	2	1.19	0.50	2.2
	3	(1)	(1)	-
One-Eighth Scale	1	0.25	0.13	9.0
	2	0.69	0.50	5.0
	3	(1)	1.25	-
One-Fifth Scale	1	1.50	0.13	2.1
	2	2.25	0.25	2.4
	3	(1)	(3)	-
One-Third Scale	1	1.62	0.13	2.0
	2	3.31	0.25	1.7
	3	(1)	1.13 (4)	-
Full Scale	1	2.18	1.25	1.0
	2	4.00	1.07	1.0
	3	(1)	-	-

- (1) Wall failed
- (2) Deflection too small to measure
- (3) Just beyond incipient failure
- (4) Scaled charge weight smaller than used in other model tests.
- (5) Deflection is sum of donor and receiver panel deflections.

TABLE 7 - MAXIMUM DEFLECTION OBTAINED FROM
ELECTRONIC DEFLECTION GAGE MEASUREMENTS

STRUCTURE	ROUND	BACK WALL DEFLECTIONS (in.)	
		DONOR PANEL	RECEIVER PANEL
One-Fifth Scale	1	(1)	(1)
	2	5.32	1.25
	3	(2)	2.20
One-Third Scale	1	< 2.50 (3)	0.28
	2	4.87	0.91
	3	(2)	3.00
Full Scale (5)	1	(4)	(4)
	2	7.30	3.60
	3	(2)	(2)

- (1) Electrical leads cut by debris
- (2) No instrumentation used
- (3) Max. deflection beyond range of recorder
- (4) Record did not function
- (5) See Table 6 for other deflection measurements

TABLE 8 - MAXIMUM DEFLECTION - SECOND ROUND-FULL SCALE BAY TEST

GAGE	TIME (ms)	DEFLECTION (in.)
1	20	3.0
2	29	7.3
3	34	3.6
4	29	3.6
5	40	1.4
6	24	6.2
7	20	5.0
8	(1)	(1)
9	35	2.6
10	20	5.5
11	31	1.1
12	(1)	(1)
13	26	3.0
14	34	0.3
15	76	0.9
16	(1)	(1)
17	30	0.7
18	56	0.8

(1) No reading

(2) See Fig. 13 for gage locations.

Strain Measurements--Several gages (whose attachment positions are indicated in Table 9) were utilized in Round 1 of the two larger scale model tests. The main electrical leads to the 1/3 scale structure were severed by flying debris close to the cubicle so no strain data was obtained for this structure. The data recorded by the strain gages of the 1/5 scale model is given in Table 9. The maximum strain recorded in this structure occurred at the top of the donor panel of the back wall where it intersects with the side wall. Visual results of the test confirmed this to be a point of maximum strain. However, other sections of the structure where gages 1 and 3 were located probably developed strains whose magnitudes were in the order of or greater than that of gage 5. Neither gage 1 nor 3 functioned during the test. Because of the difficulty in obtaining reliable data in the first rounds of these tests, strain gages were not used in subsequent tests.

Concrete Fragments--Although there was fragmentation of the floor slab at the onset of testing of each structure, the formation of concrete fragments from the walls did not materialize until the final test of each structure was performed. Wall fragmentation occurred chiefly in the back wall between the vertical reinforcing bars situated at the section of failure. As the horizontal tension reinforcement failed, the concrete retained by the failed flexural and lacing reinforcement was ejected from the structure. Except where complete collapse of the 1/10 scale model (10,000 lbs. full scale equivalent) took place, the weight of the concrete rubble was small in comparison to the weight of the wall. Also, the velocities of the small fragments were low. This is indicated by the results of Round 3 of the 1/10 model test where a maximum fragment velocity of 31 fps and an overall average fragment velocity of 74 fps (Table 10) were produced.

Photography--The most significant use of camera coverage was documentation of blast results with the still camera. Motion pictures of the structural motion and concrete fragments were not practical since the dust created by the detonation obscured these pictures.

TABLE 9 - SUMMARY OF STRAIN GAGE MEASUREMENTS

GAGE	MAXIMUM STRAIN INDICATED	ATTACHMENT(1)
1	Circuit opened before gage could respond.	A
2	0.19; 7 milliseconds after detonation.	A
3	This gage damaged during concrete pouring.	B
4	0.35; 4 milliseconds after detonation.	B
5	2.4%; 5 milliseconds after detonation	B
6	No output recorded from this gage.	B
7	1.23%; 3 milliseconds after detonation.	B

- (1) A - Attached to side of vertical reinforcing bars
 B - Attached to top of horizontal reinforcing bars,
 second row from top

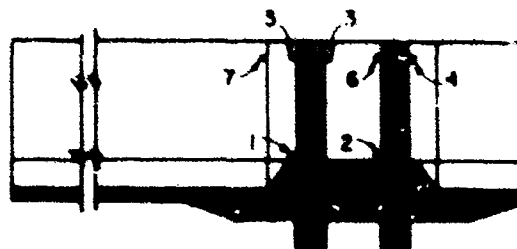
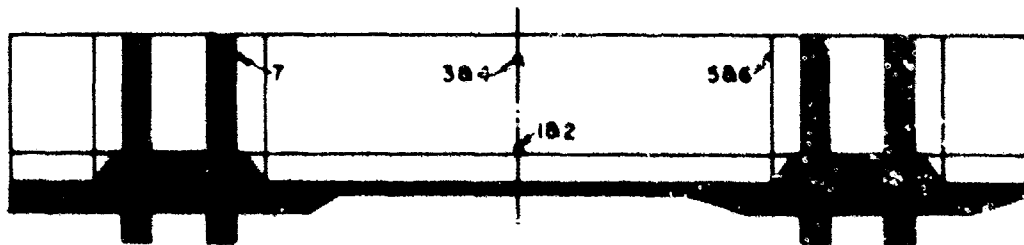



TABLE 10 - BACK WALL FRAGMENT VELOCITIES (Round 3)

FRAGMENT	FRAGMENT VELOCITY (fps)				AVERAGE	OVERALL AVERAGE
	SPACE 1	SPACE 2	SPACE 3	SPACE 4		
1	78	78	78	78	78	
2	78	78	70	66	73	
3	81	71	71	71	74	74
4	76	73	73	71	73	
5	76	71	71	71	72	

S	P	A	C	E	1
S	P	A	C	E	2
S	P	A	C	E	3
S	P	A	C	E	4

Direction of
Fragments



SECTION III

ULTIMATE CAPACITY BAY TESTS

3-1 General

The bay structures tested in the Scaling Test Series withstood detonations of quantities of explosives in excess of the 2000 pounds of HE for which the structure was originally designed. Therefore, a supplementary test series was developed to evaluate the maximum explosive (quantity of explosive which will produce incipient failure) capacity of the structure.

Two composite bay models were tested in the Ultimate Capacity Series, namely a 1/10 and 1/8 scale model. The design of these two models was the same as comparative models tested in the Scaling Test Series. As will be shown, the test results of the two models were significantly dissimilar.

To determine the feasibility of utilizing plain reinforced concrete in lieu of composite construction, a second 1/8 scale model of the bay structure was designed, built and tested. This second 1/8 scale model had the same interior cell dimensions as that of the composite structure, but all three walls were constructed of plain laced reinforced concrete. The thickness of the individual walls of the model was 6.5 inches or $\frac{1}{4}$ ft. - $\frac{1}{4}$ in. full scale. Because the plain concrete bay was designed to simulate the explosive capacity of the composite bay, the tests of these two models were performed in the same manner.

Table 11 lists some of the dimensions of the three models as well as the dimensions of the full scale structure.

Table 11

TEST STRUCTURE DIMENSIONS (FEET)

Unit	1/10 Scale Composite	1/8 Scale		Full Scale
		Composite	Plain	
Length	4.0	5.0	5.0	40
Width	2.0	2.5	2.5	20
Height	1.0	1.25	1.25	10
Thickness	0.8	1.0	0.54	8

The damage sustained by the three models tested in the Ultimate Capacity Test Series is listed in Table 4.

3-2 One-Tenth Scale Composite Bay Test

The 1/10 scale composite model was tested in a fashion similar to that used in the performance of the 1/8 scale model test of the Scaling Test Series. The model was positioned adjacent to the opening in the side of a steel tunnel used for recording the flight of spalled concrete fragments. The explosive used in the 1/10 scale test consisted of 2-5 pound spherical charges of Composition B (full scale equivalent of 10,000 pounds) which were located at the geometric center of the cell (Fig. 36).

The results of the 1/10 scale test are shown in Figure 37. The back wall and floor slab split in half forming separate sections of the structure. The space between the two sections was as large as 10 inches indicating translation of each section in the direction of its respective side wall. It is theorized that the motion imparted to each section of the structure was produced by the blast loading acting on the side walls. It was also theorized that the initial failure of the back walls and floor was produced by the excessive tension stresses occurring in the longitudinal reinforcement of these elements as a result of the side wall reactions imparted to these elements. It will be shown later that the above failure characteristics of the structure, in conjunction with the fact that the explosive quantity used in the test was too large, were borne out by the results of the subsequent 1/8 scale model tests.

3-3 One-Eighth Scale Composite Bay Test

Like the 1/10 scale composite cubicle, the 1/8 scale composite bay was tested at Picatinny Arsenal. However, because of the damage inflicted on the smaller model, the testing technique was altered to more fully simulate a multi-cubicle arrangement. Here, a buttress tie system (Figure 38) for both the floor slab and back wall of the model was used to resist the additional tension forces in the back wall produced by the blast loads acting on the side walls. In this system, the model was placed partly into the previously mentioned opening in the steel tunnel with both ends of the back wall buttressed by the steel plates which formed the donor side of the tunnel. The spaces between the ends of the back wall and tunnel plates were shimmed to form positive contacts. In addition, a rigid steel collar was placed around the slab. The spaces between the collar and the slab were also shimmed. The collar plus the mass afforded by the side wall of the tunnel produced the required strength necessary to resist the applied loads.

NOT REPRODUCIBLE

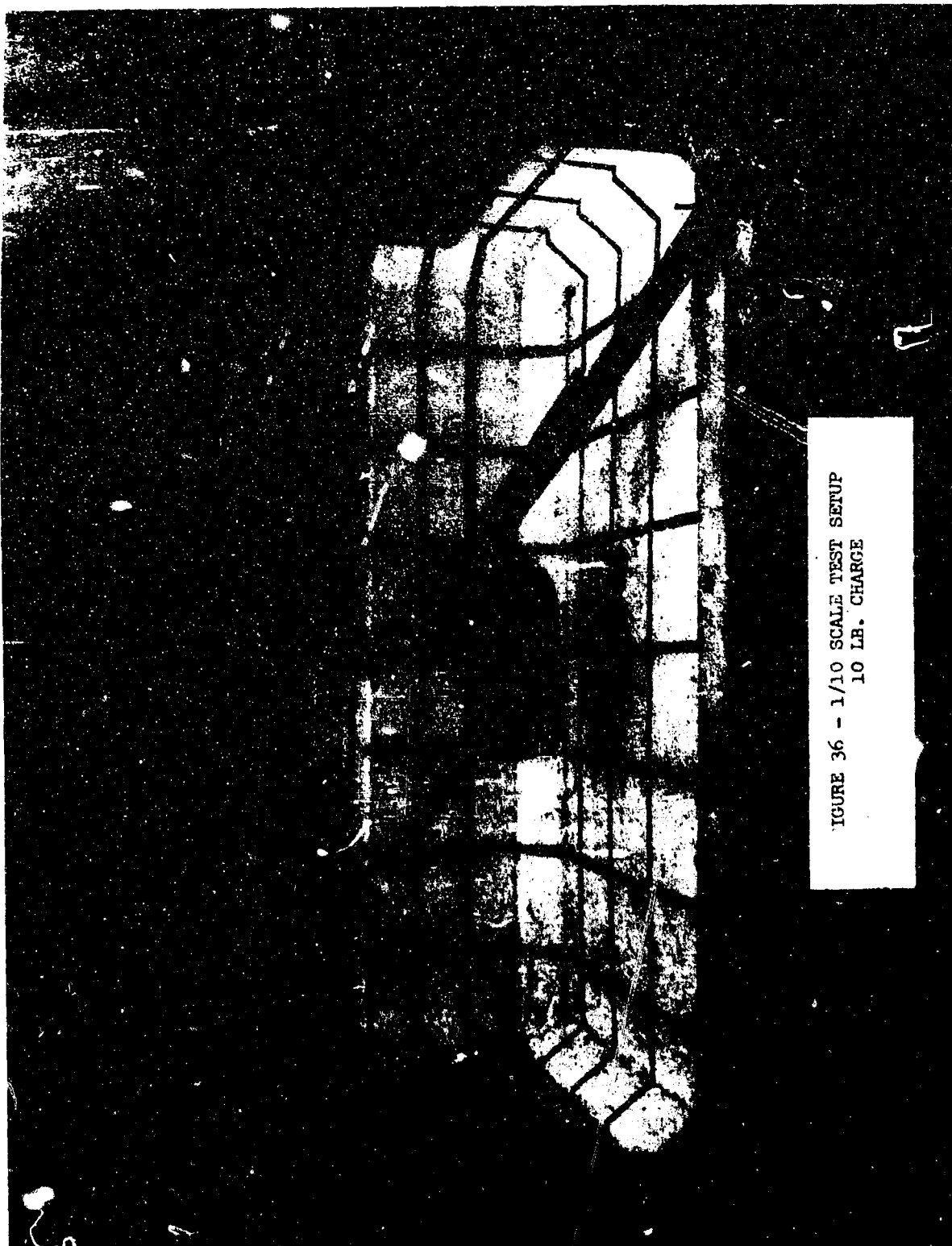


FIGURE 36 - 1/10 SCALE TEST SETUP
10 LB. CHARGE



DONOR SIDE



NOT REPRODUCIBLE
RECEIVER SIDE

FIGURE 37 - ONE TENTH SCALE BAY TEST - 10LB. CHARGE

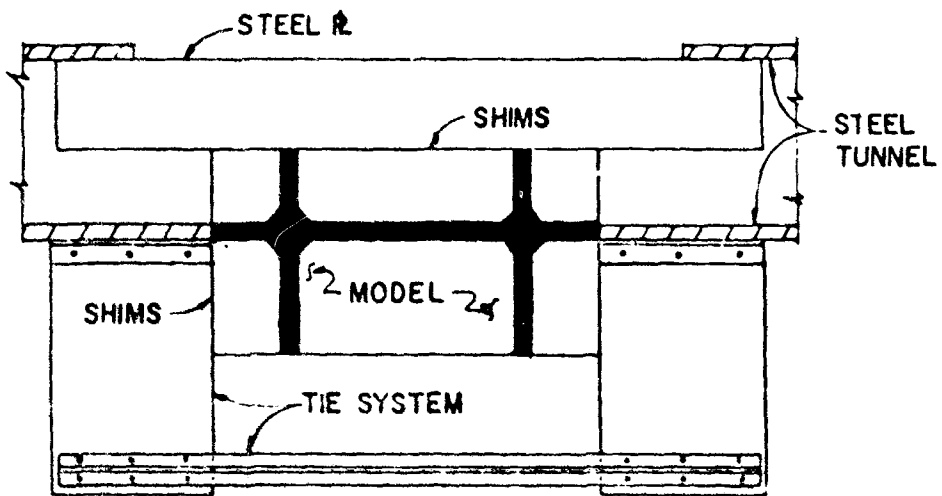


FIGURE 38 - SIMULATION OF MULTI-CUBICLE STRUCTURE
USING STEEL PLATE TIE SYSTEM

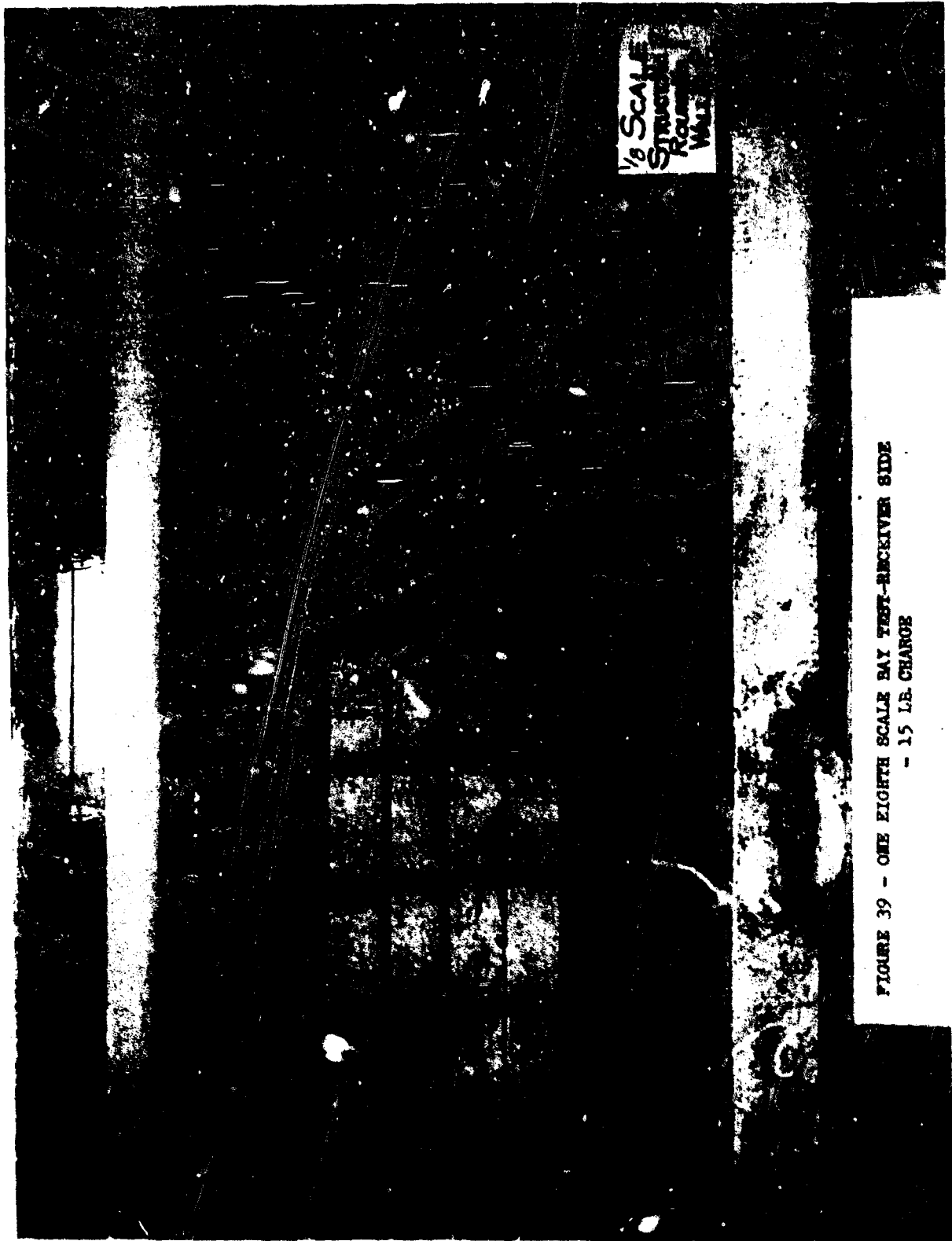
Because of the improved testing arrangement, the 1/8 scale model was found to be capable of resisting without failure the blast effects of an explosion equivalent to 7,500 lbs. of Composition B. This was approximately 10% less than the ultimate capacity as predicted by the pre-shot analysis.

As in the case of the smaller model, the damage to the back wall of the 1/8 scale model was greater than that sustained by the side walls. Although the tension reinforcement at the supports (back wall panel supported by the base slab and by the two side walls of the cubicle) and at the center of the donor panel failed, the compression steel at these sections remained intact. It can be noted from Figure 39 that a typical concrete yield line pattern was formed.

The receiver panel of the back wall remained intact with the magnitude of the panel's deflection indicating less than incipient failure conditions. Spalling of the receiver surface of the receiver panel did occur at the supports. This spalling was attributed to the high compression forces which crushed the concrete cover over the compression reinforcement (Figure 39).

Figures 39 and 40 indicate that the damage to the side walls of the 1/8 scale structure was nearly as severe as that sustained by the side walls of the 1/10 scale model even though a somewhat larger equivalent explosive was used in the smaller model test. The large degree of damage to the 1/8 scale model side walls was attributed to the fact that the structure remained intact. Therefore, all the energy imparted to the side walls by the blast had to be absorbed entirely by the walls themselves. In the case of the 1/10 scale model, a portion of the applied blast loads acting on the side walls was dissipated by translation of the two sections of the structure after the back wall failed. Hence, the amount of blast energy to be absorbed by the flexural action of the model was reduced.

The results of the 1/8 scale test were significant insofar as they established an ultimate single-shot capacity of the full scale structure equal to approximately 7,500 lbs. However, in the Scaling Test Series the full scale structure was capable of resisting without failure the effects of several explosions whose total quantity was in excess of 10,000 lbs. of HE. Furthermore, the full scale structure failed when subjected to the effects of a single explosive quantity of 7,500 lbs. of TNT. The reason that the full scale structure had a larger ultimate capacity under a multiple-shot arrangement than when a single detonation was involved was because the total kinetic energy of the structural elements associated with the blast loads of the multi-shot arrangement was less than the kinetic energy associated with a single shot having an explosive charge equal to the sum of the charges used in the multi-shots. Also, the effects of the elastic recovery of the elements contributed to the increased explosive capacity of the structure in the multiple detonation tests.



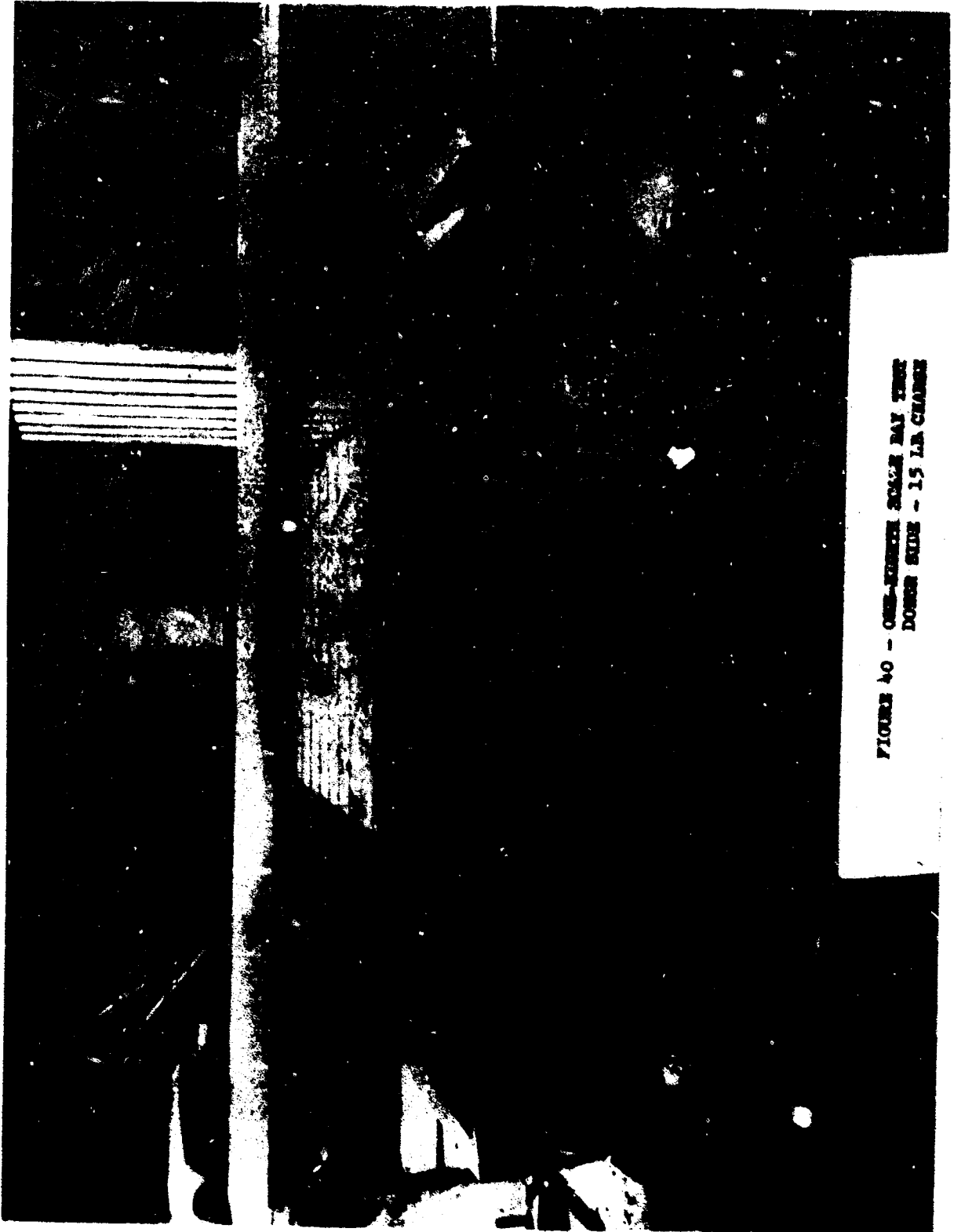


FIGURE 40 - ONE-THIRD SCALE DAY TIME
DOWNER SLIDE - 15 LB CHANGE

-76-

NOT REPRODUCIBLE

3-4 One-Eighth Scale Plain Reinforced Concrete Bay Test

The plain reinforced concrete bay was also tested utilizing the buttress-type tie system described for the composite model. The equivalent explosive quantity used in the test was 7,500 lbs. of Composition B. The results of the test are shown in Figure 41.

The donor and receiver surfaces of all three walls were severely spalled. This was significantly different from the results of the one-eighth scale composite structure test where only the donor surfaces of the structure sustained spalling. The spalling of the receiver surfaces of the plain concrete structure was primarily a result of the shock transmission of the blast loads through the concrete. Also, the resultant large deflections of the walls also contributed to the production of the concrete spalls. It is evident from the comparative results of both one-eighth scale structure tests that one would expect the production of larger amounts of secondary fragments when plain concrete construction is used in place of composite construction. However, in facilities other than those utilized for the protection of personnel and/or equipment, the possible occurrence of spalling will not be a significant factor in design.

The magnitude of the post-shot permanent deflection (measured at the center and top of the back wall) was 1-3/4 inches which is approximately 70% of the magnitude of the deflection predicted by the pre-shot analysis. Part of this discrepancy was the fact that the strength of the reinforcement was approximately 30% higher than that assumed in the analysis. The remainder of the differences which occurred between the calculated and measured deflection may be attributed to the inherent conservatism of the analytical procedures used for design of plain reinforced concrete elements.

Based upon the above results, it appears that except in those cases where spalling is a problem, plain reinforced concrete construction will be as useful as composite construction in the design of structures to resist the effects of HE explosions.

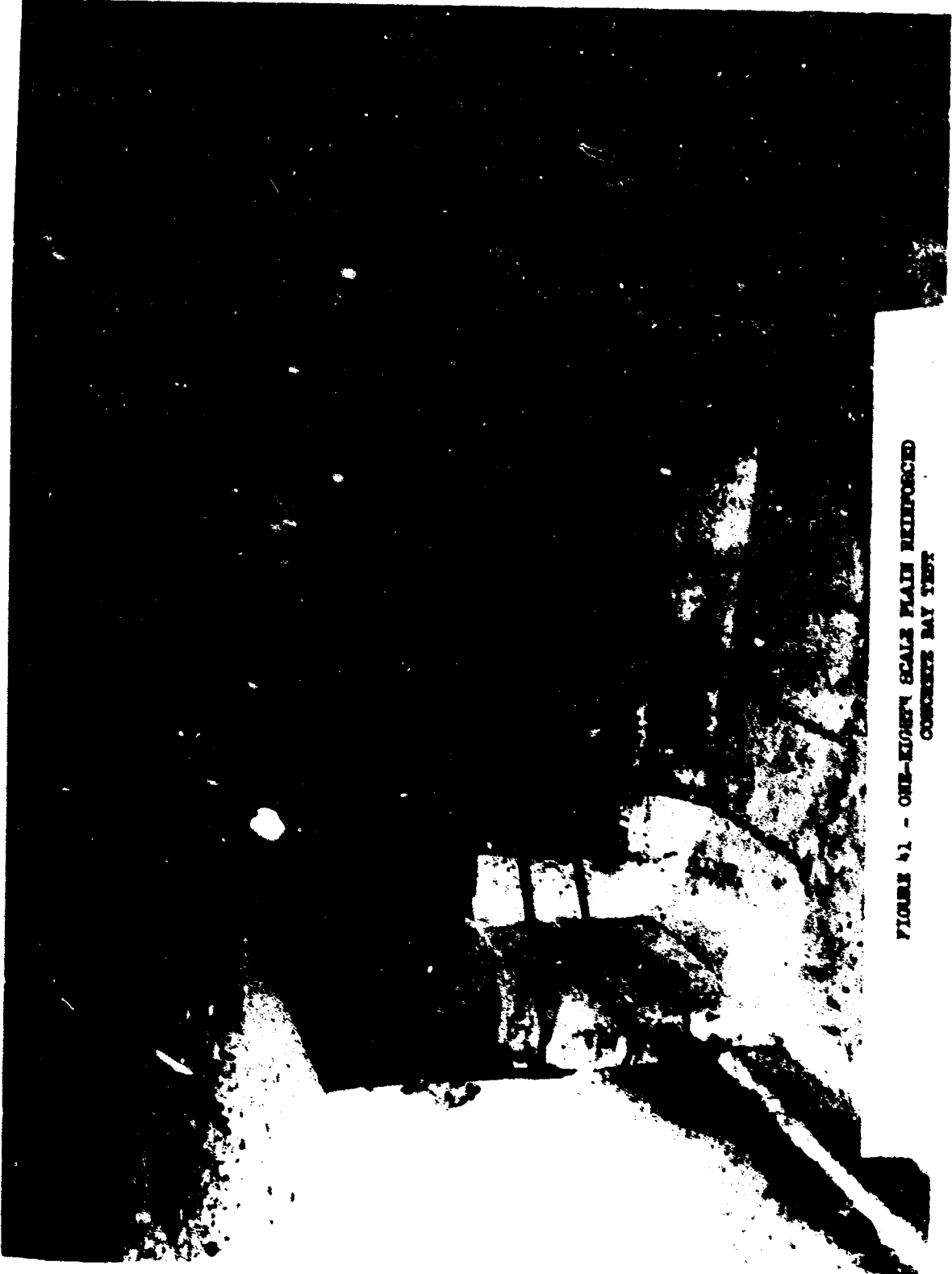


FIGURE 61 - ONE-EIGHTH SCALE PLAN REINFORCED
CONCRETE BAY TEST

REFERENCES

1. Richard Rindner et al, Establishment of Safety Design Criteria for Use in Engineering of Explosive Facilities and Operations - Supporting Studies: January-December 1965, Report No. 8, Picatinny Arsenal Technical Report 3484, December 1966.
2. Edward Cohen and Norval Dobbs, Design Procedures and Details for Reinforced Concrete Structures Utilized in Explosive Storage and Manufacturing Facilities, Ammann & Whitney, Consulting Engineers, New York City, Annals of the New York Academy of Science Conference on Prevention of and Protection Against Accidental Explosion of Munitions, Fuels and Other Hazardous Mixtures, Volume 152, Article 1, October 1968.
3. Structures to Resist the Effects of Accidental Explosions, Department of the Army Technical Publication TM 5-1300, Department of the Navy Publication NAVFAC P-397, Department of the Air Force Manual AFM 88-22, U.S. Government Printing Office, Washington, D.C., June 1969.
4. Richard Rinder et al, Establishment of Safety Design Criteria for Use in Engineering of Explosive Facilities and Operations, Report No. 9, Summary Studies: January-December 1966, Picatinny Arsenal Technical Report 3594, June 1967.
5. C. N. Kingery, Air Blast Parameters Versus Distance for Hemispherical TNT Surface Bursts, Report 1344, Ballistic Research Laboratories, Aberdeen Proving Ground, Maryland, September 1966.
6. Edward Cohen et al, Establishment of Safety Design Criteria for Use in Engineering of Explosive Facilities and Operations - Report No. 10, Blast Pressures and Impulse Loads Produced by Explosions in Cubicle-Type Structures, Technical Report 3604, by Ammann & Whitney, Consulting Engineers, New York City for Picatinny Arsenal, Dover, New Jersey under Contract DAAA-21-67-C-0217, May 1967.
7. H. R. Richey, Armed Forces Explosives Safety Board Wall Program, Phase C, Tests 1 - 13, Technical Progress Report 346 (SECRET RESTRICTED DATA) U.S. Naval Ordnance Test Station, China Lake, California, April 1964.
8. A. R. Sound, Summary Report of Earth-Covered, Steel-Arch Magazine Tests, Technical Progress Report 401, U. S. Naval Ordnance Test Station, China Lake, California, July 1965.

9. Stanley Wachtell, Methods of Measurement of Structure Response to Blast Loads, Picatinny Arsenal, Dover, New Jersey, Annals of the New York Academy of Sciences Conference on Prevention of and Protection Against Accidental Explosion of Munitions, Fuels and Other Hazardous Mixtures, Volume 152, Article 1, October 1968.
10. R. H. Cole, Underwater Explosions, Princeton University Press, Princeton, New Jersey, 1948.
11. W. E. Baker, Modeling of Large Transient and Plastic Deformations of Structures Subjected to Blast Loading, Paper No. 60-APM-18, American Society of Mechanical Engineers, Applied Mechanics Division, July 1959.
12. I. Davies, Model Analysis, Proceedings of the Symposium on Protective Structures for Civilian Populations, National Academy of Sciences, National Research Council, Washington, D.C., April 1965.

APPENDIX A
Geometrical Scaling

GEOMETRICAL SCALING

Certain laws of similitude must be observed to insure that the model test data can be applied to the prototype. These laws, in turn, provide a means for designing model tests and for correlating and interpreting test results.

It has been demonstrated in References 10 to 12 that the model law for high explosives can be determined by a consideration of the equations describing the motion of a shocked fluid. In essence, this law states that "pressure and other properties of the shock wave will be unchanged if the length and time scales are changed by the same factor, n , as the dimensions of the explosive loading source", that is:

$$L_p = nL_m \quad (1)$$

$$T_p = nT_m \quad (2)$$

$$W_p = n^3W_m \quad (3)$$

where L , T , and W are dimensional symbols for length, time and charge weight, respectively, and the subscript p designates the prototype and m designates the model. Since the density scale must therefore be unity, the scaling factor for the mass of the explosive is:

$$M_p = n^3M_m \quad (4)$$

where M is the dimensional symbol for mass.

It has been shown in Reference 10 that the same geometric scaling which governs the shock transmission process also provides the proper modeling for the structural response to the pressures generated during the blast process. The motion of the structure due to the applied blast loads is expressed by Newton's second law, $F = M(T)^{-2}L$, and it follows that:

$$F_p = n^2F_m \quad (5)$$

where F is the dimensional symbol for force. those structures where the mode of action is primarily in the plastic range, similitude between the model and the prototype systems will be realized when the dimensionless ratio of the external work to the stored strain energy is the same for both systems, that is, the kinetic energy, associated with the momentum of the structure, imparted by the blast loads will be numerically equal to the strain or potential energy of the structure for both the model and prototype systems.

The kinetic energy may be expressed in terms of the impulse, I , of the blast loads or $KE = I^2/2M$, where the impulse is a function of force and time. Therefore:

$$(KE)_p = n^3(KE)_m \quad (6)$$

The potential energy of a structure is numerically equal to the area under its resistance-deflection curve and, therefore, is a function of force and length. Thus:

$$(PE)_p = n^3(PE)_m \quad (7)$$

On the basis of the above relationships, it may be concluded that the similarity principle which applies to the blast loads applies equally well to the modeling of the structural response to the transient forces generated by the interaction of the blast waves and the structure. Certain limitations do appear in application of these scaling laws. The rate of strain associated with the structural response of the prototype may differ significantly from that of the model. This variation will depend on the model size and differences in the materials used in both systems.

According to the scaling laws, the strains in the model and prototype are identical whereas the time scale for the model is $1/n$ times that of the prototype. Hence, the strain rate for the model is $1/n$ times that of the prototype:

$$\frac{d\epsilon_m}{dt} = (1/n) \frac{d\epsilon_p}{dt} \quad (8)$$

In assessing the effects of strain rate on model response, it is first necessary to predict the effect to be expected from the physical properties of the materials. Under the rapid rates of strain that occur in structural elements subjected to blast loads, both the reinforcement and concrete exhibit higher strengths than in the case of statically loaded elements. Hence, it would be expected that the model test data will provide an over-estimate of the storage capabilities of the prototype since the model is strained at a faster rate and thereby has "increased" strength.

It is apparent that strain rates are greater for smaller models than for larger models at the same maximum levels of strain. Hence, at any given scaled distance, the greater the effect of strain rate on similitude, the larger the scale factor n . Since the effect is to "strengthen" the models, maximum strains at equal scaled distances will be less for smaller models.

For small values of n (large models), the difference in strain rate effects between the model and prototype structures should be small, so that approximate coincidence can be maintained for maximum strain versus scaled distance. Under such conditions the scaled distance which causes incipient flexural failure in the model should likewise cause similar failure in the prototype. Differences between the responses will become more pronounced as n increases. If responses are limited to the elastic range strain rate, the effects should not be significant regardless of the scale factor since the elastic modulus of the reinforcing steel is unaffected and that of the concrete is affected only slightly.

Another limitation imposed by the scaling laws is due to the invariance of gravitational forces which will distort the scaling effects for parameters such as dead loads and distances traveled by fragments. In blast-resistant design the effects of dead loads and other such physical parameters will usually be small in comparison to the effects of the blast environment and, therefore, may usually be neglected in the model design.

With the "ideal" scale for length, time and force (or mass), it is possible to derive an ideal scale for each specific parameter involved in the model design. These scales are obtained by proceeding in a manner already described for kinetic and potential energies. A summary of the more pertinent quantities and their ideal scales is presented in Table A-1.

TABLE A-1 - COMPUTATIONS OF IDEAL SCALES

<u>Quantity</u>	<u>Symbol</u>	<u>Typical Units</u>	<u>Ideal Scale</u>
Length of Slab	L	ft.	$L_p/L_m = n$
Depth of Slab	d	ft.	$d_p/d_m = n$
Area of Slab	A	ft ²	$A_p/A_m = n^2$
Mass of Slab	M	lb-sec ² /ft	$M_p/M_m = n^3$
Area of Reinf.	A _s	in. ²	$A_{sp}/A_{sm} = n^2$
Area of Reinf./ft.	A' _s	in.	$A'_{sp}/A'_{sm} = n$
Unit Resistance	w	lb/in ²	$w_p/w_m = 1$
Total Resistance	R	lb.	$R_p/R_m = n^2$
Charge Weight	W	lb.	$W_p/W_m = n^3$
Distance	r	ft.	$r_p/r_m = n$
Scaled Distance	Z	ft/lb ^{1/3}	$Z_p/Z_m = 1$
Total Impulse	I	lb-ms.	$I_p/I_m = n^3$
Unit Impulse	i	lb-ms/in ²	$i_p/i_m = n$
Scaled Impulse	I	lb-ms/in ² -lb ^{1/3}	$I_p/I_m = 1$
Pressure	P	lb/in ²	$P_p/P_m = 1$
Kinetic Energy	KE	ft-lb.	$KE_p/KE_m = n^3$
Density	ρ	lb-sec ² /ft ⁴	$ρ_p/ρ_m = 1$
Elastic Modulus	E	lb/in ²	$E_p/E_m = 1$

TABLE A-1 - COMPUTATIONS OF IDEAL SCALES (Cont'd)

<u>Quantity</u>	<u>Symbol</u>	<u>Typical Units</u>	<u>Ideal Scale</u>
Deflection	δ	in.	$\delta_p/\delta_m = n$
Moment	M	ft-lb.	$M_p/M_m = n^3$
Moment/ft.	\bar{M}	lb.	$\bar{M}_p/\bar{M}_m = n^2$
Shear	V	lb.	$V_p/V_m = n^2$
Shear/ft.	\bar{V}	lb/ft	$\bar{V}_p/\bar{V}_m = n$
Stress	σ	lb/in ²	$\sigma_p/\sigma_m = 1$
Strain	ϵ	in/in	$\epsilon_p/\epsilon_m = 1$
Velocity	v	ft/sec	$v_p/v_m = 1$
Time	t	sec	$t_p/t_m = n$
Moment of Inertia	I	in ⁴	$I_p/I_m = n^4$
Frequency	f	cycles/sec	$f_p/f_m = 1/n$

APPENDIX B

**ANALYSIS OF DYNAMIC RESPONSE OF
BACK WALL OF FULL SCALE BAY STRUCTURE
(ROUND NO. 1)**

SECTION B.1

INTRODUCTION

1. General

This structure was designed as part of the scaling investigation tests of the bay-type (cubicle) explosive structure utilizing composite wall construction (two concrete panels separated by sand fill). The tests included one-tenth, one-eighth, and one-third scale models and the full scale structure. The full scale structure was initially tested using a spherical charge of 2,000 pounds of Composition B located at the center of the cubicle. Three subsequent tests were performed on the same structure using spherical charges of 3,000 pounds of Composition B in the second round, and 5,000 and 7,500 pounds of TWT in rounds three and four, respectively.

The data presented in this appendix pertains to the analysis of the dynamic response of the back wall resulting from the 2,000 pound test (Round No. 1).

2. Method of Analysis

In general, the analysis of a structure subjected to H. E. type blast loadings may be based on the solution of the equation of motion,

$$F - R = Ma$$

where F is the applied blast force, R is the resistance the structure offers against motion, M is the mass of an equivalent single-degree-of-freedom system and, a is the acceleration of the mass. This equation of motion can be readily solved by any of several numerical integration methods. The method employed in this appendix for analyzing the response of the back wall is the semi-graphical method of analysis described in Reference B-1 which provides the analytical means of obtaining the applied blast force and the associated structural response of the member.

To evaluate the test results, a procedure for the structural analysis was developed whereby the potential energy of the resisting element was determined and then compared to the kinetic energy of the element induced by the applied blast loads. The applied blast loading was obtained utilizing the procedures of Reference B-1 which are based on semi-empirical data developed from impulse load tests previously performed. The structure response (potential energy) on the other hand was calculated using the analytical relationships presented in Reference B-1.

However, to solve these relationships, values for some of the terms involved were ascertained from the test data. For example, the ultimate flexural and shear capacities of the wall panels were based on the results of tension tests of the reinforcing steel and compression tests of concrete cylinders. In addition, the deflection criteria required for the solution of the structure response equations was obtained from electronic deflection-time measurements taken during the test. This data in combination with density measurements of the sand fill was sufficient to specify the overall structural response of the composite wall.

The above test evaluation procedure differs from most test evaluation methods in which overall test results are compared with similar data obtained by analytical means. This variation in procedure was predetermined by the solution of the response of composite walls which requires that the response of the individual panels be known before the response of the overall wall can be evaluated.

SECTION B.2

APPLIED BLAST LOADING

1. General

At close distances from high explosive detonations, the peak pressures associated with the shock front are extremely high and the duration of the blast wave is relatively short, thereby, producing an impulse (area under pressure-time curve) loading in which the actual pressure-time relationship is not required for the analytical solution of the structure response.

When an explosion occurs within a cubicle, amplification of the initial shock front due to reflections within the structure occurs. At any given point on a particular surface, the total impulse loading is a combination of the contributions from the initial shock and from the shock reflected from adjacent surfaces.

A method of calculating the average blast impulse (Reference B-1) was developed using a theoretical procedure based on semi-empirical blast data. The total reflected impulses acting at various points on each surface of the cubicle were calculated and then integrated to obtain the total impulse load. The total impulse was assumed to be distributed uniformly giving an average value of the impulse acting on any one surface.

The use of the average impulse load is based on the assumption that the structural element subjected to the blast loading is capable of transferring the localized high shear stresses produced by the high intensity and highly irregular blast loads to regions of lower stress. For the case at hand, where the concrete portions of the structure are reinforced with lacing, this shear transfer will take place.

2. Average Impulse Load

Structural and Charge Parameters

The average impulse load acting on an element of a cubicle-type structure is a function of the configuration and size of the structure, and the size, type, shape and location of the explosive within the structure. The cubicle configuration and charge location parameters are given in Figure B-1.

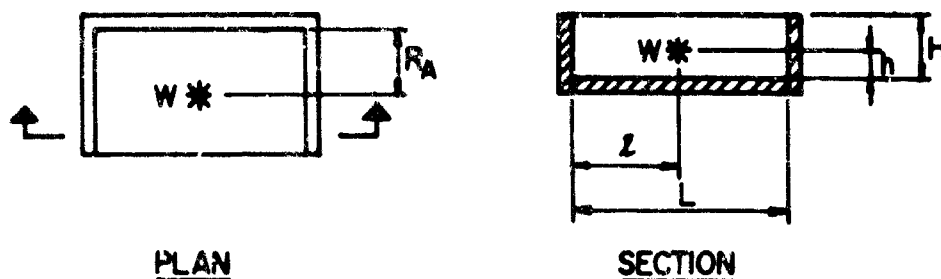


FIGURE B-1
CUBICLE CONFIGURATION AND CHARGE LOCATION PARAMETERS

Charge Characteristics

The impulse load charts of Reference B-1 were prepared based on the blast output of bare spherical TNT charges. However, the data may be extended to other explosives with various shapes by equating their blast output to that of TNT, that is, obtaining the TNT equivalent of the explosive in question. Equivalent weight ratios (weight of given explosive to that of TNT) for both peak pressure and impulse are given in Table 4-1 of Reference B-1.

Since the actual charge is spherical, shape is not a factor in determining its equivalent. Hence, for an impulse loading the TNT equivalent of the 2,000 pound charge of Composition B is:

$$W = 2000 (1.06) = 2120 \text{ lbs}$$

Charge Location Parameters

Normal Distance to Back Wall - $R_A = 10 \text{ ft.}$

Height of Charge - $h = 5 \text{ ft}$

Location Relative to Side Wall - $z = 20 \text{ ft}$

Structural Characteristics

Type - element with three adjacent reflecting surfaces ($N = 3$)

Length - $L = 40 \text{ ft}$

Height - $H = 10 \text{ ft}$

Impulse Load Chart Parameters

The required chart parameters are listed in Figure 4-15 of Reference B-1.

$$Z_A = \frac{R_A}{W^{1/2}} = \frac{10}{(2120)^{1/2}} = 0.778 \text{ ft/lb}^{1/2}$$

$$\frac{l}{L} = \frac{20}{40} = 0.5$$

$$\frac{h}{H} = \frac{5}{10} = 0.5$$

$$\frac{L}{H} = \frac{40}{10} = 4$$

$$\frac{L}{R_A} = \frac{40}{10} = 4$$

Blast Impulse Load

The blast impulse load acting on the back wall is determined from Figure 4-51 of Reference B-1 (see Figure 4-16 of Reference B-1 for $N = 3$, $h/H = 0.5$ and $l/L = 0.5$). Interpolation is required for $Z_A = 0.778$ and $L/H = 4$.

Interpolation for Z_A and L/H

The scaled impulse is obtained from Figure 4-51 for the required L/R_A for various values of Z_A and L/H . These values are presented in Table B-1 and plotted in Figure B-2. For the required L/H , scaled impulses are read from Figure B-2, tabulated in Table B-1 and plotted in Figure B-3.

TABLE B-1

$Z_A \backslash L/H$	0.75	1.50	3	6	4 (1)
0.35	640	775	1520	2050	1840
0.50	395	495	850	1090	990
0.75	224	328	465	565	515
1.00	153	215	305	350	335
1.50	108	127	175	203	191
3.00	59	67	81	88	85

(1) From Figure B-2

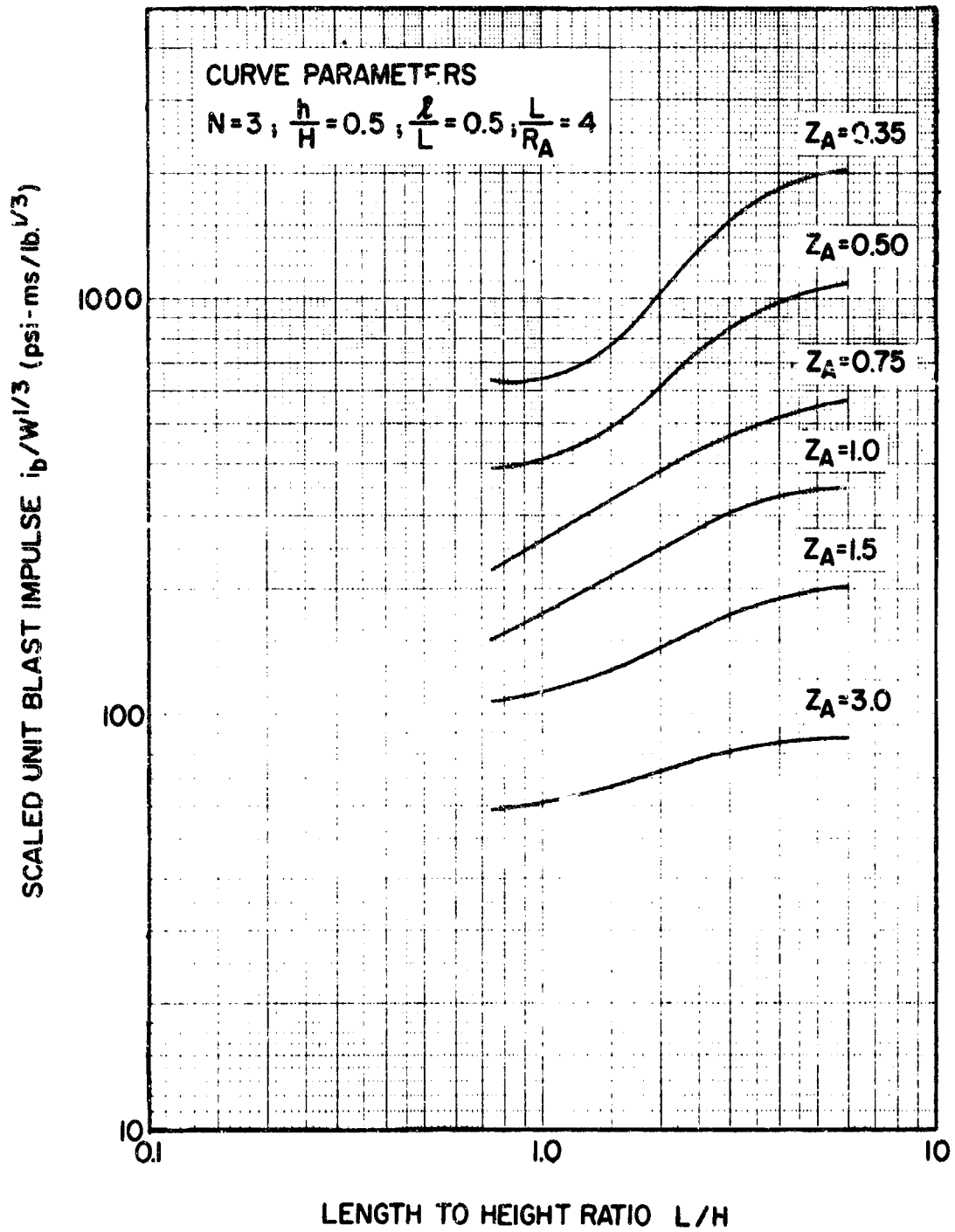


FIGURE B-2
 INTERPOLATION OF SCALED UNIT BLAST IMPULSE FOR L/H

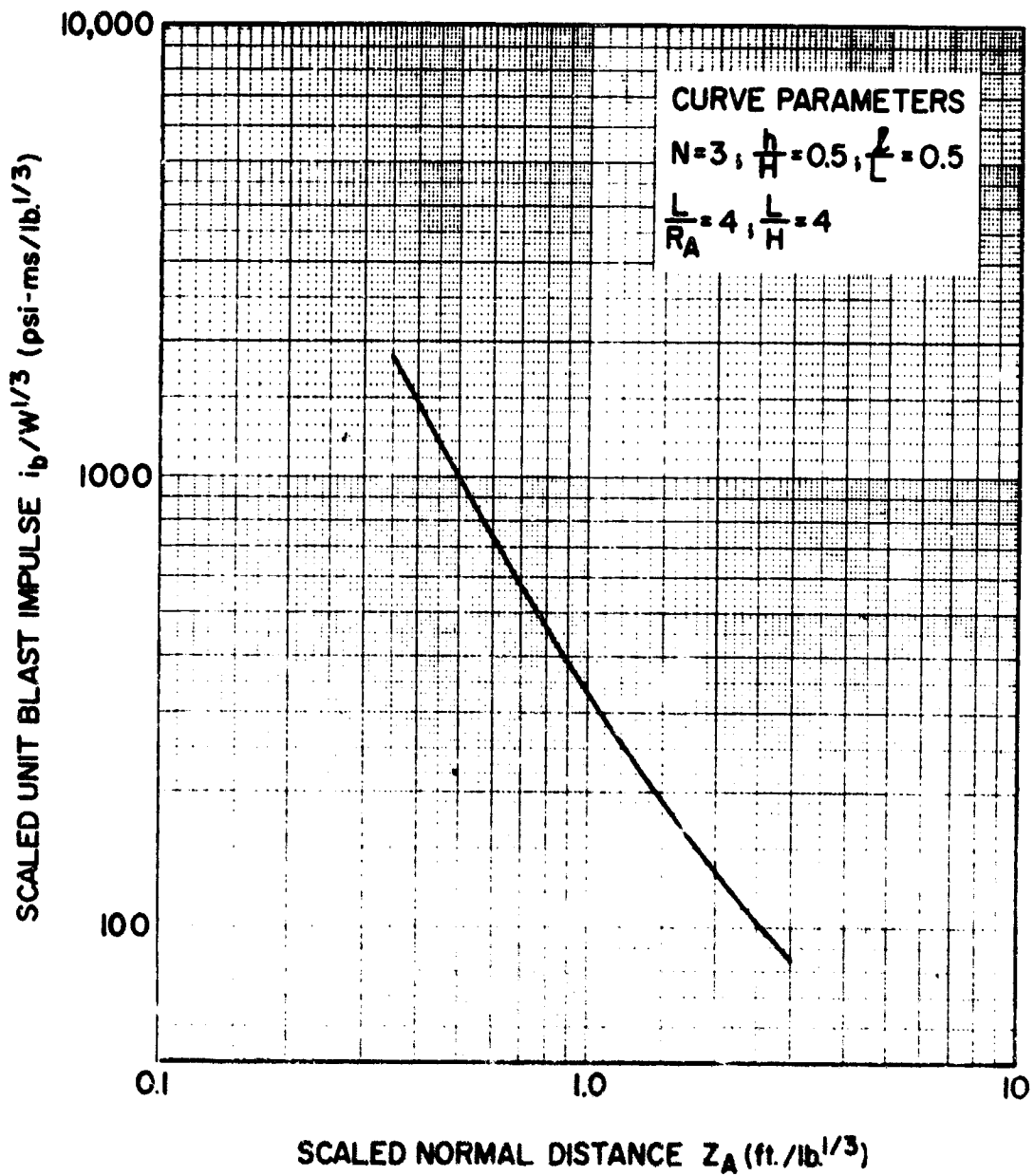


FIGURE B-3
 INTERPOLATION OF SCALED UNIT BLAST IMPULSE FOR Z_A

Average Impulse Load

From Figure B-2 for $Z_A = 0.778$,

$$\frac{I_b}{W^{1/2}} = 485 \text{ psi-ms/lb}^{1/2}$$

3. Duration of Applied Load

The duration of the applied pressures acting on the entire element is estimated by adding the time increments corresponding to the time required for the blast wave to fully engulf the element and the duration of the blast load at the section of the element furthest removed from the explosion. This relationship is represented by Equation 4-1 of Reference B-1:

$$t_o = (t_A)_F - (t_A)_A + 1.5 (t_o)_F$$

where:

$$\begin{aligned} t_o &= \text{duration of load (ms)} \\ (t_A)_F &= \text{arrival time of the blast wave at the point on the element furthest from the explosion (ms)} \\ (t_A)_A &= \text{arrival time of the blast wave at the point on the element nearest to the explosion (ms)} \\ (t_o)_F &= \text{duration of the blast pressure at the point on the element furthest from the explosion (ms)} \end{aligned}$$

The arrival time of the blast wave for the two points of interest as well as the duration of the load at the furthest point on the element are obtained from Figure 4-5 of Reference B-1.

Arrival Time and Load Duration at Furthest Point

$$R = \sqrt{(10)^2 + (5)^2 + (20)^2} = 22.9 \text{ ft}$$

$$Z = \frac{R}{W^{1/2}} = \frac{22.9}{(2120)^{1/2}} = 1.78 \text{ ft/lb}^{1/2}$$

$$\frac{t_A}{W^{1/2}} = 0.21 \text{ ms/lb}^{1/2} \therefore t_A = 0.21 (2120)^{1/2} = 2.70 \text{ ms}$$

$$\frac{t_o}{W^{1/2}} = 0.119 \text{ ms/lb}^{1/2} \therefore t_o = 0.119 (2120)^{1/2} = 1.53 \text{ ms}$$

Arrival Time at Nearest Point

$$Z_A = 0.778 \text{ ft/lb}^{1/2}$$

$$\frac{t_A}{W^{1/2}} = 0.049 \text{ ms/lb}^{1/2} \quad \therefore t_A = 0.049 (2120)^{1/2} = 0.63 \text{ ms}$$

Duration of Load on Back Wall

$$t_o = 2.70 - 0.63 + 1.5 (1.53) = 4.37 \text{ ms}$$

SECTION B.3

IMPULSE CAPACITY OF BACK WALL

1. General

Strength Criteria

The ultimate strength of the back wall was calculated in accordance with ultimate strength theory (Reference B-1) using average stresses obtained from post-shot compression cylinder and reinforcement bar tension tests. The average ultimate compressive strength of the concrete cylinders was 4,935 psi. The reinforcing steel was high-strength reinforcing bars conforming to ASTM specification A615 Grade 60 and had static yield and ultimate stresses as shown in Table B-3.

Under the rapid rates of strain which occur in structural elements subjected to blast loads, both the reinforcement and the concrete exhibit higher strengths than when the element is loaded slowly (static condition). The ratio of the dynamic to static stresses is known as the dynamic increase factor (DIF).

In flexural members the above increase in capacity is primarily a function of the rate of strain of the reinforcement and in particular the time required to yield the reinforcing steel. Therefore, to establish the dynamic stresses, the static deflection at yield was calculated for the wall panels using the average yield stresses of the reinforcement and the average static ultimate compressive strength of the concrete. This deflection was then compared to that of the deflection-time history obtained from the test to determine the time to reach yield for each panel. The times to reach yield were then utilized to determine the dynamic increase factors (References B-2 and B-3) for each panel. In this example the time to reach ultimate strength of the concrete was assumed equal to the time to reach yield of the reinforcing steel.

For an element which responds in the plastic range, the magnitude of the reinforcement stresses in the strain hardening region cannot be related directly to the strains. However, an average stress can be estimated by approximating the energy absorbed in the post-yield and strain hardening regions of the reinforcement (Figure B-4).

For the problem at hand, the above approximation of the average stress was achieved by relating the average stress to the deflection of the wall panel according to the procedure of Reference B-1.

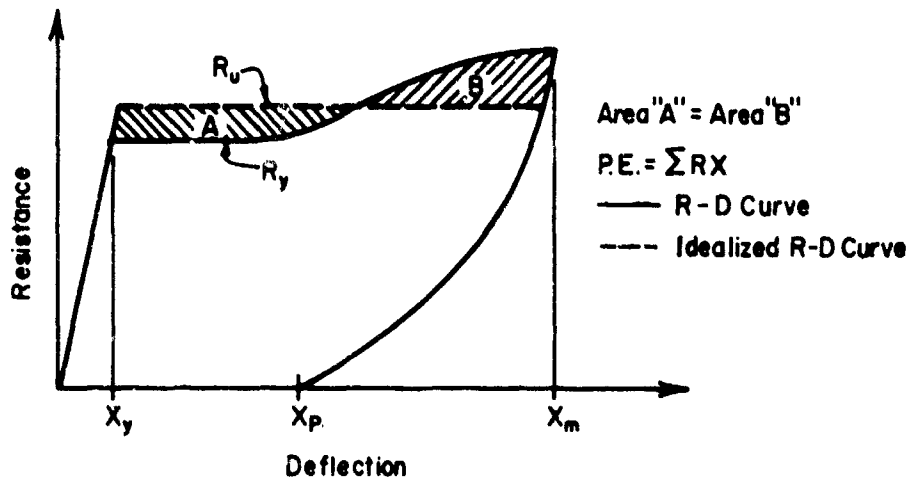


FIGURE B-4
IDEALIZED RESISTANCE-DEFLECTION CURVE OF WALL PANEL

The ultimate dynamic resistance of each panel was calculated using dynamic stresses (static stress multiplied by dynamic increase factor) for both the concrete and reinforcement. Dynamic yield stresses for the reinforcement were used for the receiver panel since the panel deflected in the post-yield range. However, since the donor panel deflected in the strain hardening region, an average dynamic stress was used to approximate the energy absorbed.

The shear capacity of each panel was checked to determine if the ultimate dynamic flexural strength was fully developed. Although the ultimate shear capacity of an element may be increased due to rapid strain rates, the effects of rapid straining were not considered for either the concrete or lacing reinforcement due to a lack of data pertaining to the increase in strength.

Dynamic Analysis

The semi-graphical method of analysis as presented in Reference B-1 is used to solve the equation of motion and, thereby, obtain the dynamic response of the back wall. In this method it is assumed that the fictitious positive phase duration of the load (t_0) is small in comparison to the time the wall takes to reach its maximum deflection (t_m). This assumption is verified in subsequent sections. Therefore, the flexural capacity which

an element must develop to resist the applied blast load may be obtained by equating the initial kinetic energy resulting from the applied blast impulse to the potential energy of the element (Figure B-5).

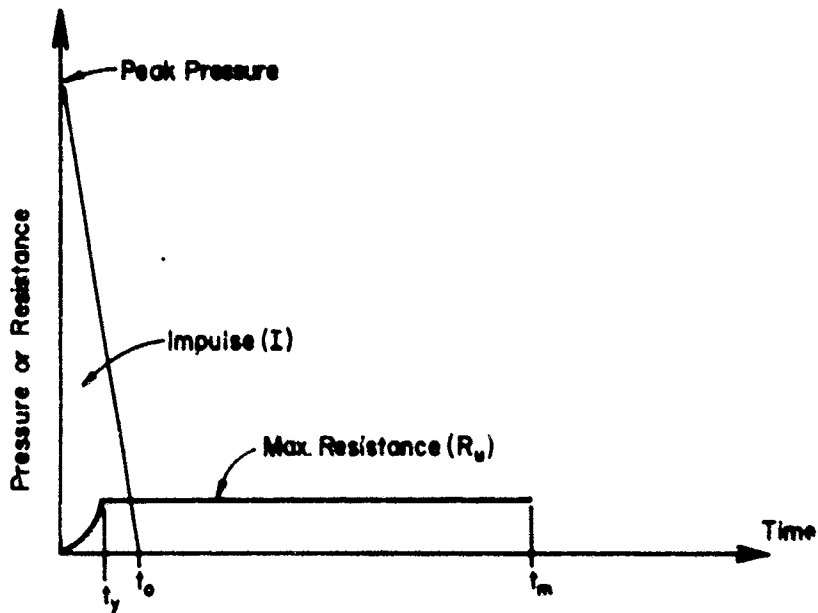


FIGURE B-5
IDEALIZED PRESSURE-TIME AND
RESISTANCE-TIME CURVES

Based upon the above method, the basic relationships for this analysis are:

$$F - R = M\ddot{X}$$

$$\int (F - R) dt = \int M dv$$

$$I = Mv$$

$$K.E. = \frac{1}{2} Mv^2 = \frac{I^2}{2M}$$

$$P.E. = I(RX)$$

where:

F = applied load (lbs)
R = resistance of the element opposing the load (lbs)
M = effective mass (single-degree-of-freedom system)
of the element (lb-sec² per ft)
 \ddot{X} = acceleration of the mass (ft per sec²)
t = time (sec)
v = velocity (fps)
I = impulse load acting on the element (lb-sec)
K.E. = Kinetic energy of the element produced by the
applied loads, (lb-ft)
P.E. = potential energy of the element (lb-ft)
X = maximum deflection (in)

By equating the kinetic energy to the potential energy of the wall, the equation for the impulse absorbed by an element due to flexure becomes:

$$I^2 = 2 \Sigma(MRX)$$

While the unit impulse absorbed is:

$$i^2 = 2 \Sigma(mrX)$$

where the values of m and r are the mass and resistance per unit area of the wall.

For the solution of the above equation, the actual element is replaced by a single-degree-of-freedom system whose dynamic properties consist of the mass, resistance and deflection. To obtain a single-degree-of-freedom system, the mass of the element is replaced by an equivalent mass while the deflection, in the expression for the potential energy, is that which occurs at the point on the wall undergoing the largest displacement. The resistance (r) is the bending resistance provided by the actual element resulting from dynamic straining.

Because the back wall of the bay structure is of composite construction (two concrete panels separated by sand fill), a portion of the blast impulse load is absorbed by dispersion (with distance) in the concrete and sand, and by compression of the sand. This attenuated impulse is calculated in accordance with the procedures of Reference B-1.

2. Structural Properties of Wall (Figure B-6)

Properties of Reinforcement

TABLE B-2

Bar Size	Direction	Diameter (in.)	Area (Sq.in.)	Spacing (in.)	Area/Foot (Sq.in./ft.)
5 (1)	E. W.	0.625	0.31	Varies	-
7	Vert.	0.875	0.60	9.93	0.726
9	Vert.	1.128	1.00	10.13	1.183
7	Horiz.	0.875	0.60	10.13	0.712
9	Horiz.	1.128	1.00	10.13	1.183

(1) Lacing (shear) reinforcement

Effective Slab Depth (d)

Total panel thickness (T_c) = 24.0 in.

Concrete cover = 1.375 in.

d (No. 7 Vertical) = 24.0 - 1.375 - 0.437 = 22.188 in.

d (No. 9 Vertical) = 24.0 - 1.375 - 0.564 = 22.061 in.

d (No. 7 Horizontal) = 24.0 - 1.375 - 1.128 - 0.437
= 21.060 in.

d (No. 9 Horizontal) = 24.0 - 1.375 - 1.128 - 0.564
= 20.933 in.

Static Stresses

Concrete

f'_c = 4935 psi - Average of 28 day concrete cylinder tests

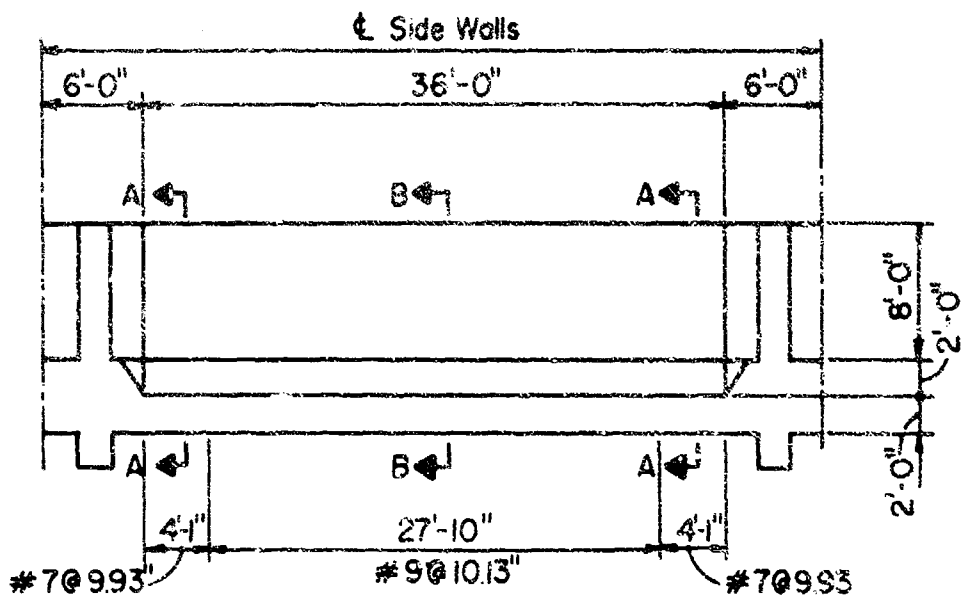
Reinforcing Bars

TABLE B-3

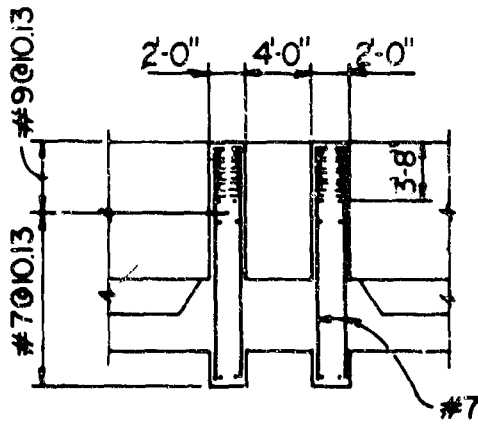
Bar Size	Yield Stress (f_y) (psi) (1)	Ult. Stress (f_u) (psi) (1)	Avg. Stress (f_a) (psi) (2)
5	71,990	100,000	78,990
7	65,140	98,560	73,000
9	73,700	108,000	82,280

(1) Average stress obtained from ten (10) test specimens

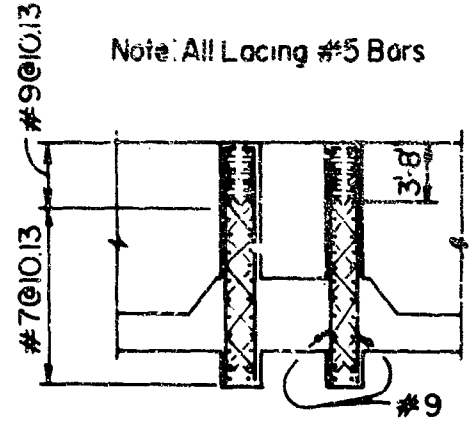
(2) $f_a = f_y + (f_u - f_y)/4$



FRONT ELEVATION



SECTION A-A



SECTION B-B

Note: All Lacing #5 Bars

FIGURE B-6
STRUCTURAL PROPERTIES OF BACK WALL

3. Static Resistance at Yield for Each Panel

The static resistance of each panel when yielding of the reinforcement occurs is determined by use of yield line procedures (Ref. B-1) in which the yield lines are determined from the condition that the unit resistance must be equal for all the sectors formed.

For the problem at hand, the wall panel is divided into sectors I and II by the positive and negative yield lines (Figure B-7). The negative yield lines form at the edge of the two-foot concrete haunches (Figure B-7) resulting in span lengths of 8 feet and 36 feet in the vertical and horizontal directions, respectively. Although the positive yield lines must be symmetrical due to the uniform concrete thickness and the symmetrical placement of the reinforcement within the panel, their position is unknown and, therefore, is given by the unknown quantity x .

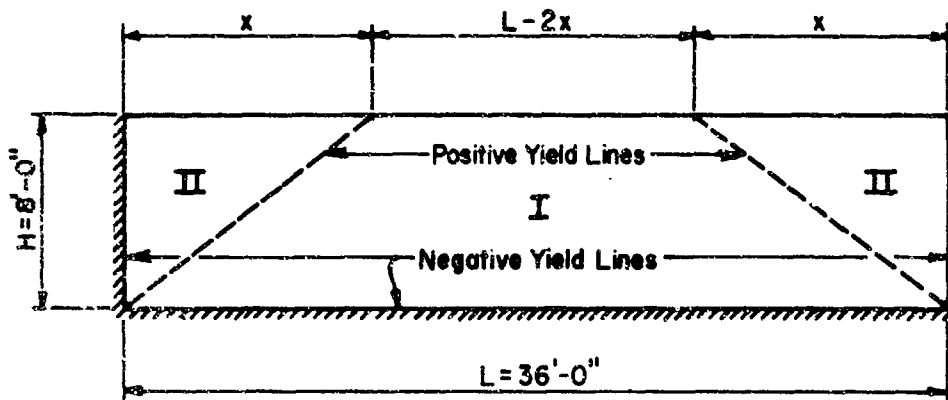


FIGURE B-7
ELEVATION OF BACK WALL
SHOWING YIELD LINE PATTERN

The unit resistance is established in terms of an unknown distance x for each sector by satisfying the equilibrium requirements of each sector. Considering the free body diagram of each sector (Figures B-8 and B-9), the summation of the moments about the axis of rotation is:

$$R_u c = EM_N + EM_P$$

where:

$$R_u = r_u A = \text{Total static resistance of the sector (Kips)}$$

r_u = Unit static resistance of wall panel (Kips per sq. ft.)

A = Area of sector (sq. ft.)

c = Centroidal distance (ft)

M_N = Total negative moment capacity of sector (Kip-ft)

M_P = Total positive moment capacity of sector (Kip-ft)

In computing the total moment capacity of each sector, corner effects must be considered. The corner sections are stiff in comparison to the remainder of the panel; therefore, straining of the reinforcement which is associated with the reduced rotations at these sections will be less. This variation is approximated by: (1) dividing the wall panel into mid and corner strips defined by the lengths $x/2$ and $H/2$ in the horizontal and vertical directions, respectively (Figures B-8 and B-9), (2) taking full straining of the reinforcement along the positive and negative yield lines in the mid strips in both the horizontal and vertical directions and, (3) assuming the reinforcement along the positive and negative yield lines in the corner strips in both the vertical and horizontal directions is strained to two-thirds of the yield strain which occurs in the mid strip.

The moments developed along the yield lines are a function of the strains produced in the reinforcement. The #9 bars in the mid strip yield while those in the corner strip are strained to two-thirds of the yield stress. All #7 bars are in the corner strip and they are strained to the lesser of either their yield stress or two-thirds of the yield stress of the #9 bars in the mid strip (constant modulus of elasticity). The moment capacity per foot of reinforcement in the various strips for either positive or negative moments in either the vertical or horizontal directions is denoted as:

M = moment capacity of #9 bars in the mid strip

M' = moment capacity of #9 bars in the corner strip

M'' = moment capacity of #7 bars in the corner strip

Static Stresses

From Table B-3

f_y (No. 7 bars) = 65,140 psi = 65.14 ksi

f_y (No. 9 bars) = 73,700 psi = 73.70 ksi

$$f'_c = 4,935 \text{ psi} = 4.935 \text{ ksi}$$

Moment Capacity per Foot of Reinforcement

Ultimate moment capacity is a function of the depth of the compression stress block (a). Therefore,

$$M_u = A_s f_y \left(d - \frac{a}{2} \right)$$

where:

$$a = \frac{A_s f_y}{0.85 b f'_c} = \text{Depth of compression block (inches)}$$

A_s = Area of reinforcement (square inches per foot)

f_y = Yield stress of the reinforcement (psi)

b = Width of one-foot-wide strip (inches)

f'_c = Ultimate compressive strength of the concrete (psi)

Also, if the negative and positive reinforcement is the same, then

$$M_N = M_P$$

where:

M_N = Ultimate moment capacity of the negative reinforcement

M_P = Ultimate moment capacity of the positive reinforcement

Vertical No. 9 Bars

Full Capacity

$$a = \frac{1.183(73.7)}{0.85(12)(4.935)} = 1.732 \text{ in.}$$

$$M_{VN} = M_{VP} = \frac{1.183(73.7)}{12} \left[22.061 - \frac{1.732}{2} \right]$$

$$= 154.0 \text{ Kip-ft./ft.}$$

Reduced Capacity

$$a = \frac{1.183(2/3)(73.7)}{0.85(12)(4.935)} = 1.155 \text{ in.}$$

$$M'_{VN} = M'_{VP} = \frac{1.183(2/3)(73.7)}{12} \left[22.061 - \frac{1.155}{2} \right]$$
$$= 104.1 \text{ Kip-ft./ft.}$$

Horizontal No. 9 Bars

$$a = \frac{1.183(73.7)}{0.85(12)(4.935)} = 1.732 \text{ in.}$$

$$M_{HN} = M_{HP} = \frac{1.183(73.7)}{12} \left[20.933 - \frac{1.732}{2} \right]$$
$$= 145.8 \text{ Kip-ft./ft.}$$

Vertical No. 7 Bars

The No. 7 bars are stressed to two-thirds of the yield stress of the No. 9 bars since this stress is lower than the yield stress of the No. 7 bars.

$$a = \frac{0.726(2/3)(73.7)}{0.85(12)(4.935)} = 0.709 \text{ in.}$$

$$M''_{VN} = M''_{VP} = \frac{0.726(2/3)(73.7)}{12} \left[22.188 - \frac{0.709}{2} \right]$$
$$= 64.9 \text{ Kip-ft./ft.}$$

Horizontal No. 7 Bars

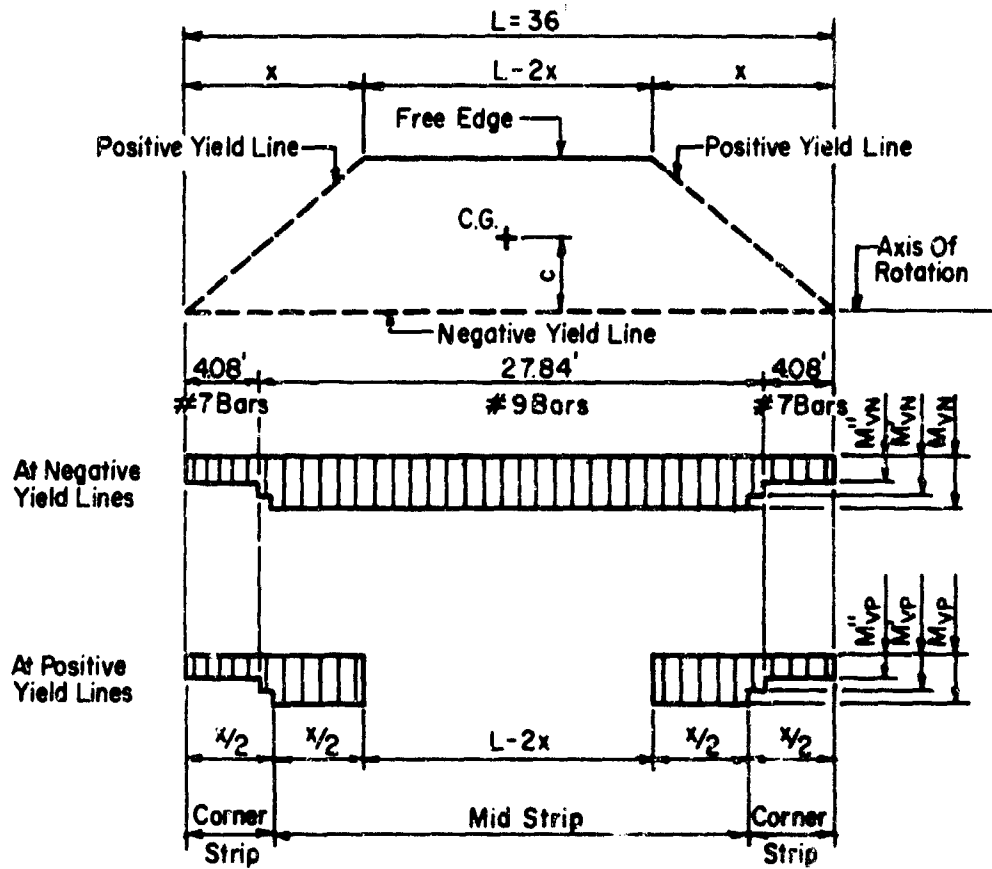
$$a = \frac{0.712(2/3)(73.7)}{0.85(12)(4.935)} = 0.695 \text{ in.}$$

$$M''_{HN} = M''_{HP} = \frac{0.712(2/3)(73.7)}{12} \left[21.060 - \frac{0.695}{2} \right]$$
$$= 60.4 \text{ Kip-ft./ft.}$$

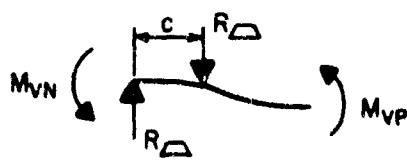
Unit Static Resistance of Sector I (Figure B-8)

Total Moment Capacity

The total moment capacity of a sector is equal to the sum



a. LAYOUT



b. FREE BODY DIAGRAM

FIGURE B-8
LAYOUT AND FREE BODY DIAGRAM OF SECTOR I

of the moment capacities of all the reinforcement crossing the yield lines and acting perpendicular to the axis of rotation (Figure B-8).

$$\begin{aligned} EM_N &= 2(4.08)(64.9) + 2\left(\frac{x}{2} - 4.08\right)(104.1) + (36-x)(154.0) \\ &= 5224 - 49.9x \end{aligned}$$

$$\begin{aligned} EM_P &= 2(4.08)(64.9) + 2\left(\frac{x}{2} - 4.08\right)(104.1) + 2\left(\frac{x}{2}\right)(154.0) \\ &= 258.1x - 320 \end{aligned}$$

$$EM_{\Delta} = EM_N + EM_P = 4904 + 208.2x$$

and,

$$R_{\Delta c} = r_u A_{\Delta c} = EM_{\Delta}$$

$$r_u \left[\frac{8[36 + (36 - 2x)]}{2} \right] \left[\frac{8[36 + 2(36 - 2x)]}{3[36 + (36 - 2x)]} \right]$$

Static Resistance

$$R_{\Delta c} = EM_{\Delta}$$

$$\therefore r_u = \frac{114.9 + 4.88x}{27 - x} \quad (1)$$

Unit Static Resistance of Sector II (Figure B-9)

Total Moment Capacity

$$EM_N = 4(60.4) + 4(145.8) = 824.8 \text{ Kip-ft.}$$

$$EM_P = EM_N = 824.8 \text{ Kip-ft.}$$

$$EM_{\Delta} = EM_N + EM_P = 1649.6 \text{ Kip-ft.}$$

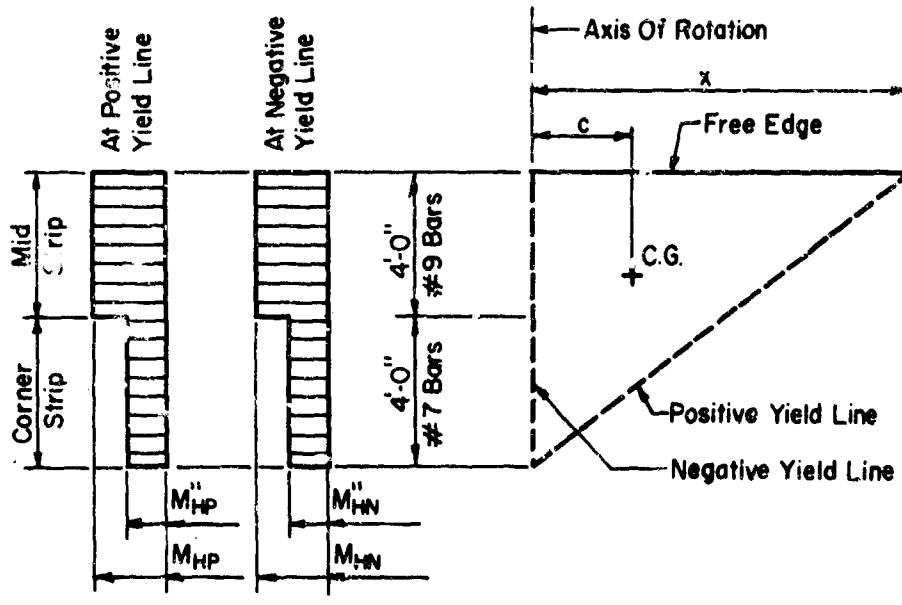
and,

$$R_{\Delta c} = r_u A_{\Delta c} = r_u \left(\frac{8x}{2} \right) \left(\frac{x}{3} \right)$$

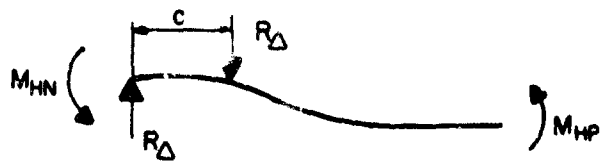
Static Resistance

$$R_{\Delta c} = EM_{\Delta}$$

$$\therefore r_u = \frac{1237.2}{x^2} \quad (2)$$



a. LAYOUT



b. FREE BODY DIAGRAM

FIGURE B-9
LAYOUT AND FREE BODY DIAGRAM OF SECTOR II

Location of Yield Lines

Since the unit resistance of all sectors must be equal,

$$\frac{114.9 + 4.88x}{27-x} = \frac{1237.2}{x^2}$$

Simplifying:

$$x^3 + 13.55x^2 + 253.5x - 6846 = 0$$

and the desired root is:

$$x = 10.89 \text{ ft.} = 130.7 \text{ in.}$$

Unit Static Resistance at Yield for Each Panel

The unit resistance is obtained by substituting the value of x into either equation (1) or (2), both of which give:

$$r_u = 10.43 \text{ Kips/sq.ft.} = 72.4 \text{ psi}$$

4. Static Resistance - Deflection Characteristics of Each Panel

In the elastic range of response, each panel of the wall is initially fixed on three adjoining sides and free on the fourth (top) side. As the panel deflects under the applied blast loads, the panel's resistance will increase uniformly until yield hinges are formed either at one or more supports and/or at the interior of the panel depending upon the length to height ratio of the panel and the amount of reinforcement at the points of maximum stress. After this first yield, the panel will deflect elasto-plastically with a different stiffness (resistance versus deflection). This change of stiffness will occur each time the panel yields until yielding occurs at all points of maximum stress at which time a flexural mechanism (ultimate strength) is formed.

The resistance-deflection curve for the elastic and elasto-plastic action of the panel is shown in Figure B-10. However, the actual curve may be replaced by an equivalent curve as indicated by the dotted lines in Figure B-10. The equivalent maximum elastic deflection and the equivalent stiffness are defined

such that the area under the dotted curve is equal to the area under the solid curve and, thereby, producing the same potential energy in each case.

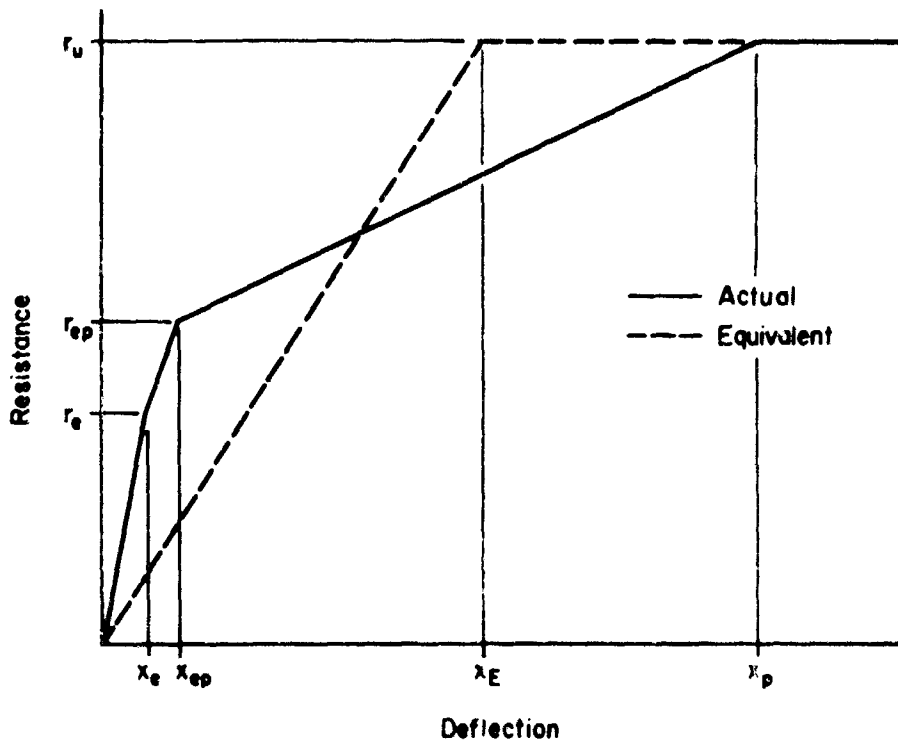


FIGURE B-10
ACTUAL AND EQUIVALENT RESISTANCE - DEFLECTION CURVES

Figure B-11 shows the critical locations P_2 and P_3 where yielding first occurs while P_1 is the point of maximum deflection. M_x indicates the moment capacity in the vertical direction, the maximum being first developed by yielding the reinforcement in the donor face of the panel at P_3 . M_y indicates the moment capacity in the horizontal direction, the maximum being first developed by yielding the reinforcement in the donor face of the panel at P_2 and the receiver face near P_1 . The means for calculating the various stiffnesses during the elastic and elasto-plastic action of the panels is given in Reference B-1 (Figures 5-14 thru 5-16) from which the coefficients (β and γ) necessary to calculate the resistance and deflection at the yield points have been obtained and are listed in Table B-4.

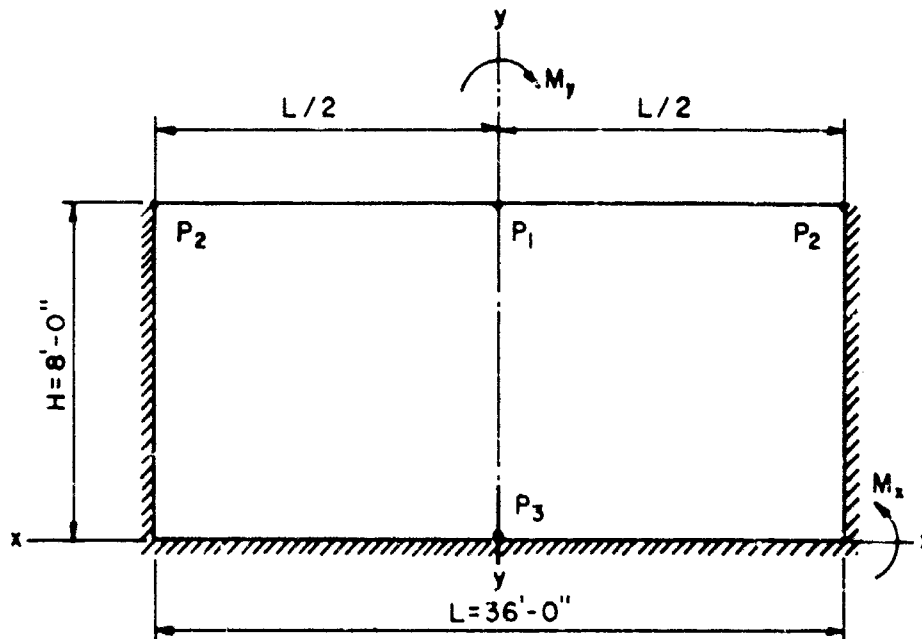


FIGURE B-11
ELEVATION OF WALL PANEL SHOWING LOCATION
OF CRITICAL POINTS IN ULTIMATE BENDING
FAILURE

Ultimate Moment Capacity in x and y Directions

At the points of maximum stress, P_2 and P_3 , the wall reinforcement consists of No. 9 bars and, therefore, the ultimate static moments at final yield are:

$$M_x = M_{VN} = 154.0 \text{ Kip-ft/ft}$$

$$M_y = M_{HN} = 145.8 \text{ Kip-ft/ft}$$

TABLE B-4
 STATIC PROPERTIES OF RECTANGULAR PLATES
 FOR VARIOUS SUPPORT CONDITIONS

Moment and Deflection	Three Sides Fixed and One Side Free	One Side Fixed, Two Sides Simple and One Side Free	Three Sides Simple and One Side Free
$M_y(P_1)$	$0.030 rH^2$	$0.039 rH^2$	$0.315 rH^2$
$M_y(P_2)$	$0.570 rH^2$	---	---
$M_x(P_3)$	$0.415 rH^2$	$0.468 rH^2$	---
$XEI(P_1)$	$0.005 rH^4$	$0.110 rH^4$	$0.800 rH^4$

Note: Poisson's ratio for reinforced concrete is usually taken to vary between 0.10 and 0.167. In this analysis, Poisson's ratio has been varied between 0.167 and 0.3 depending on the wall support conditions considered. Previous experience has indicated that the effect of Poisson's ratio may be considered negligible over the entire range from elastic to plastic behavior of the structural member.

Properties at First Yield

Unit Resistance (r) Expressed in Terms of Wall Height (H)

$$M_y(P_2) = M_{HN} = 145.8 = 0.57 r(P_2)H^2$$

$$\therefore r(P_2) = \frac{256}{H^2}$$

$$M_x(P_3) = M_{VN} = 154.0 = 0.415r(P_3)H^2$$

$$\therefore r(P_3) = \frac{371}{H^2}$$

NOTE: Because $r(P_2) < r(P_3)$, the reinforcement will yield first at P_2 . Therefore, the panel will then assume a simple-simple-free stiffness.

Unit Resistance at First Yield at (P₂)

$$r_e = r(P_2) = \frac{256}{(8)^2} = 4.0 \text{ Kips/sq.ft.}$$

Positive Moment at P₁

$$M_p(r_e) = 0.030 r_e H^2 = 0.030(4.0)(8)^2 = 7.7 \text{ Kip-ft./ft.}$$

Negative Moment at P₃

$$\begin{aligned} M_N(r_e) &= 0.415 r_e H^2 = 0.415(4.0)(8)^2 \\ &= 106.2 \text{ Kip-ft./ft.} \end{aligned}$$

Deflection at P₁

$$\begin{aligned} X_e EI(P_1) &= 0.085 r_e H^4 = 0.085(4.0)(8)^4(144) \\ &= 2.00 \times 10^5 \text{ Kip-in}^2 \end{aligned}$$

Properties at Second Yield

Change in Unit Resistance (Δr) Expressed in Terms of (H)

$$\begin{aligned} M_y(P_1) &= M_{HN} - M_p(r_e) = 145.8 - 7.7 = 138.1 \\ &= 0.039 \Delta r (P_1)H^2 \therefore \Delta r(P_1) = \frac{3541}{H^2} \end{aligned}$$

$$M_x(P_3) = M_V - M_N(r_e) = 154.0 - 106.2 = 47.8$$

$$= 0.468 \Delta_r(P_3) H^2 \therefore \Delta_r(P_3) = \frac{102.1}{H^2}$$

NOTE: Because $r(P_3) < r(P_1)$, the reinforcement will yield at location P_3 next. Therefore, the panel will then assume a simple-simple-simple-free stiffness.

Change in Unit Resistance Between the First and Second Yield

$$\Delta r = \Delta r(P_3) = \frac{102.1}{(8)^2} = 1.6 \text{ Kips/sq.ft.}$$

Change in Deflection at P_1 Between First and Second Yield

$$\Delta X EI(P_1) = 0.110 \Delta r H^4 = 0.110(1.6)(8)^4(144)$$

$$= 1.04 \times 10^5 \text{ Kip-in}^2$$

Total Deflection at P_1

$$X_{ep} EI(P_1) = (2.00 + 1.04)10^5 = 3.04 \times 10^5 \text{ Kip-in}^2$$

Total Unit Resistance

$$r_{ep} = 4.0 + 1.6 = 5.6 \text{ Kips/sq.ft.}$$

Properties at Final Yield

Change in Unit Resistance Between Second and Final Yield

$$\Delta r = r_u - r_{ep} = 10.43 - 5.60$$

$$= 4.83 \text{ Kips/sq.ft.}$$

Change in Deflection at P_1 Between Second and Final Yield

$$\Delta X EI(P_1) = 0.80 \Delta r H^4 = 0.80(4.83)(8)^4(144)$$

$$= 22.79 \times 10^5 \text{ Kip-in}^2$$

Total Deflection at P₁

$$\sum EI(P_1) = (3.04 + 22.79)10^5 = 25.83 \times 10^5 \text{ Kip-in}^2$$

Total Unit Resistance

$$r_u = 10.43 \text{ Kips/sq.ft.}$$

Determination of Deflection at Final Yield (Location P₁)

Modulus of Elasticity

E_c = Modulus for Concrete

E_s = Modulus for Steel

$$\begin{aligned} E_c &= w^{1.5}(33)\sqrt{f'_c} = (150)^{1.5}(33)\sqrt{4935} \\ &= 4.27 \times 10^6 \text{ psi (Ref. B-1)} \end{aligned}$$

$$E_s = 29 \times 10^6 \text{ psi}$$

$$n = \frac{E_s}{E_c} = \frac{29}{4.27} = 6.79$$

Weighted Percent Reinforcement (p_w) For Entire Panel

$$p_w = \frac{A_s}{bd_v}$$

where:

A_s = Total area of reinforcement acting along supports (sq. in.)

b = Length of supports (in.)

d_v = Weighted effective depth (in.)

Therefore,

$$\begin{aligned} p_w &= \frac{2(49)(0.726) + 334(1.183) + 2(48)(1.183) + 2(48)(0.712)}{12(96 + 96 + 432)(21.75)} \\ &= 0.00398 = 0.398\% \end{aligned}$$

Cracked Moment of Inertia (I_c)

$F = 0.0195$ (See Figure 5-5 of Ref. B-1)

$$I_c = Fbd_v^3 = 0.0195(1)(21.75)^3 = 200 \text{ in.}^4/\text{in.}$$

Gross Moment of Inertia

$$I_G = \frac{bT_c^3}{12} = \frac{1(24)^3}{12} = 1152 \text{ in.}^4/\text{in.}$$

Average Moment of Inertia

$$I_a = \frac{I_c + I_G}{2} = \frac{200 + 1152}{2} = 676 \text{ in.}^4/\text{in.}$$

Deflection at Final Yield (Location P_1)

$$X_p EI(P_1) = 25.83 \times 10^5 \text{ Kip-in}^2$$

$$X_p = \frac{25.83 \times 10^5}{E_c I_a} = \frac{25.83 \times 10^5}{(4.27 \times 10^3)(676)} = 0.895 \text{ in}$$

Elastic and Elasto-Plastic Deflections (Location P_1)

$$X_e = \frac{2.0 \times 10^5}{25.83 \times 10^5} (0.895) = 0.069 \text{ in}$$

$$X_{ep} = \frac{3.04 \times 10^5}{25.83 \times 10^5} (0.895) = 0.105 \text{ in}$$

Equivalent Elastic Deflection

From Equation 5-51 of Reference B-1:

$$X_E = X \left(\frac{r_{ep}}{r_u} \right) + X_{ep} \left(1 - \frac{r_e}{r_u} \right) + X_p \left(1 - \frac{r_{ep}}{r_u} \right)$$

$$X_E = 0.069 \left(\frac{5.60}{10.43} \right) + 0.105 \left(1 - \frac{4.0}{10.43} \right) + 0.895 \left(1 - \frac{5.60}{10.43} \right)$$

$$X_E = 0.516 \text{ in.}$$

5. Dynamic Increase Factors for Each Panel

As previously mentioned, the increase in strength of both the reinforcement and concrete due to a rapid rate of strain is a function of the time to reach the yield stress of the reinforcement.

The reinforcement crossing the lines of maximum stress (yield lines) reach yield stress at various times; the negative reinforcement at the side supports yields first, the negative reinforcement at the base next and the positive reinforcement at the interior of the panel last. Therefore, the dynamic increase in strength will vary for the reinforcement and concrete at these various locations.

For the problem at hand, an average dynamic increase factor is obtained for the reinforcement and concrete of each panel. This average is obtained by considering the maximum equivalent elastic deflection as the deflection necessary to yield all the reinforcement.

The time to reach yield for each panel is obtained by comparing the deflection at yield (equivalent elastic deflection) with the deflection-time history of each panel as recorded during the test. Unfortunately, due to a malfunction of the electronic gages during Round no. 1, the deflection-time history recorded in Round No. 2 had to be utilized. This data (Round No. 2) would produce a conservative estimate of the time to reach yield of the panels in the first round as can be seen from Figure B-12 which shows the idealized resistance-deflection curve of a concrete element subjected to multiple loadings. Therefore, to compensate for this conservatism, the static deflection has been used to determine the time at which each panel yields.

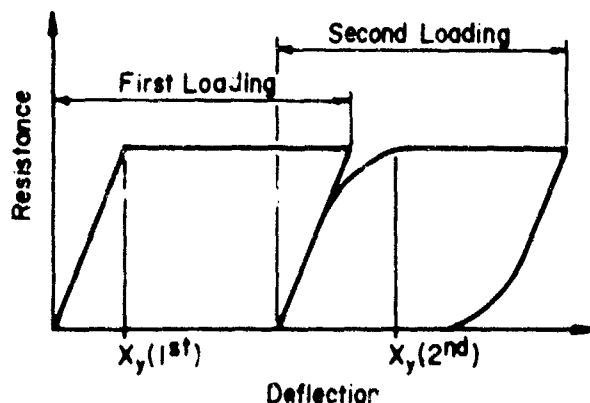


FIGURE B-12
IDEALIZED RESISTANCE-DEFLECTION CURVE FOR MULTIPLE LOADINGS

The complete deflection-time history for each panel of the back wall as measured in Round No. 2 is shown in Figure B-13. An enlarged section of the initial deflection-time curve for each panel is shown in Figure B-14.

The dynamic increase factors versus strain rate for the reinforcement and concrete were obtained from References B-2 and B-3, respectively, and are presented in Figure B-15.

Static Deflection at Yield for Each Panel

$$X_y = X_E = 0.516 \text{ in}$$

Time to Reach Yield (Figure B-14)

Donor Panel

$$t_y = 0.0026 \text{ sec}$$

Receiver Panel

$$t_y = 0.0132 - 0.007 = 0.0062 \text{ sec}$$

Dynamic Increase Factor for Reinforcement of Each Panel

Strain at Yield

$$\epsilon = \frac{f_y}{E_s} = \frac{73,700}{29 \times 10^6} = 0.00254 \text{ in/in}$$

Strain Rate

Donor Panel

$$\dot{\epsilon} = \frac{\epsilon}{t_y} = \frac{0.00254}{0.0026} = 0.977 \text{ in/in/sec}$$

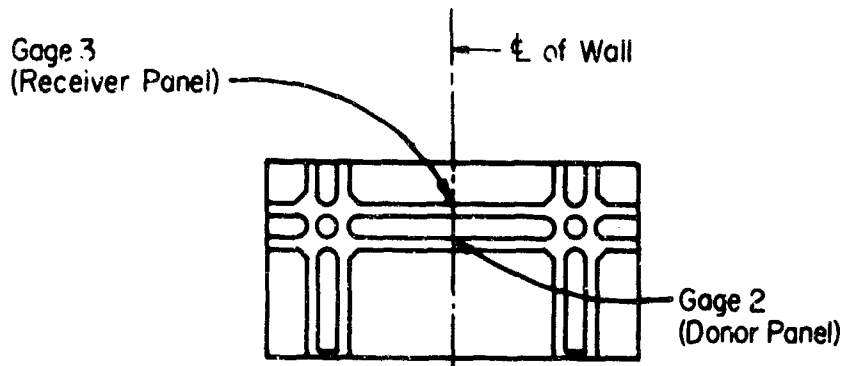
Receiver Panel

$$\dot{\epsilon} = \frac{\epsilon}{t_y} = \frac{0.00254}{0.0062} = 0.410 \text{ in/in/sec}$$

Dynamic Increase Factor (Figure B-15)

Donor Panel

$$DIF = 1.104$$



NOTE: Attachment Points for Gage
Located 6 inches Below
Top of Wall

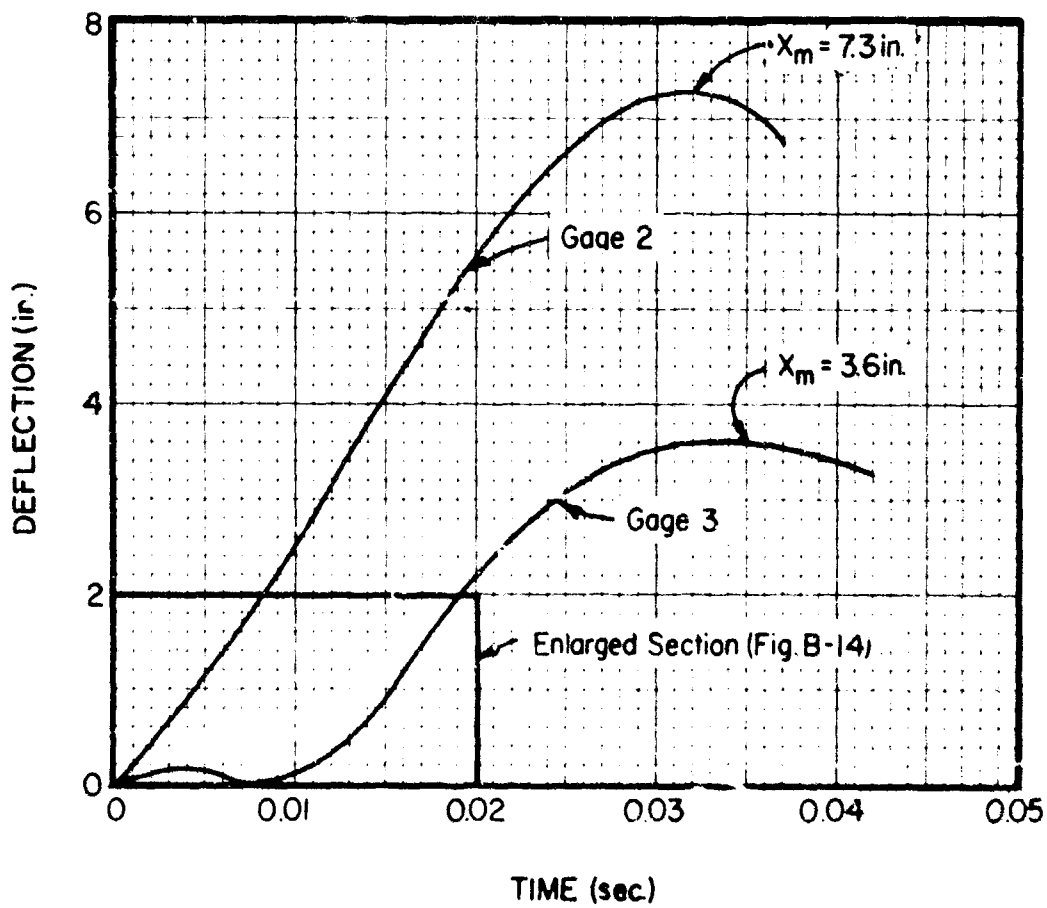


FIGURE B-13
DEFLECTION-TIME HISTORY OF BACK WALL
(ROUND No. 2)

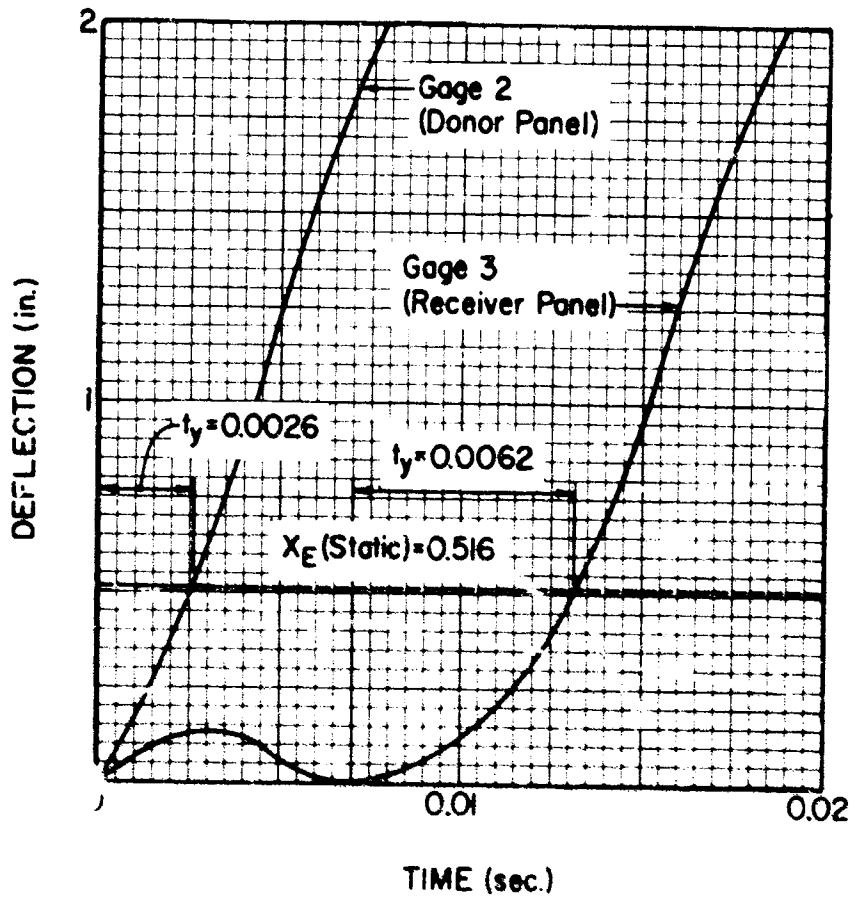
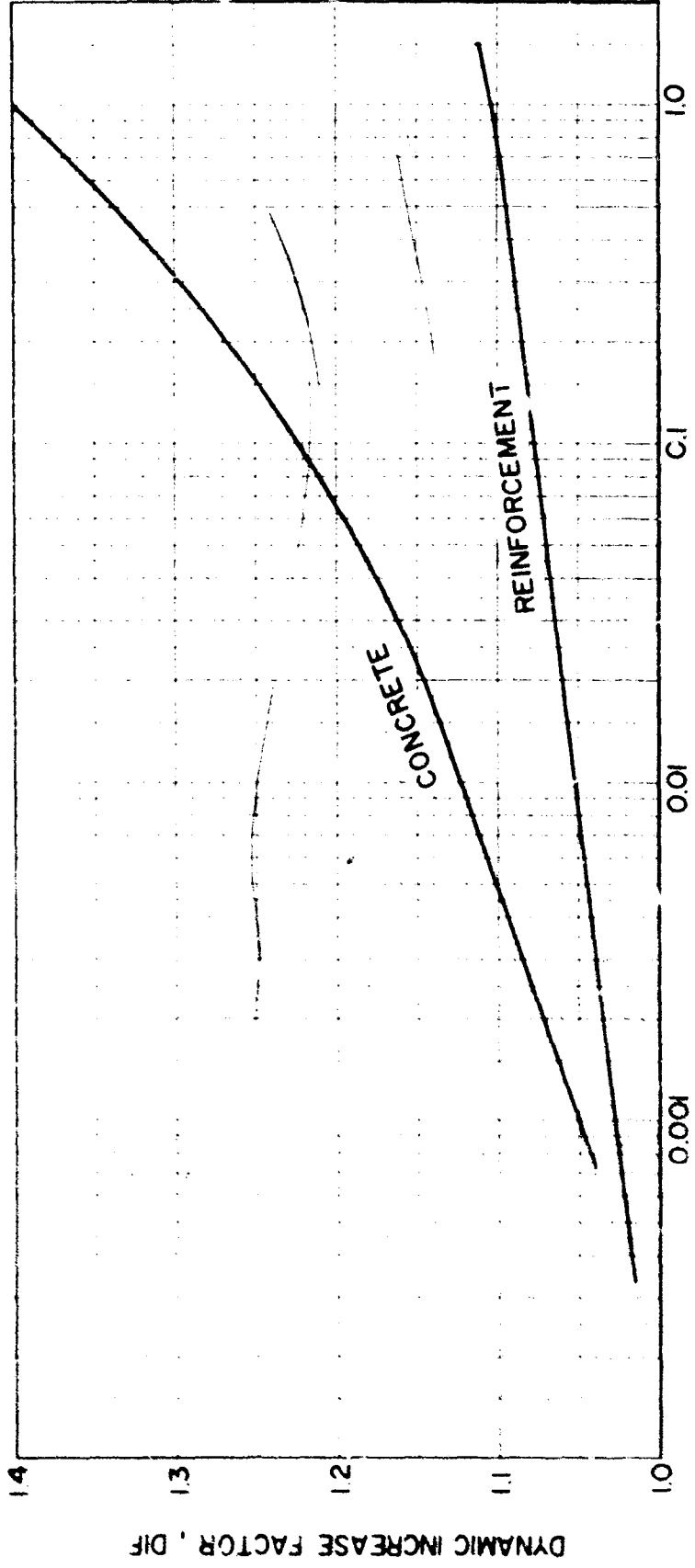


FIGURE B-14
 ENLARGED SECTION OF DEFLECTION-TIME CURVE OF
 BACK WALL (ROUND No. 2)



STRAIN RATE, $\dot{\epsilon}$ (in./in./sec.)

FIGURE B-15
DYNAMIC STRENGTH OF CONCRETE AND REINFORCEMENT

Receiver Panel

$$DIF = 1.093$$

Dynamic Increase Factor for Concrete of Each Panel

Strain at Ultimate Strength

$$\epsilon = \frac{f'_c}{E_c} = \frac{4935}{4.27 \times 10^6} = 0.00115 \text{ in/in}$$

Strain Rate

Donor Panel

$$\dot{\epsilon} = \frac{\epsilon}{t_y} = \frac{0.00115}{0.0026} = 0.442 \text{ in/in/sec}$$

Receiver Panel

$$\dot{\epsilon} = \frac{\epsilon}{t_y} = \frac{0.00115}{0.0062} = 0.185 \text{ in/in/sec}$$

Dynamic Increase Factor (Figure B-15)

Donor Panel

$$DIF = 1.33$$

Receiver Panel

$$DIF = 1.264$$

6. Ultimate Unit Dynamic Resistance of Donor Panel

The ultimate dynamic resistance of the donor panel is calculated in the same manner as the static resistance except that the concrete and reinforcement stresses used are obtained by considering the dynamic action of the panel.

The maximum deflection of the donor panel is in excess of that deflection which causes a support rotation of two degrees and, therefore, the reinforcement is stressed in the strain hardening region. An average static stress was obtained to approximate

the energy absorbed according to the procedure of Reference B-1. This static stress was then multiplied by the dynamic increase factor to obtain an average dynamic stress.

It should be noted that a small reduction in moment capacity occurs due to the large deflection of the donor panel (greater than two degrees support rotation) because the concrete in the compression zone is crushed. As the concrete fails, the compression stresses are transferred (for laced reinforced concrete elements only) from the concrete to the compression reinforcement. Since this reduction in moment capacity is small, its effect on the resistance of the panel was neglected. The ultimate moment capacity was calculated considering the concrete as attaining and maintaining its ultimate dynamic stress.

Dynamic Stresses for Concrete and Reinforcement

Maximum Deflection of Panel

The maximum deflection of the donor panel is estimated from Figure B-13.

$$X_m \approx 6.1 \text{ in.}$$

Panel Rotation at Supports

The support rotations for the dynamic action of the panel are approximated by considering the yield line locations which were determined for the static resistance of the panel.

$$\theta_V = \tan^{-1} \left(\frac{X_m}{H} \right) = \tan^{-1} \left(\frac{6.1}{96} \right) = 3.63^\circ$$

$$\theta_H = \tan^{-1} \left(\frac{X_m}{x} \right) = \tan^{-1} \left(\frac{6.1}{130.7} \right) = 2.67^\circ$$

Static Stresses (Table B-3)

Reinforcement

For support rotations within the range $2^\circ < \theta < 5^\circ$, the absorbed energy is approximated by considering the average stress given by:

$$f_s = f_a = f_y + \frac{1}{4} (f_u - f_y)$$

Therefore, from Table B-3:

$$f_s \text{ (No. 7 bars)} = 73,000 \text{ psi} = 73.0 \text{ ksi}$$

$$f_s \text{ (No. 9 bars)} = 82,280 \text{ psi} = 82.28 \text{ ksi}$$

Concrete

$$f'_c = 4,935 \text{ psi} = 4.935 \text{ ksi}$$

Dynamic Increase Factors

$$\text{Reinforcement} - \text{DIF} = 1.104$$

$$\text{Concrete} - \text{DIF} = 1.33$$

Ultimate Dynamic Stresses

$$f \text{ (dynamic)} = \text{DIF} \times f \text{ (static)}$$

Reinforcement

$$f_{ds} \text{ (No. 7 bars)} = 1.104(73.0) = 80.6 \text{ ksi}$$

$$f_{ds} \text{ (No. 9 bars)} = 1.104 (82.28) = 90.8 \text{ ksi}$$

Concrete

$$f'_{dc} = 1.33 (4.935) = 6.56 \text{ ksi}$$

Moment Capacity per Foot of Reinforcement

The ultimate dynamic moment capacity is obtained in the same manner as the static moment capacity except that dynamic stresses are used. Therefore, the formula for moment capacity becomes:

$$M_u = A_s f_{ds} \left(d - \frac{a}{2} \right)$$

where:

$$a = \frac{A_s f_{ds}}{0.85 b f'_{dc}}$$

Vertical No. 9 Bars

Full Capacity

$$a = \frac{1.183(90.8)}{0.85(12)(6.56)} = 1.605 \text{ in.}$$

$$M_{VN} = M_{VP} = \frac{1.183(90.8)}{12} \left[22.061 - \frac{1.605}{2} \right]$$
$$= 190.3 \text{ Kip-ft./ft.}$$

Reduced Capacity

$$a = \frac{1.183(2/3)(90.8)}{0.85(12)(6.56)} = 1.070 \text{ in}$$

$$M'_{VN} = M'_{VP} = \frac{1.183(2/3)(90.8)}{12} \left[22.061 - \frac{1.070}{2} \right]$$
$$= 128.5 \text{ Kip-ft./ft.}$$

Horizontal No. 9 Bars

$$a = \frac{1.183(90.8)}{0.85(12)(6.56)} = 1.605 \text{ in}$$

$$M_{HN} = M_{HP} = \frac{1.183(90.8)}{12} \left[20.933 - \frac{1.605}{2} \right]$$
$$= 180.2 \text{ Kip-ft./ft.}$$

Vertical No. 7 Bars

The No. 7 bars are stressed to two-thirds of the yield stress of the No. 9 bars since this stress is lower than the yield stress of the No. 7 bars.

$$a = \frac{0.726(2/3)(90.8)}{0.85(12)(6.56)} = 0.657 \text{ in.}$$

$$M_{VN}'' = M_{VP}'' = \frac{0.726(2/3)(90.8)}{12} \left[22.188 - \frac{0.657}{2} \right]$$

$$= 80.1 \text{ Kip-ft./ft.}$$

Horizontal No. 7 Bars

$$a = \frac{0.712(2/3)(90.8)}{0.85(12)(6.56)} = 0.644 \text{ in}$$

$$M_{HN}'' = M_{HP}'' = \frac{0.712(2/3)(90.8)}{12} \left[21.060 - \frac{0.644}{2} \right]$$

$$= 74.5 \text{ Kip-ft./ft.}$$

Ultimate Unit Dynamic Resistance of Sector I (Figure B-8)

Total Moment Capacity

$$\Sigma M_N = 2(4.08)(80.1) + 2\left(\frac{x}{2} - 4.08\right)(128.5) + (36-x)(190.3)$$

$$= 6456 - 61.8x$$

$$\Sigma M_P = 2(4.08)(80.1) + 2\left(\frac{x}{2} - 4.08\right)(128.5) + 2\left(\frac{x}{2}\right)(190.3)$$

$$= 318.8x - 395$$

$$\Sigma M_D = \Sigma M_N + \Sigma M_P = 6061 + 257x$$

and,

$$R_{DC} = r_u A_c$$

$$= r_u \left[\frac{8[36+(36-2x)]}{2} \right] \left[\frac{8[36+2(36-2x)]}{3[36+(36-2x)]} \right]$$

Unit Dynamic Resistance

$$R_{DC} = \Sigma M_D$$

$$\therefore r_u = \frac{142.1 + 5.02x}{27 - x} \quad (1)$$

Ultimate Unit Dynamic Resistance of Sector II (Figure B-9)

Total Moment Capacity

$$EM_N = 4(180.2) + 4(74.5) = 1019 \text{ Kip-ft}$$

$$EM_P = EM_N = 1019 \text{ Kip-ft.}$$

$$EM_\Delta = EM_N + EM_P = 2038 \text{ Kip-ft.}$$

and,

$$R_{\Delta c} = r_u A_{\Delta c} = r_u \left(\frac{8x}{2}\right) \left(\frac{x}{3}\right)$$

Unit Dynamic Resistance

$$R_{\Delta c} = EM_\Delta$$

$$\therefore r_u = \frac{1520}{x^2} \quad (2)$$

Location of Yield Lines

Since the unit resistance of all the sectors must be equal,

$$\frac{142.1 + 5.02x}{27 - x} = \frac{1520}{x^2}$$

Simplifying:

$$x^3 + 23.58x^2 + 253.7x - 6850 = 0$$

And the desired root is:

$$x = 10.89 \text{ ft.} = 130.7 \text{ in.}$$

Ultimate Unit Dynamic Resistance

The unit resistance is obtained by substituting the value of x into either equation (1) or (2), both of which give:

$$r_u = 12.89 \text{ Kips/sq.ft.} = 89.5 \text{ psi}$$

7. Check of Shear Capacity of Donor Panel

To fully develop its ultimate dynamic flexural capacity, a reinforced concrete element must fully resist the high shear stresses produced at its supports by the applied blast loads. These shear stresses are a function of the elements's geometry, yield line locations, and flexural resistance.

The shear capacity (diagonal tension) of the donor panel was checked at the critical section occurring at a distance d from the supports, where d is a weighted value, according to the procedures of Reference B-1. The shear stresses were computed at the critical section for the panel's ultimate dynamic flexural resistance and corresponding yield line locations which divide the panel into Sectors I and II. Since the shear is assumed equal to zero along the positive yield lines, the total shear force for each sector at the critical section is equal to the resistance times the area between the critical section and the positive yield lines.

To account for the higher stiffness of the corners, the shear along the supports is assumed to vary in the same manner as the moment. Therefore, the shear per inch along the critical section in either the vertical or horizontal directions is denoted as:

- V = shear in the mid strip
- V' = shear corresponding to moment capacity of #9 bars in the corner strip
- V'' = shear corresponding to moment capacity of #7 bars in the corner strip

Shear resistance is provided by both the concrete and lacing reinforcement. The ultimate capacity of the concrete and the shear resisted by the lacing were calculated in accordance with the procedures of Reference B-1. An increase in shear strength due to rapid rate of strain was not considered for either the concrete or lacing reinforcement due to a lack of data pertaining to the increase in strength.

It should be noted that the donor panel responded in the strain hardening region of the flexural reinforcement and the maxi-

mum shear forces produced correspond to its peak dynamic resistance (resistance corresponding to the maximum dynamic stress attained in the reinforcement in the strain hardening region). However, in this analysis the shear stresses at the critical section were calculated based on the equivalent dynamic resistance rather than on the peak dynamic resistance. The variation in shear stresses produced by the equivalent and peak resistance was compensated for by utilizing an average stress for the lacing reinforcement since the lacing will also be stressed in its strain hardening region. The average stress for the lacing reinforcement was obtained by relating the average stress to the deflection of the donor panel in accordance with the procedures of Reference B-1.

Check of Shear Capacity of Sector I (Figure B-16)

Weighted Effective Depth d_v

The weighted effective depth is taken at the plane 1-1 (critical section for shear). Therefore, it becomes necessary to first assume a value of d_v .

Assume $d_v = 22.1$ in.

Strip	Length (in)	d (in)
Corner	18.9	22.188
Mid	334	22.061

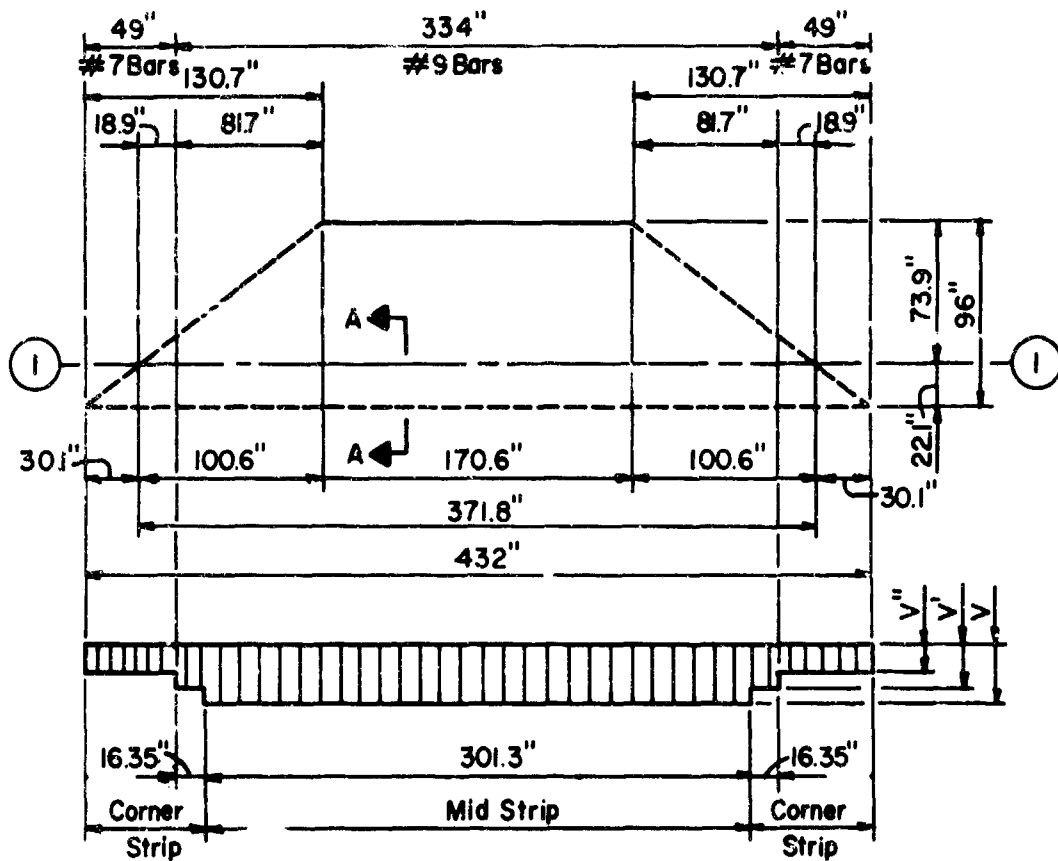
Therefore,

$$d_v = \frac{2(18.9)(22.188) + 334(22.061)}{2(18.9) + 334} = 22.1 \text{ in}$$

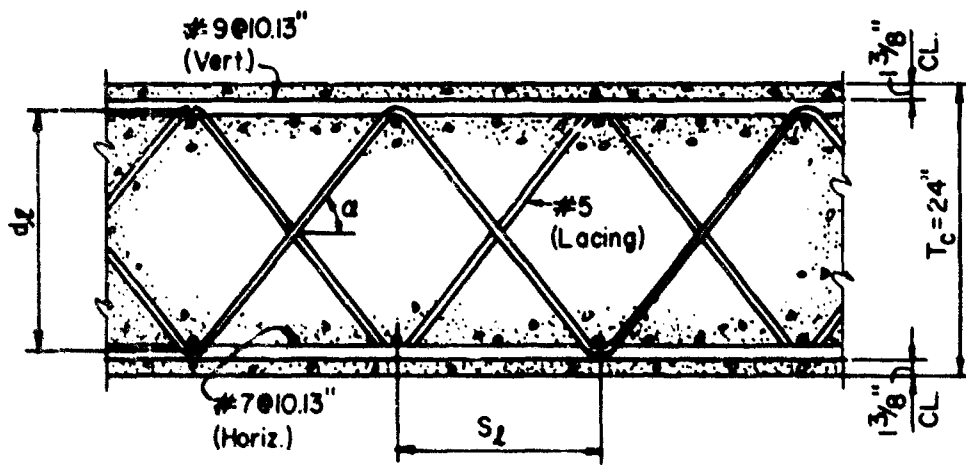
Total Effective Shear Force

The total shear force acting at the critical section (Plane 1-1) is equal to the area between the critical section and the positive yield lines times the ultimate dynamic flexural resistance of the panel.

$$EV = Ar_u = \left[\frac{73.9(170.6 + 371.8)}{2} \right] (89.5) \\ = 1,794,000 \text{ lbs}$$



a. LAYOUT



b SECTION A-A

FIGURE B-16
LAYOUT OF SECTOR I AND LOCATION OF LACING REINFORCEMENT

Shear per Inch Along Critical Section

The unit shear force is assumed to be proportional to the ultimate dynamic moment capacity at all sections. Therefore,

$$\frac{V'_{dV}}{V_{dV}} = \frac{M'_{VN}}{M_{VN}} = \frac{128.5}{190.3} = 0.675$$

$$\frac{V''_{dV}}{V_{dV}} = \frac{M''_{VN}}{M_{VN}} = \frac{80.1}{190.3} = 0.421$$

Hence,

$$V'_{dV} = 0.675 V_{dV}$$

$$V''_{dV} = 0.421 V_{dV}$$

and,

$$\begin{aligned} \Sigma V &= \Sigma V_{dV} + \Sigma V'_{dV} + \Sigma V''_{dV} \\ &= 301.3 V_{dV} + 2(16.35)(0.675V_{dV}) + 2(18.9)(0.421V_{dV}) \\ &= 339.3 V_{dV} \end{aligned}$$

from which

$$V_{dV} = \frac{\Sigma V}{339.3} = \frac{1,794,000}{339.3} = 5290 \text{ lbs./in.}$$

Maximum Shear Stress at Critical Section

$$v_{uV} = \frac{V_{dV}}{bd_v} = \frac{5290}{(1)(22.1)} = 239 \text{ psi}$$

Ultimate Shear Stress of Concrete

The ultimate shear stress for concrete as given by Reference B-1 with the capacity reduction factor ϕ eliminated is

$$v_c = 1.9 \sqrt{f'_c} + 2500 p$$

where:

- v_c = ultimate shear stress for concrete (psi)
 f_c' = ultimate compressive strength of concrete (psi)
 p = p_w = weighted percentage of reinforcement at critical section

$$p = p_w = \frac{A_s}{bd_w} = \frac{2(18.9)(0.726) + 334(1.183)}{12(371.8)(22.1)} = 0.00428$$

Therefore,

$$v_c = 1.9 \sqrt{4935} + 2500(0.00428) = 144 \text{ psi}$$

Shear Stress Resisted by the Lacing Reinforcement

The ultimate shear stress of the concrete is less than the shear stress produced by the resistance of the panel. Therefore, the lacing reinforcement must resist the excess stress.

$$v' = v_{uV} - v_c = 239 - 144 = 95 \text{ psi}$$

Required Cross-Sectional Area of Lacing Reinforcement

The required area of lacing reinforcement as given by Reference B-1 with the capacity reduction factor eliminated is

$$A_v = \frac{v' b_l s_l}{f_s (\sin \alpha + \cos \alpha)}$$

where:

- A_v = cross-sectional area of lacing reinforcement in tension within a width b_l and a distance s_l (sq. in.)
 v' = excess shear stress resisted by lacing reinforcement (psi)
 b_l = width of concrete strip in which the diagonal tension stresses are resisted by lacing of area A_v (in)
 s_l = spacing of lacing in the direction parallel to

the longitudinal reinforcement (in)

f_s = maximum stress permitted on lacing reinforcement (psi)

α = angle formed by the plane of the lacing and the plane of the longitudinal reinforcement (degrees)

The angle of inclination of the lacing bars (α) is obtained from Figure 6-19 of Reference B-1

where:

d_l = distance between centerlines of lacing bends measured normal to flexural reinforcement (in)

R_l = radius of lacing bend (in)

D_o = nominal diameter of lacing bar (in)

For #5 lacing bars,

$$d_l = 24 - 2\left(1.375 + 1.128 - \frac{0.625}{2}\right) = 19.619 \text{ in}$$

$$\frac{R_l}{d_l} = \frac{2(10.13)}{19.619} = 1.03$$

Note: Lacing bars have a minimum radius of bend $R_l = 3D_o$

$$\frac{2R_l + D_o}{d_l} = \frac{7D_o}{d_l} = \frac{7(0.625)}{19.619} = 0.223$$

From Figure 6-19 of Reference B-1,

$$\alpha = 47^\circ$$

For the donor panel, $f_s = f_a = 78,990$ psi (Table B-3).

Therefore,

$$A_v \text{ (req'd)} = \frac{95(10.13)(20.26)}{78,990(0.731 + 0.682)} = 0.175 \text{ sq. in.}$$

$$A_v \text{ (provided)} = 0.31 \text{ sq. in.} > A_v \text{ (req'd)}$$

Check of Shear Capacity of Sector II (Figure B-17)

The analysis for determining the shear capacity of Sector II is similar to that of Sector I.

Weighted Effective Depth (d_w)

Assume $d_v = 21.0$ in.

Strip	Length (in)	d (in)
Mid	32.6	21.060
Corner	48.0	20.933

Therefore,

$$d_w = \frac{20.933(48) + 21.060(32.6)}{80.6} = 21.0 \text{ in.}$$

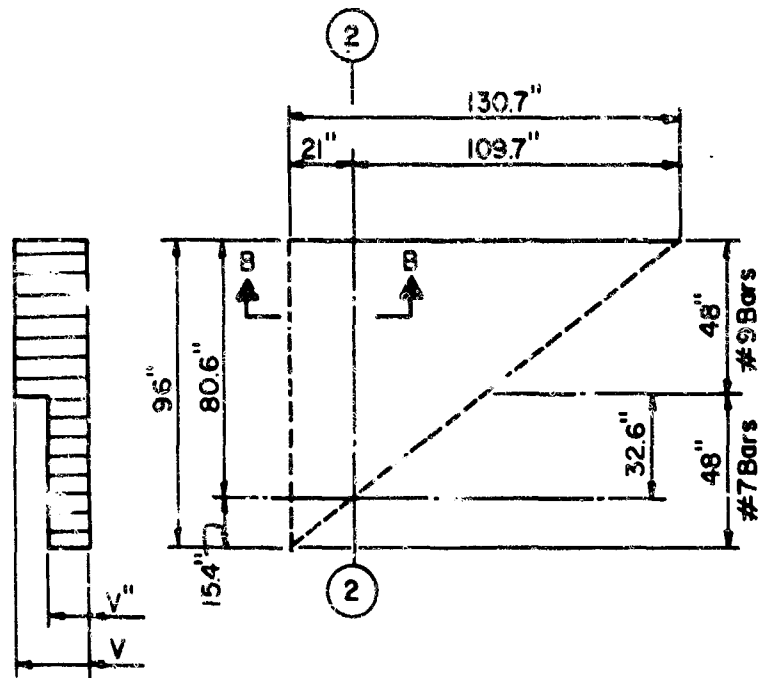
Total Effective Shear Force

$$V = A_r u = \left[\frac{80.6(109.7)}{2} \right] (89.5) = 395,700 \text{ lbs}$$

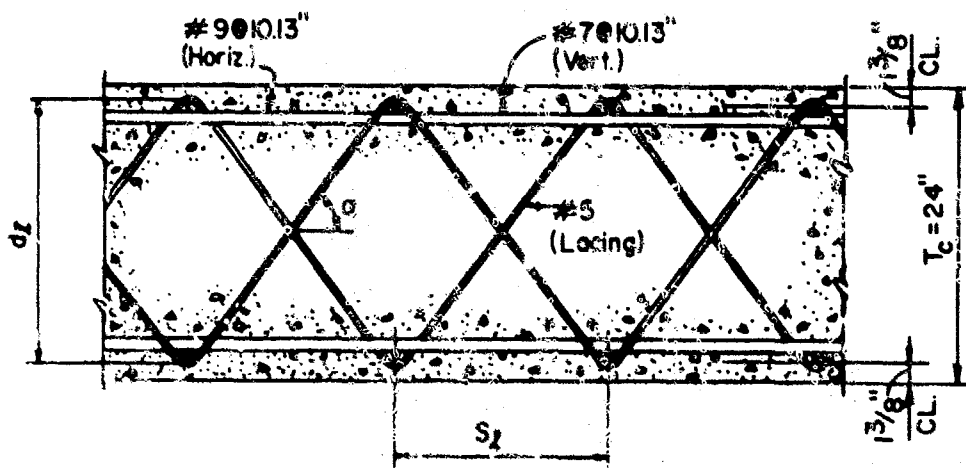
Shear per Inch Along Critical Section

$$\frac{V_{dH}''}{V_{dH}} = \frac{M_{HN}''}{M_{HN}} = \frac{74.5}{180.2} = 0.413$$

$$V_{dH}'' = 0.413 V_{dH}$$



a. LAYOUT



b. SECTION B-B

FIGURE B-17
LAYOUT OF SECTOR II AND LOCATION OF LACING REINFORCEMENT

$$\begin{aligned} \Sigma V &= \Sigma V_{dH} + \Sigma V_{dH}'' = 48V_{dH} + 32.6 (0.413V_{dH}) \\ &= 61.5 V_{dH} \end{aligned}$$

$$V_{dH} = \frac{\Sigma V}{61.5} = \frac{395,700}{61.5} = 6,430 \text{ lbs./in.}$$

Maximum Shear Stress at Critical Section

$$v_{uH} = \frac{V_{dH}}{l_v} = \frac{6,430}{1(21.0)} = 306 \text{ psi}$$

Ultimate Shear Stress of Concrete

$$p = p_w = \frac{A_s}{bd_v} = \frac{0.712(32.6) + 1.183(48)}{12(80.6)(21.0)} = 0.00394$$

$$\begin{aligned} v_c &= 1.9\sqrt{f'_c} + 2500p = 1.9\sqrt{4935} + 2500(0.00394) \\ &= 142 \text{ psi} \end{aligned}$$

Shear Resisted by Lacing Reinforcement

$$v' = v_{uH} - v_c = 306 - 142 = 164 \text{ psi}$$

Required Cross-Sectional Area of Lacing Reinforcement

For #5 lacing bars,

$$d_l = 24 - 2\left(1.375 - \frac{0.625}{2}\right) = 21.875 \text{ in}$$

$$\frac{2R_l + D_o}{d_l} = \frac{7D_o}{d_l} = \frac{7(0.625)}{21.875} = 0.200$$

$$\frac{s_l}{d_l} = \frac{2(9.93)}{21.875} = 0.908$$

$$\alpha = 50.5^\circ \text{ (Figure 6-19 of Ref. B-1)}$$

$$A_v \text{ (req'd)} = \frac{v' b_s s_s}{f_s (\sin \alpha + \cos \alpha)}$$

$$= \frac{164(10.13)(19.86)}{78,990(0.772 + 0.636)} = 0.297 \text{ sq. in.}$$

$$A_v \text{ (provided)} = 0.31 \text{ sq. in.} > A_v \text{ (req'd)}$$

Note: The lacing reinforcement provided is greater than that required for both sectors I and II, and therefore, a shear failure will not occur and the ultimate dynamic flexural resistance can be fully developed.

8. Ultimate Unit Dynamic Resistance of Receiver Panel

The ultimate dynamic resistance of the receiver panel is calculated in the same manner as the static resistance except that dynamic concrete and reinforcement stresses are used.

The maximum deflection of the panel is less than that corresponding to two degrees support rotation. Therefore, the reinforcement is stressed within the post-yield range and the concrete remains effective in resisting moments. The static yield stress and the static ultimate compressive strength of the concrete were multiplied by their respective dynamic increase factors to obtain the dynamic reinforcement and concrete stresses, respectively.

Dynamic Stresses for Concrete and Reinforcement

Maximum Deflection of Panel

The maximum deflection of the receiver panel is estimated from Figure B-13.

$$X_m = 3.0 \text{ in.}$$

Panel Rotation at Supports

The support rotations for the dynamic action of the panel are approximated by considering the yield line locations which were determined for the static resistance of the panel.

$$\theta_v = \tan^{-1} \left(\frac{X_m}{H} \right) = \tan^{-1} \left(\frac{3.0}{96} \right) = 1.68^\circ$$

$$\theta_H = \tan^{-1} \left(\frac{X_m}{x} \right) = \tan^{-1} \left(\frac{3.0}{130.7} \right) = 1.32^\circ$$

Static Stresses (Table B-3)

Reinforcement

$$f_s \text{ (No. 7 bars)} = 65,140 \text{ psi} = 65.14 \text{ ksi}$$

$$f_s \text{ (No. 9 bars)} = 73,700 \text{ psi} = 73.7 \text{ ksi}$$

Concrete

$$f'_c = 4,935 \text{ psi} = 4.935 \text{ ksi}$$

Dynamic Increase Factors

$$\text{Reinforcement - DIF} = 1.093$$

$$\text{Concrete - DIF} = 1.264$$

Ultimate Dynamic Stresses

$$f(\text{dynamic}) = \text{DIF} \times f(\text{static})$$

Reinforcement

$$f_{ds} \text{ (No. 7 bars)} = 1.093 (65.14) = 71.1 \text{ ksi}$$

$$f_{ds} \text{ (No. 9 bars)} = 1.093 (73.7) = 80.5 \text{ ksi}$$

Concrete

$$f'_{dc} = 1.264 (4.935) = 6.24 \text{ ksi}$$

Ultimate Unit Dynamic Resistance

Once the dynamic concrete and reinforcement stresses are established, the solution for the location of the yield lines and the resistance of the panel is performed using the same general procedure utilized to establish the static resistance of each panel and the dynamic resistance of the donor panel. Therefore, the calculations are not shown.

Location of Yield Lines

$$x = 10.89 \text{ ft} = 130.7 \text{ in}$$

Ultimate Unit Dynamic Resistance

$$r_u = 11.45 \text{ Kips/sq. ft} = 79.5 \text{ psi}$$

9. Check of Shear Capacity of Receiver Panel

The shear capacity (diagonal tension) of the receiver panel is checked to verify the assumption that its ultimate dynamic flexural resistance is fully developed. The calculations are performed in the same manner as that for the donor panel except that the yield stress is used for the lacing reinforcement since the panel responded within the post-yield range.

Check of Shear Capacity of Sector I (Figure B-16)

Note: The values of d_v , p_v and α for Sector I of the receiver panel are identical to those for Sector I of the donor panel. Hence, the appropriate calculations are omitted. Also, the values for the various moment capacities are merely stated with the calculations being excluded.

Weighted Effective Depth

$$d_v = 22.1 \text{ in}$$

Total Effective Shear Force

$$\begin{aligned} EV &= Ar_u = \left[\frac{73.9 (170.6 + 371.8)}{2} \right] (79.5) \\ &= 1,593,500 \text{ lbs} \end{aligned}$$

Shear per Inch Along Critical Section

$$\frac{V'_{dv}}{V_{dv}} = \frac{M'_{VN}}{M_{VN}} = \frac{114.1}{169.1} = 0.675$$

$$\frac{v_{dv}''}{v_{dv}} = \frac{M_{VN}''}{M_{VN}} = \frac{71.0}{169.1} = 0.420$$

Hence,

$$v_{dv}' = 0.675 v_{dv}$$

$$v_{dv}'' = 0.420 v_{dv}$$

and,

$$\begin{aligned} EV &= \Sigma V_{dv} + \Sigma V_{dv}' + \Sigma V_{dv}'' \\ &= 301.3 v_{dv} + 2(16.35)(0.675 v_{dv}) \\ &\quad + 2(18.9)(0.420 v_{dv}) \\ &= 339.2 v_{dv} \end{aligned}$$

from which

$$v_{dv} = \frac{EV}{339.2} = \frac{1,593,500}{339.2} = 4700 \text{ lbs/in}$$

Maximum Shear Stress at Critical Section

$$v_{uv} = \frac{v_{dv}}{bd_v} = \frac{4700}{1(22.1)} = 213 \text{ psi}$$

Ultimate Shear Stress of Concrete

$$p = p_w = 0.00428$$

$$\begin{aligned} v_c &= 1.9 \sqrt{f_c'} + 2500p = 1.9 \sqrt{4935} + 2500(0.00428) \\ &= 144 \text{ psi} \end{aligned}$$

Shear Resisted by Lacing Reinforcement

$$v' = v_{uv} - v_c = 213 - 144 = 69 \text{ psi}$$

Required Cross - Sectional Area of Lacing Reinforcement

For the receiver panel, $f_s = f_y = 71,990$ psi (Table B-3)

and for #5 lacing bars, $\alpha = 47^\circ$

$$A_v \text{ (req'd)} = \frac{v' b_l s_l}{f_s (\sin \alpha + \cos \alpha)}$$
$$= \frac{69 (10.13)(20.26)}{71,990 (0.731 + 0.682)} = 0.139 \text{ sq in}$$

$$A_v \text{ (provided)} = 0.31 \text{ sq in} > A_v \text{ (req'd)}$$

Check of Shear Capacity of Sector II (Figure B-17)

The analysis for determining the shear capacity of Sector II is similar to that of Sector I.

Note: The values of d_v , p_v and α for Sector II of the receiver panel are identical to those for Sector II of the donor panel. Hence, the appropriate calculations are omitted. Also, the values for the various moment capacities are merely stated with the calculations being excluded.

Weighted Effective Depth

$$d_v = 21.0 \text{ in}$$

Total Effective Shear Force

$$EV = Ar_u = \left[\frac{80.6 (109.7)}{2} \right] (79.5) = 351,500 \text{ lbs.}$$

Shear per Inch Along Critical Section

$$\frac{V''}{dH} = \frac{M''_{HN}}{M_{HN}} = \frac{66.1}{160.2} = 0.413$$

$$V''_{dH} = 0.413 V_{dH}$$

$$\begin{aligned}\Sigma V &= \Sigma V_{dH} + \Sigma V''_{dH} = 48 V_{dH} + 32.6 (0.413 V_{dH}) \\ &= 61.5 V_{dH}\end{aligned}$$

$$V_{dH} = \frac{\Sigma V}{61.5} = \frac{351,500}{61.5} = 5715 \text{ lbs/in}$$

Maximum Shear Stress at Critical Section

$$v_{uH} = \frac{V_{dH}}{bd_v} = \frac{5715}{1(21.0)} = 272 \text{ psi}$$

Ultimate Shear Stress of Concrete

$$p = p_v = 0.00394$$

$$\begin{aligned}v_c &= 1.9 \sqrt{f'_c} + 2500 p = 1.9 \sqrt{4935} + 2500(0.00394) \\ &= 142 \text{ psi}\end{aligned}$$

Shear Resisted by Lacing Reinforcement

$$v' = v_{uH} - v_c = 272 - 142 = 130 \text{ psi}$$

Required Cross-Sectional Area of Lacing Reinforcement

For #5 lacing bars, $\alpha = 50.5^\circ$

$$\begin{aligned}A_v \text{ (req'd)} &= \frac{v' b_t s_t}{f_s (\sin \alpha + \cos \alpha)} \\ &= \frac{130 (10.13)(19.86)}{71,990 (0.772 + 0.636)} = 0.258 \text{ sq. in.}\end{aligned}$$

$$A_v \text{ (provided)} = 0.31 \text{ sq in} > A_v \text{ (req'd)}$$

Note: The lacing reinforcement provided is greater than that required for both sectors I and II, and therefore, a shear failure will not occur and the ultimate dynamic flexural resistance can be fully developed.

10. Equivalent Dynamic Resistance - Deflection Curve for Donor Panel

In this analysis the equivalent dynamic resistance - deflection curve is considered to describe the dynamic response of the donor panel rather than the actual resistance-deflection curve. The use of the equivalent curve greatly reduces the amount of calculations necessary to obtain the flexural impulse capacity of the panel.

The parameters required to describe the equivalent dynamic curve are the ultimate dynamic unit resistance (r_u), the maximum equivalent elastic deflection (X_p) and the maximum deflection (X_m) of the panel. The ultimate dynamic unit resistance is an average value which includes the effect of straining hardening in the flexural reinforcement and has been previously calculated. The dynamic maximum equivalent elastic deflection was obtained from consideration of the static resistance - deflection curve (Figure B-10) since the stiffness of the panel does not change for static and dynamic loadings. Lastly, the maximum deflection (X_m) of the panel was estimated from the deflection-time history obtained from Round No. 2 (Figure B-13) and the measured permanent deflections of Round Nos. 1 and 2 (time history records of Round No. 1 were not obtained due to a malfunction of the electronic gages).

The measured permanent deflection of the donor panel was shown on the resistance-deflection curve (Figure B-18) for comparative purposes. This deflection is smaller than what would normally be expected since the elastic rebound portion of the resistance-deflection curve usually has the same stiffness as the initial elastic portion of the curve. However, in the case of the bay structure (single cell arrangement), rotations which occurred at both intersections of the back and side walls distorted the unloading portion of the curve. This dissimilarity between the two portions of the curve would not occur when sufficient mass to prevent rotation is provided by adjoining cells in multi-cubicle arrangements.

Dynamic Equivalent Elastic Deflection (X_p)

Since the stiffness of the panel is the same under static and dynamic loadings:

$$X_E \text{ (dynamic)} = \frac{r_u \text{ (dynamic)}}{r_u \text{ (static)}} X_E \text{ (static)}$$

where from previous calculations:

$$r_u \text{ (dynamic)} = 89.5 \text{ psi}$$

$$r_u \text{ (static)} = 72.4 \text{ psi}$$

$$X_E \text{ (static)} = 0.516 \text{ in}$$

Therefore,

$$X_E = \frac{89.5}{72.4} (0.516) = 0.638 \text{ in}$$

Maximum Deflection (X_m)

$$X_m = 6.1 \text{ in (estimated from Figure B-13)}$$

Permanent Deflection (X_p)

$$X_p = 2.81 \text{ in (obtained from pre- and post-shot measurements)}$$

Equivalent Dynamic Resistance-Deflection Curve

The equivalent dynamic resistance-deflection curve for the donor panel is shown in Figure B-18.

11. Equivalent Dynamic Resistance - Deflection Curve for Receiver Panel

As was the case for the donor panel, the equivalent dynamic resistance-deflection curve is considered to describe the dynamic response of the receiver panel rather than the actual resistance-deflection curve. The equivalent curve for the receiver panel is obtained in the same manner as that for the donor panel.

Dynamic Equivalent Elastic Deflection (X_p)

From previous calculations:

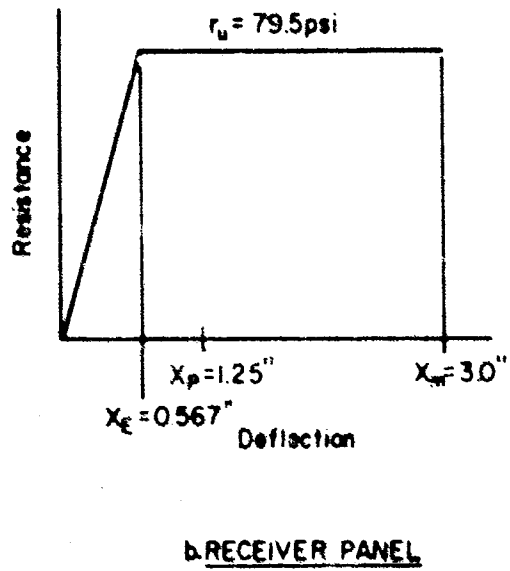
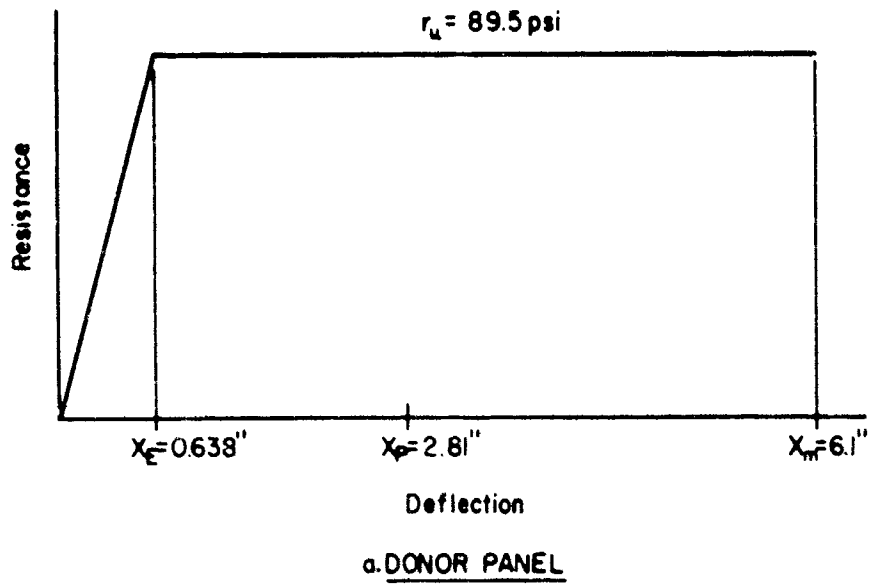


FIGURE B-18
EQUIVALENT RESISTANCE-DEFLECTION CURVES FOR EACH PANEL OF JACK WALL

$$r_u \text{ (dynamic)} = 79.5 \text{ psi}$$

$$r_u \text{ (static)} = 72.4 \text{ psi}$$

$$X_E \text{ (static)} = 0.516 \text{ in}$$

Therefore,

$$\begin{aligned} X_E \text{ (dynamic)} &= \frac{r_u \text{ (dynamic)}}{r_u \text{ (static)}} X_E \text{ (static)} \\ &= \frac{79.5}{72.4} (0.516) = 0.567 \text{ in} \end{aligned}$$

Maximum Deflection (X_m)

$$X_m = 3.0 \text{ in (estimated from Figure B-13)}$$

Permanent Deflection (X_p)

$$X_p = 1.25 \text{ in (obtained from pre- and post-shot measurements)}$$

Equivalent Dynamic Resistance-Deflection Curve

The equivalent dynamic resistance-deflection curve for the receiver panel is shown in Figure B-18.

12. Effective Mass for Each Panel

The value of the mass used in the equation of motion is equal to the actual mass only if all particles of the mass move as a unit. For each panel of the back wall the motion of the particles of mass varies along the length of the panel in both the vertical and horizontal directions. Therefore, each panel has an infinite number of degrees of freedom since an infinite number of independent displacement variables are needed to specify completely the configuration of the system. However, the equation of motion of a single particle may be used if the actual mass is replaced by an effective mass, that is, the mass of an equivalent single-degree-of-freedom system in which a single displacement variable X is sufficient to describe its motion.

The effective mass (m_e) of the equivalent single-degree-of-freedom system is related to the unit mass (m) of the actual system by

$$m_e = K_{LM} m$$

where K_{LM} is the load-mass factor determined by equating the work done, strain energy and kinetic energy of the actual system to that of the equivalent system.

The value of the effective mass is dependent upon the deflected shape of the panels which varies with the type of spanning, end conditions, etc. Therefore, the effective mass is different in the elastic, elasto-plastic, and plastic ranges of behavior. The load-mass factors in the elastic and elasto-plastic ranges of response of the panels are obtained from Table 6-1 of Reference B-1 and are then averaged to obtain the average load-mass factor for the equivalent elastic range of the panels (Figure B-18 for deflection range $0 < X \leq X_E$). The load-mass factor for the plastic range of response (Figure B-18 for deflection range $X_E < X \leq X_U$) is obtained from Figure 6-5 of Reference B-1 for the known yield line location of each panel.

Actual Unit Mass of Each Panel

The mass of each panel of the wall is assumed to consist of the mass of one-half the sand fill.

Unit Weight of Concrete and Sand for Each Panel

$$\begin{aligned} \text{Thickness of Concrete Panel} &= T_c = 2 \text{ ft} \\ \text{Thickness of Sand} &= T_s/2 = 2 \text{ ft} \\ \text{Density of Concrete} &= w_c = 150 \text{ lb/ft}^3 \\ \text{Average Density of Sand} &= w_s = 85 \text{ lb/ft}^3 \end{aligned}$$

$$w = w_c + w_s = 2(150) + 2(85) = 470 \text{ lb/sq.ft}$$

Actual Unit Mass of Each Panel

$$m = \frac{w}{g} = \frac{470}{32.2} = 14.6 \text{ lb-sec}^2/\text{ft}^3 = 8450 \text{ lb-ms}^2/\text{in}^3$$

Effective Unit Mass of Each Panel for Equivalent Elastic Range (m_e)

Load-Mass Factor

From Table 6-1 of Reference B-1 for three edges supported and one edge free, and $L/H \geq 2$ (actual $L/H = 4.5$):

$$\text{Elastic Range (all edges fixed)} - K_{LM} = 0.65$$

First Elasto-Plastic Range (two edges simple, other edge fixed) - $K_{LM} = 0.65$

Second Elasto-Plastic Range (all edges simple) -
 $K_{LM} = 0.66$

Therefore, the average load-mass factor for the equivalent elastic range is

$$K_{LM} = \frac{1}{3} (0.65 + 0.65 + 0.66) = 0.653$$

Effective Unit Mass (m_E)

$$m_E = K_{LM} m = 0.653(8450) = 5520 \text{ lb-ms}^2/\text{in}^3$$

Effective Unit Mass of Each Panel for Plastic Range (m_P)

Load Mass Factor

The location of the yield lines for both panels is given by

$$\frac{x}{L} = \frac{10.89}{36} = 0.303$$

Therefore, from Figure 6-5 of Reference B-1 for three edges supported and one free, and $x/L = 0.303$

$$K_{LM} = 0.577$$

Effective Unit Mass (m_P)

$$m_P = K_{LM} m = 0.577(8450) = 4880 \text{ lb-ms}^2/\text{in}^3$$

13. Unit Flexural Impulse Capacity of Donor Panel

The unit flexural impulse capacity of an element, if the time for the element to reach its maximum deflection (t_m) is greater than three times the duration (t_m) of the applied load but where the support rotations are equal to or less than 5 degrees in which case the elastic and elasto-plastic ranges of behavior of the element must be taken into account, is given by Equation 6-23 of Reference B-1:

$$i^2 = 2m_a \left[\frac{r_u X_E}{2} + \frac{m_a}{m_p} r_u (X_m - X_E) \right]$$

where m_a is the average of the effective masses for the equivalent elastic and plastic ranges of behavior. Since the average effective mass is used, the above equation assumes that the blast load is applied to the element during its elastic, elasto-plastic and plastic ranges of response.

For the problem at hand, the support rotations of the donor panel have previously been established to be less than 5 degrees and it will be shown that the response time (t_m) is less than three times the load duration. However, the blast load is applied only during the elastic and elasto-plastic ranges of behavior of the donor panel. Therefore, the above equation is used to obtain the flexural impulse capacity of the panel but the average effective mass (m_a) is replaced by the effective equivalent elastic mass (m_E). It should be noted that using the average effective mass in the above equation is conservative.

Verification of Assumptions

Comparison of Response Time (t_m) to Load Duration (t_o)

$$t_m = 22.3 \text{ ms (from Figure B-13 for } X_m = 6.1 \text{ in)}$$

$$t_o = 4.37 \text{ ms (from Section B.2)}$$

$$\frac{t_m}{t_o} = \frac{22.3}{4.37} = 5.10$$

Note: Since $t_m > 3t_o$, the wall panel must be analyzed for an impulse loading.

Comparison of Time to Reach Ultimate Resistance (t_p) to Load Duration (t_o)

The deflection at which the panel reaches its ultimate dynamic resistance (end of elasto-plastic range of behavior) is:

$$\begin{aligned} X_p \text{ (dynamic)} &= X_p \text{ (static)} \left[\frac{r_u \text{ (dynamic)}}{r_u \text{ (static)}} \right] \\ &= 0.895 \left(\frac{89.5}{72.4} \right) = 1.11 \text{ in.} \end{aligned}$$

and from Figure B-14:

$$t_p = 4.70 \text{ ms}$$

Therefore,

$$\frac{t_o}{t_p} = \frac{4.37}{4.70} = 0.930$$

Note: Since $t_o < t_p$, the blast load is applied only during the elastic and elasto-plastic ranges of behavior of the panel.

Unit Flexural Impulse Capacity of Donor Panel

From previous calculations:

$$m_E = 5520 \text{ lb-ms}^2/\text{in}^3$$

$$m_p = 4880 \text{ lb-ms}^2/\text{in}^3$$

$$r_u = 89.5 \text{ psi}$$

$$X_E = 0.638 \text{ in}$$

$$X_m = 6.1 \text{ in}$$

$$i_D^2 = 2m_E \left[\frac{r_u X_E}{2} + \frac{m_E}{m_p} r_u (X_m - X_E) \right]$$

$$= 2(5520) \left[\frac{(89.5)(0.638)}{2} + \frac{5520}{4880} (89.5)(6.1 - 0.638) \right]$$

$$= 6.42 \times 10^6 \text{ (psi-ms)}^2$$

Therefore,

$$i_D = 2530 \text{ psi-ms}$$

14. Unit Flexural Impulse Capacity of Receiver Panel

The unit flexural impulse capacity of the receiver panel is obtained in the same manner as that for the donor panel.

Verification of Assumptions

Comparison of Response Time (t_m) to Load Duration (t_o)

$$t_m = 24.3 - 7.0 = 17.3 \text{ ms (from Figure B-13 for } X_m = 3.0)$$

$$t_o = 4.37 \text{ ms (from Section B.2)}$$

$$\frac{t_m}{t_o} = \frac{17.3}{4.37} = 3.96$$

Note: Since $t_m > 3 t_o$, the wall panel must be analyzed for an impulse loading.

Comparison of Time to Reach Ultimate Resistance (t_p) to Load Duration (t_o)

$$\begin{aligned} X_p \text{ (dynamic)} &= X_p \text{ (static)} \left[\frac{r_u \text{ (dynamic)}}{r_u \text{ (static)}} \right] \\ &= 0.895 \frac{(79.5)}{(72.4)} = 0.983 \text{ in} \end{aligned}$$

$$t_p = 15.2 - 7.0 = 8.2 \text{ ms (from Figure B-14)}$$

$$\frac{t_o}{t_p} = \frac{4.37}{8.20} = 0.533$$

Note: Since $t_o < t_p$, the blast load is applied only during the elastic and elasto-plastic ranges of behavior of the panel.

Unit Flexural Impulse Capacity of Receiver Panel

From previous calculations:

$$m_E = 5520 \text{ lb-ms}^2/\text{in}^3$$

$$m_p = 4880 \text{ lb-ms}^2/\text{in}^3$$

$$r_H = 79.5 \text{ psi}$$

$$X_E = 0.567 \text{ in}$$

$$X_m = 3.0 \text{ in}$$

$$\begin{aligned}
i_R^2 &= 2m_E \left[\frac{r_u X_E}{2} + \frac{m_E}{m_p} r_u (X_m - X_E) \right] \\
&= 2(5520) \left[\frac{(79.5)(0.567)}{2} + \frac{5520}{4880} (79.5)(3.0 - 0.567) \right] \\
&= 2.66 \times 10^6 \text{ (psi-ms)}^2
\end{aligned}$$

Therefore,

$$i_R = 1630 \text{ psi-ms}$$

15. Impulse Capacity of Back Wall

The total blast impulse load that the back wall is capable of resisting consists of those impulses resisted by the flexural action of the concrete panels, the impulse attenuation due to dispersion of the blast wave in the concrete and sand, and the impulse absorbed by the compression of the sand fill. The impulse capacity of the concrete panels has already been obtained while the impulse absorbed by dispersion and compression of the sand fill is determined from Figure B-19 (reproduced from Figure 6-30 of Reference B-1).

Scaled Unit Flexural Impulse Capacity of Each Panel

Donor Panel

$$\bar{i}_D = \frac{i_D}{w^{1/3}} = \frac{2530}{(2120)^{1/3}} = 197 \text{ psi-ms/lb}^{1/3}$$

Receiver Panel

$$\bar{i}_R = \frac{i_R}{w^{1/3}} = \frac{1630}{(2120)^{1/3}} = 127 \text{ psi-ms/lb}^{1/3}$$

Scaled Unit Impulse Attenuated By Dispersion and Absorption Through Sand Compression

Scaled Thickness of Concrete and Sand

$$\text{Concrete} - \frac{T_c}{W^{1/3}} = \frac{2}{(2120)^{1/3}} = 0.156 \text{ ft/lb}^{1/3}$$

$$\text{Sand} - \frac{T_s}{W^{1/3}} = \frac{4}{(2120)^{1/3}} = 0.311 \text{ ft/lb}^{1/3}$$

Scaled Unit Impulse Attenuated by Dispersion and Absorption

With the use of the scaled unit flexural impulse capacity of the receiver panel and the scaled thickness of the concrete and sand, the value of \bar{i}_a , which includes the impulse attenuated by dispersion in the concrete and sand, and by absorption through compression of the sand fill as well as the impulse capacity of the receiver panel, is determined from Figure B-19. Therefore,

$$\bar{i}_a = 275 \text{ psi-ms/lb}^{1/3} \text{ (from Figure B-19)}$$

$$\bar{i}_A - \bar{i}_a - \bar{i}_R = 275 - 127 = 148 \text{ psi-ms/lb}^{1/3}$$

where \bar{i}_A = scaled unit impulse attenuated by dispersion in the concrete and sand, and by absorption through compression of the sand fill.

Scaled Unit Impulse Capacity of the Back Wall

The scaled unit impulse capacity (\bar{i}_c) of the back wall is the sum of the scaled impulse resisted by the flexural action of the donor and receiver panels (\bar{i}_D and \bar{i}_R , respectively) and the scaled impulse attenuated by dispersion and absorption (\bar{i}_A).

$$\begin{aligned} \bar{i}_c &= \bar{i}_D + \bar{i}_A + \bar{i}_R = 197 + 148 + 127 \\ &= 472 \text{ psi-ms/lb}^{1/3} \end{aligned}$$

Note:

$$\bar{i}_c = 472 = \bar{i}_b = 485 \text{ psi-ms/lb}^{1/3} \text{ (Section B.2)}$$

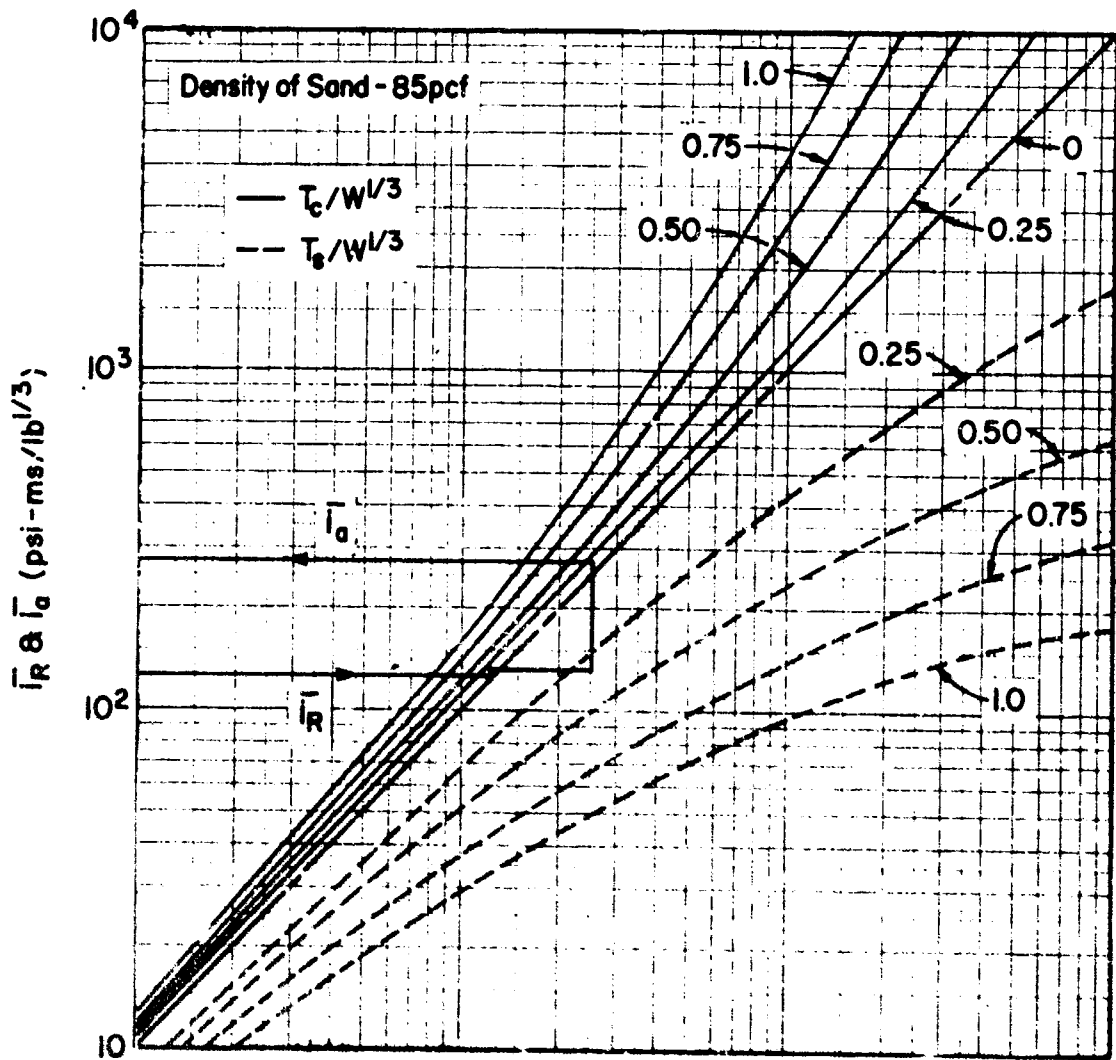


FIGURE B-19
 ATTENUATION OF BLAST IMPULSE IN SAND AND CONCRETE

NOMENCLATURE

a	(1) acceleration (2) depth of equivalent rectangular stress block
A	area of sector
A_S	area of tension reinforcement within a width b
A_V	total area of lacing reinforcement in tension within a distance s_l and a width b_l
b	width of compression face of flexural member
b_l	width of concrete strip in which the diagonal tension stresses are resisted by lacing of area A_V
c	centroidal distance
d	distance from extreme compression fiber to centroid of tension reinforcement
d_l	distance between centerlines of adjacent lacing bends measured normal to flexural reinforcement
d_w	weighted d
D_o	nominal diameter of reinforcing bar
DIF	dynamic increase factor
E_c	modulus of elasticity of concrete
E_s	modulus of elasticity of reinforcement
f_a	average stress of reinforcement
f'_c	static ultimate compressive strength of concrete
f'_{dc}	dynamic ultimate compressive strength of concrete
f_{ds}	dynamic stress of reinforcement
f_s	static stress of reinforcement
f_y	static yield stress of reinforcement
f_u	static ultimate stress of reinforcement
F	(1) total applied blast force (2) coefficient for moment of inertia of cracked concrete section
g	acceleration due to gravity
h	height to center of charge above floor slab
H	(1) span height (2) distance between reflecting surface (floor slab) and free edge

i_a unit impulse attenuated by concrete and sand plus impulse capacity of receiver panel
 i_A unit impulse attenuated by concrete and sand
 i_b unit blast impulse
 i_D unit flexural impulse capacity of donor panel
 i_R unit flexural impulse capacity of receiver panel
 I total impulse
 I_a average of gross and cracked moments of inertia of width b
 I_c moment of inertia of cracked concrete section width b
 I_G moment of inertia of gross concrete section of width b
 K_{LM} load-mass factor
 K.E. kinetic energy
 l charge location relative to vertical reflecting surface
 L (1) span length
 (2) distance between reflecting surfaces (side walls)
 m unit mass
 m_e effective unit mass
 m_E effective unit mass for equivalent elastic range
 m_p effective unit mass for plastic range
 M (1) moment capacity of #9 bars in mid strip
 (2) total mass of equivalent single-degree-of-freedom system
 M' moment capacity of #9 bars in corner strip
 M'' moment capacity of #7 bars in corner strip
 M_N negative moment capacity
 M_p positive moment capacity
 M_u ultimate moment capacity
 n modular ratio
 N number of adjacent reflecting surfaces
 p_v weighted percentage of reinforcement
 P.E. potential energy
 r_e elastic unit resistance
 r_{ep} elasto-plastic unit resistance
 r_u ultimate unit resistance

R (1) slant distance between charge and wall
 (2) total internal resistance of structural element
 R_A normal distance between charge and wall
 R_l radius of lacing bend
 R_u ultimate resistance
 R_y resistance at yield
 s_l spacing of lacing in the direction parallel to the longitudinal reinforcement
 t_A arrival time of blast wave
 t_m time at which maximum deflection occurs
 t_o duration of positive phase of blast pressure
 t_p time to reach ultimate resistance
 t_y time to reach yield
 T_c thickness of concrete section
 T_s thickness of sand fill
 v velocity
 v' shear stress resisted by lacing reinforcement
 v_c ultimate shear stress permitted on an unreinforced concrete web
 v_u shear stress at critical section
 V shear in the mid strip
 V' shear corresponding to moment capacity of #9 bars in the corner strip
 V'' shear corresponding to moment capacity of #7 bars in the corner strip
 V_d unit shear force at critical section
 w_c weight density of concrete
 w_s weight density of sand
 W charge weight
 x yield line location
 δ deflection
 \ddot{X} acceleration of the mass
 δ_e elastic deflection
 δ_E equivalent elastic deflection

X_{ep}	elasto-plastic deflection
X_m	maximum deflection
X_p	plastic deflection
X_p	permanent deflection
X_y	deflection at yield
Z	scaled slant distance between charge and wall
Z_A	scaled normal distance between charge and wall
α	angle formed by the plane of lacing reinforcement and the plane of the longitudinal reinforcement
β	coefficient for determining elastic and elasto-plastic resistances
γ	coefficient for determining elastic and elasto-plastic deflections
ϵ	strain
$\dot{\epsilon}$	strain rate
θ	support rotation angle
ν	Poisson's ratio

REFERENCES

- B-1 Structures to Resist the Effects of Accidental Explosions, Department of Army Technical Manual 5-1300, Department of Air Force Manual 88-22, Department of Navy Publication P-397, U. S. Government Printing Office, Washington, D. C., October, 1969.
- B-2 Cowell, W. L., Dynamic Tests of Concrete Reinforcing Steels, Technical Report R394, U.S. Naval Civil Engineering Laboratory, Port Hueneme, California, September 1965.
- B-3 Keenan, W. A., Strength and Behavior of Laced Reinforced Concrete Slabs Under Static and Dynamic Load, Technical Report R620, Naval Civil Engineering Laboratory, Port Hueneme, California, April, 1969.

TABLE OF DISTRIBUTION

UNCLASSIFIED

Security Classification

DOCUMENT CONTROL DATA - R & D

(Security classification of title, body of abstract and indexing annotation must be entered when the overall report is classified)

1. ORIGINATING ACTIVITY (Corporate author) Picatinny Arsenal Dover, New Jersey		2a. REPORT SECURITY CLASSIFICATION UNCLASSIFIED	
3. REPORT TITLE FULL AND MODEL SCALE TESTS OF BAY STRUCTURE		2b. GROUP	
4. DESCRIPTIVE NOTES (Type of report and inclusive dates)			
5. AUTHOR(S) (First name, middle initial, last name) Stuart Levy Richard Rindler - Picatinny Arsenal Leon Saffian Stanley Wachtell		Edward Cohen Michael Dede - Ammann & Whitney Norval Dobbs	
6. REPORT DATE February 1971	7a. TOTAL NO. OF PAGES 176	7b. NO. OF PAGES 12	
8a. CONTRACT OR GRANT NO.		8b. ORIGINATOR'S REPORT NUMBER(S) Technical Report 4168	
9. PROJECT NO.		9d. OTHER REPORT NO(S) (Any other numbers that may be assigned this report)	
9c.			
9d.			
10. DISTRIBUTION STATEMENT			
11. SUPPLEMENTARY NOTES Report completed in collaboration with Ammann & Whitney, New York, N.Y.		12. SPONSORING MILITARY ACTIVITY Armed Services Explosives Safety Board Washington, D. C.	
13. ABSTRACT <p>This report contains the results of two explosive test series: (1) The Scaled Explosive Bay Test Series whose purpose was to validate the "Scaling Laws" as applied to model bays and (2) The Ultimate Capacity Bay Test Series whose purpose was to determine the ultimate explosive resistance of a given explosive bay configuration.</p> <p>The results of these tests indicated that scale models may be used to evaluate the blast-resistant capabilities of a laced reinforced concrete cubicle-type structure and that the total explosive capacity of the tested structure (at incipient failure) is at least equal to 7,500 lbs. of high explosives.</p> <p>The Explosive Bay Test Series was carried out under the supervision of the Ammunition Engineering Directorate's Process Engineering Laboratory with technical assistance relating to structural design and testing provided by Ammann & Whitney of New York, New York.</p> <p>The smaller models (1/10 and 1/8 scale) were fabricated at the Civil Engineering Laboratories, Columbia University, and Ohio River Division Laboratories, Cincinnati, Ohio and tested at Picatinny Arsenal. The 1/3 and 1/5 scale models were built and tested by the Arthur D. Little Corporation at its Keene, New Hampshire test facility and the full scale structure was constructed and tested at the U.S. Naval Weapons Center, China Lake, California.</p>			

DD FORM 1473

REPLACES DD FORM 1473, 1 JAN 64, WHICH IS OBSOLETE FOR ARMY USE.

-175-

UNCLASSIFIED

Security Classification

UNCLASSIFIED

Security Classification

14. KEY WORDS	LINK A		LINK B		LINK C	
	ROLE	WT	ROLE	WT	ROLE	WT
Safety Design Criteria Program Explosive Bay Test Series Scaling Laws Ultimate Capacity Bay Test Series Explosive bay configuration Armed Forces Explosives Safety Board Blast-resistant capabilities Incipient failure Scale model testing						

UNCLASSIFIED

Security Classification